MSc Dissertation
September 1998

Engineering Seismology and Earthquake Engineering

Identification of Response Mechanisms in RC Beam-Column Connections

A.Orlando

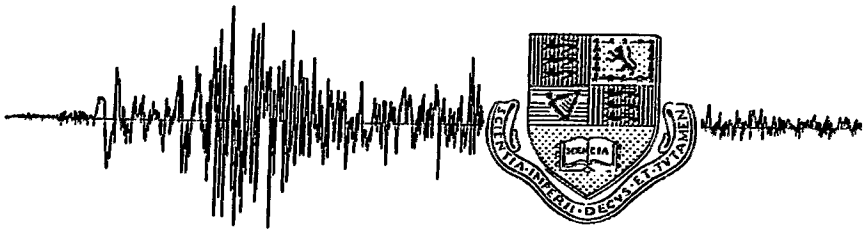

Civil and Environmental Engineering Department
Imperial College, London SW7 2BU, UK

Acknowledgements

I would like to express my sincere and deep gratitude to my supervisor Prof. A.S. Elnashai for his unfailing support, for all his advice and constructive criticism during the development of this research.

I am also grateful to all the staff of Earthquake Engineering and Seismology Section for the enthusiasm that have transmitted during the lectures of the MSc in EESD well interpreting their mission of lecturer.

I would also like to thank MS. K. Crook and S. Parry in the Civil Engineering Library who always joked with me thinking I was a 'rich man' for the enormous amount of papers I have had the fortune to consult and photocopy.

Words of thanks would fail to express my indebtedness to Prof. E. Cosenza, Dr. G. Manfredi and Dr. G. Serino of University of Naples. They all made me enthuse over pursuing the MSc at the Imperial College.

My infinite love and thanks are due to my parents, because all what I have accomplished in life is the result of their love and years of sacrifice.

This research is dedicated to the memory of my beloved and esteemed grandpa:
Nonno Antonio.

TABLE OF CONTENTS

Quelli che s'innamoran di pratica sanza scienza,
son come il nocchiere,
ch'entra in navilio sanza timone o bussola,
che mai ha certezza dove si vada.
Leonardo da Vinci

(Whoever loves practice without science,
is like a sailor,
he drives his boat without helm or compass,
he will be never sure where he is going).

Fuggi i precetti di quelli speculatori
che le loro ragioni non sono confermate
dalla sperienza.
Leonardo da Vinci

(Stay away from the concepts by those researchers
that cannot prove their reasons
with the experience).

CHAPTER 1

INTRODUCTION

1.1 Significance of beam-column connections

The analysis and design of reinforced concrete beam-column joints in ductile moment resisting frames is an area of earthquake engineering in which there is still no consensus as to the best analytical and design procedures. In the design of these structures following the ductile design approach known as weak-beam strong-column behaviour, it is desirable that the joints and columns remain essentially elastic in order to insure proper energy dissipation and lateral stability of the structure.

With significant progress made in the understanding and design of beams and columns, and particularly with the detailing of the reinforcement to achieve the necessary ductility in appropriate regions of these members, the importance of joints has gradually emerged. Using well-designed beams and columns, a joint may well become the weakest link of the chain of resistance within a ductile reinforced concrete frame [Paulay and Priestley, 1992].

As a consequence of seismic moments in columns of opposite signs immediately above and below the joint and similar beam moment reversal across the joint, the joint region is subjected to high values of shear forces. The reversal in moment across the joint also means that if for example plastic hinges occur in the beam adjacent to the column, the beam reinforcement is required to be in compression on one side of the joint and at tensile yield on the other side of the joint. Hence, high bond stresses are required to transmit the above force gradient across the joint [Paulay and Priestley, 1992].

For the aforementioned reasons the beam-column connection becomes a region of high distress and due to the brittle nature of the concrete and the poor hysteretic performance of the shear and bond mechanisms, strength and deformability are aspects of the joint behaviour which must be addressed carefully. In fact, stiffness and/or strength deterioration in the joint region endanger the overall stability of the structure leading to substantial drifts with possibility of collapse due to P-delta effects.

It is sometimes claimed that the importance of the joints in seismic design is overemphasized because there is little evidence from past earthquakes of major damage or collapse that could be attributed to joint failures. This observation is largely due to the inferior standard of design of beams and particularly, the poor detailing of columns. These members thus became the weak links in the structural system. Many failures of framed buildings resulted from soft-story mechanisms in which column failure due to shear or inadequate confinement of the concrete occurred before the development of available beam strengths [Paulay and Priestley, 1992]. However, when in the past seismic events joint failures have occurred, they have always had catastrophic consequences as shown for example in **Fig. 1.1** and **Fig. 1.2**. Owing to the high standard reached in the design and detailing of beams and columns and the use of high strength materials which lead to have beam and column sections with small dimensions and heavy reinforcement, it is expected the above failure

percentage may increase if the joint is not adequately and carefully designed. Also damage to the joint is required to be avoided so as to eliminate the need for a repair in a relatively inaccessible region. On the other hand, over-reinforcing the joint is clearly not always a viable solution as it can cause undue construction difficulties, as it is evident from **Fig. 1.3**. Hence, the importance of estimating accurately the joint performance is required to be necessary.

1.2 Scope of the study

Experimental studies and observation in field have shown that joint shear deformation and fixed-end rotations due to the slippage of the longitudinal bars may contribute up to 50% to ioverall deflections of the subassemblages. If these effects are not accurately accounted for, the stiffness of a structure is overestimated, the lateral displacements are underestimated and an erroneous assessment of the stability of the structure will be expressed, especially in the case of high-rise buildings.

Though many experimental and analytical studies have been carried out for more than thirty years, a thorough understanding of the connection behaviour seems still far from having reached a unanimous agreement among the several researchers. This incompleteness is evident both on the experimental side and analytical one.

It is claimed that the experience must be the fundament to devise an accurate analytical model. This statement is true if the experimental study allows the influence of one parameter at time to be evaluated. Unfortunately, only very few experimental tests have been conceived with this purpose, hence important information on aspects of the joint behaviour has not completely been clarified. The experimental deficiency reflects oneself in the analytical modelling. The current models which account for the source of deformability related to the joint are generally global models. These models describe joint behaviour with hysteretic models defined on the basis of deterioration and degradation mechanisms which are expected to occur within the joint. Hence, this choice is made by the analyst and is not the result of the interaction between system and input.

The aforementioned ideas have given rise to the present research. The intention was to establish underlying principles and mechanisms which a predictive model should rely on. At this end, a finite element analysis has been carried out. From the theoretical standpoint of view, finite element method has the potentiality of being a predictive model as it can take into account the single materials and their interaction. Nevertheless, such numerical simulation is meant basically for research purpose due to the complexity of the models required to carry out the analysis. However, its use is usually conceived to clarify the basic joint response mechanisms and to derive from these studies simplified models for more common design applications.

1.3 Organisation of the Report

This research aims to study the shear deformation of a reinforced concrete interior beam-column connection of a one way bare frame by means of a non-linear finite element analysis.

Owing to the complexity of the topic, this research should be regarded as first step of a more thorough analysis aimed at describing the joint behaviour by means of combination of single mechanical elements defined by only geometrical and material properties.

Accurate prediction of the joint behaviour by means of a theoretical model may be best developed if phenomenological understanding of the problem is known so as to serve as guide for the modelling. Hence, the importance of a premise on experimental and analytical studies is recognised and is presented in chapter 2 and chapter 3, respectively.

In chapter 2, after illustrating the two basic joint failure modes a list of the key design variables is given. Thereafter, a survey of experimental investigations which have proposed to study the influence of the above design variables on the connection behaviour is presented. Some considerations on conflicting results from the several experiences are expressed on the basis of the most recent findings of concrete modelling, as well.

Chapter 3 presents the current analytical models adopted to describe the influence of the joint behaviour on the frame response. These have been classified as global and finite element models. The former describe the joint by means of analytical hysteretic models which are usually chosen a priori by the analyst on the basis of the hysteretic mechanisms which are expected to occur within the joint. The latter adopts a finite element idealisation of the joint.

In chapter 4, after having given the basic concepts of the strut and ties models adopted to evaluate the joint shear strength, a global model which allows to describe the primary response of the joint under increasing monotonically loads is illustrated in great detail. Also, an effective algorithm to solve the system of non-linear equations and its implementation into a Fortran program are given. The model has been applied to study the complete response of three specimens which exhibited the three different shear failure modes. It has been also pointed out and shown with a detailed numerical example that the study of the reinforced concrete membrane by adopting total average stresses, such as in the Modified Compression Field theory, can give rise to inconsistencies in the behaviour of the membrane.

In chapter 5, non-linear analyses of three finite element models of a subassemblage are carried out. The three models are different because of assumptions made on the material behaviour which allowed to evaluate the importance of the joint boundary conditions on the joint performance. An attempt to give a simple model which considers only the strut contribution to control the joint shear deformation is done, as well.

In the final chapter, conclusions from the present study are drawn and suggestions for further investigation are outlined.

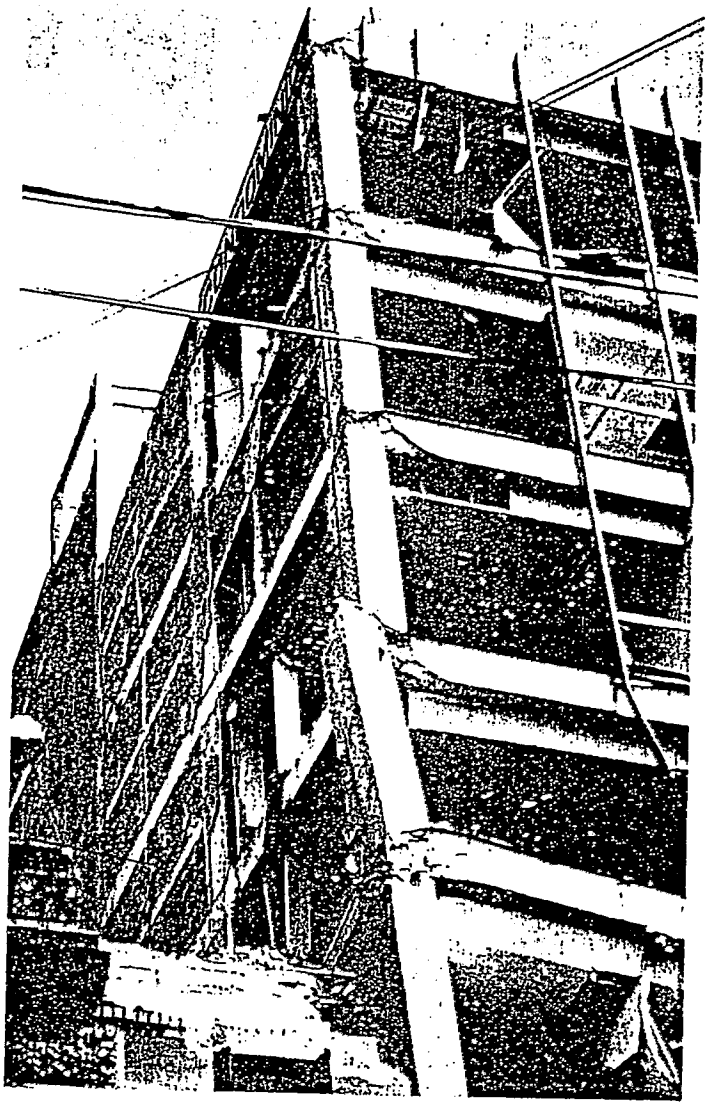

Fig. 1.1 Beam-column joint failures in the 1985 Mexico earthquakes

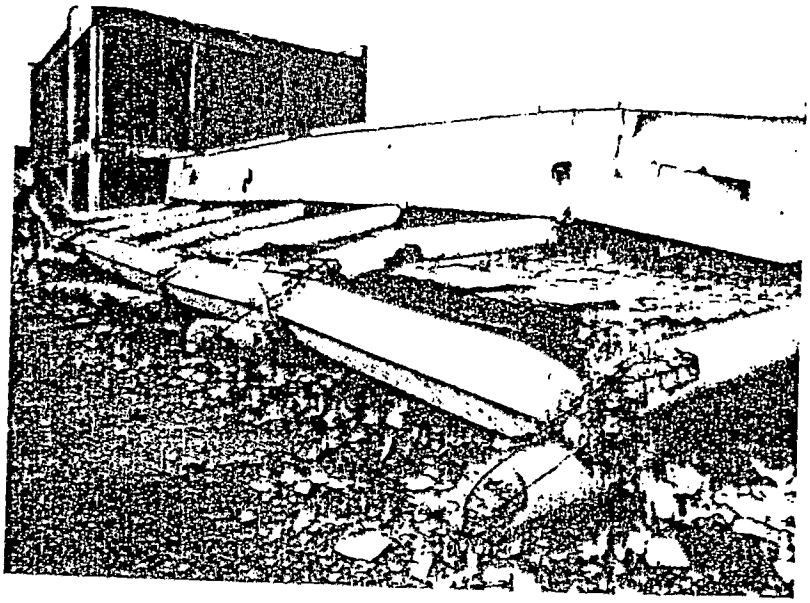

Fig. 1.2 Beam-column joint failure in the 1980 El Asnam earthquake

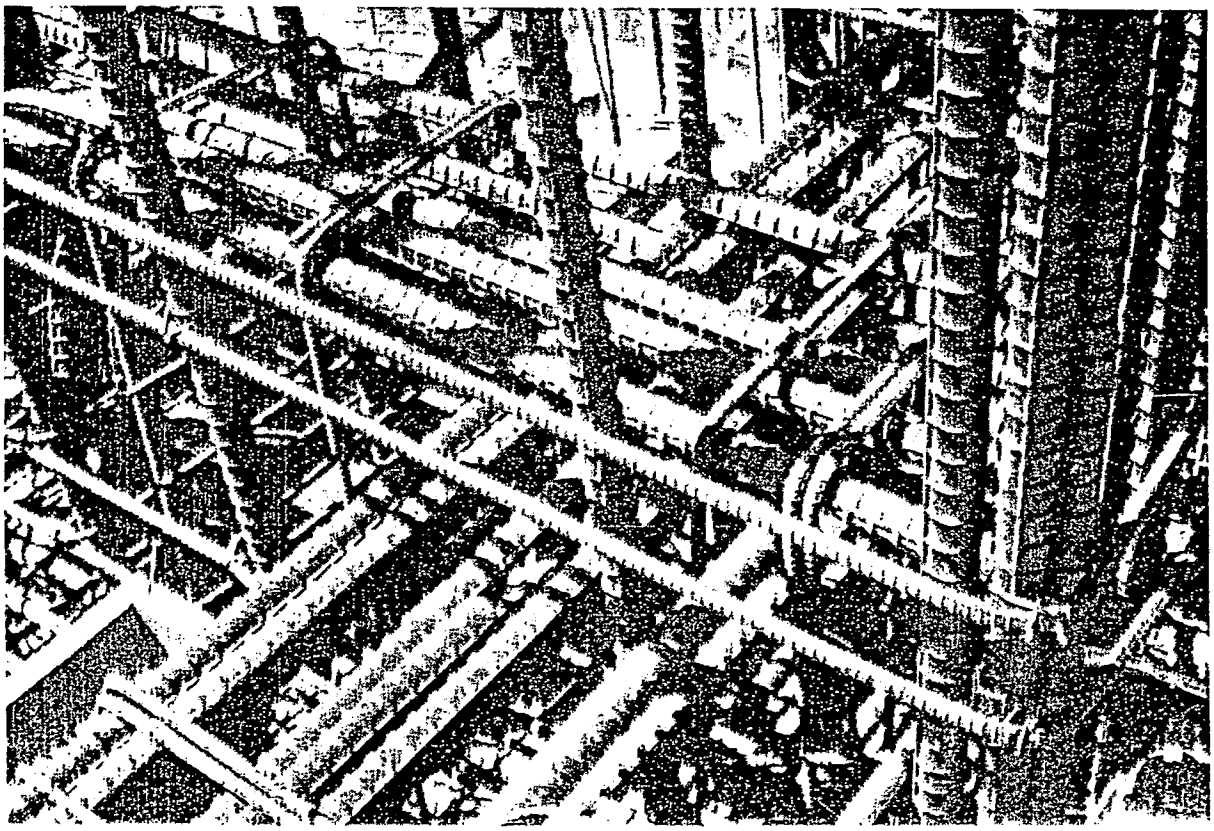

Fig. 1.3 Joint reinforcement arrangement for ductile reinforced concrete

CHAPTER 2

EXPERIMENTAL STUDIES

2.1 Introduction

In the study of the reinforced concrete beam column connections under the action of cycling loading the experimental investigation has an important role. Much of the current knowledge about joint behaviour has been obtained by interpreting results of cyclic tests done on assemblies representing frame connections. Usually, these assemblies are made statically determinate to facilitate data reduction. However, due to the non-linear interaction of the two materials, i.e. reinforcement and concrete, and the material non-linearity the above interpretation is also the most demanding task of the whole experimentation and is subject to considerable numerical scatter.

Since the first experimental investigations conducted in the United States by the Portland Cement Association in the early 1960's and published in 1967 [Hanson and Connor, 1967], the importance of design variables such as joint transverse reinforcement, axial column load, anchorage bar length has long been recognised. However, all experimental research available up to now has not been always able to clarify and quantify the influence of the above parameters. This difficulty is basically due to the two fundamental failure modes, which the different experiments have recognised to occur in the joint, and to different way the design variables influence each of them.

After reviewing the two basic joint failure modes a list of the key design variables is given. Thereafter, a survey of experimental investigations which have proposed to study the influence of the above design variables on the connection behaviour is presented.

2.2 Basic Joint Failure Modes and Key Design Variables

Under seismic actions, the joint is the region of the column where large variation of effect actions must take place giving rise a complex stress-state. The main actions transmitted to an interior joint are from bearing of the compressive concrete blocks and from the bond stresses by which the forces applied to the column and beam longitudinal reinforcement are transferred to the concrete. **Fig. 2.1** depicts these forces in the case of a joint of a laterally loaded frame. Both of these two modes of force application develop what is referred to as **joint shear**. Any corresponding failure of either the concrete or reinforcement to resist the application of these forces is referred to as **joint shear failure**. Hence, this type of failure may appear as either diagonal tension failure or concrete crushing or reinforcement rupture. The joint is not able to bear further increment of actions and dramatic loss of load carrying capacity of the column arises. **Fig. 2.2** shows a typical shear failure due to crushing of concrete after yielding of the horizontal joint shear reinforcement. The

breakdown of the interaction between longitudinal bars through the joint and the surrounding concrete such that no longer bond stresses can be transferred to the core concrete is referred to as **joint bond failure**. As result, the bars slip through the joint. The anchorage failure by itself does not necessarily result in sudden loss of joint strength. The joint is still capable of bearing further increments of load as the longitudinal bars are anchored in the beams on the opposite side of the joint [Paulay, 1981]. The slippage of the bars bring the far beam compression zone in contact with the side of the joint while opening a wide crack on the tensile face of the near beam [Hanson, 1971], **Fig. 2.3**. In this case larger compressive strains occur in the joint and consequently losses of section in the corners of the column may arise [Leon, 1990a]. However, before getting to this stage, which is still denounced by concrete crushing, the earlier stage of bond deterioration is assumed as failure condition because it produces large reduction in both stiffness and energy dissipation of the whole subassemblages, **Fig. 2.4**.

A large number of beam-column subassemblies have been tested to date. The different types of configurations are shown in **Fig. 2.5** where are depicted bare frames, frames with slab contribution and transverse beams, interior and exterior joints. In the following, only the experimental investigations of interior joint of one way bare frame, i.e. without slab contribution and transverse beam, are considered. An overall exam of the test results show that the performance of these beam-column connections may be made depending on the following parameters: **joint transverse reinforcement, column bars arrangement, column axial load, column depth, bar diameter, ratio of bottom to top steel area bars, concrete strength and steel strength**. Also the loading history and its severity is an important parameter as may influence the behavioural pattern. However, it has not been included in the above list as the main goal of the report is the characterisation of the system of which the loading history is the input.

Hereafter, the experimental results are reported to show the influence of the previous design variables on shear strength, shear deformational capacity and bond deterioration.

2.3 Effect of Joint Reinforcement

In 1967 Hanson and Connor reported the results of a series of investigations conducted on full-size beam-column subassemblages. The purpose of their research was to determine joint reinforcement required ensuring maintaining ultimate capacity for cast-in-place beams and columns subjected to multiple reversals of loading of major earthquake magnitude. Although the experiences were referred to exterior beam-column, the results of their research become the standard reference for subsequent investigations as contained useful and general indications. The major test variable was the degree of confinement of concrete in the joint. With regard to this aspect, the comparison of behaviour of two identical specimens but the joint reinforcement was of interest. In one the joint hoops were purposely omitted whereas the other one the hoops were designed so as to provide full confinement of concrete. Regarding the joint as a segment of the vertical column, the hoops were designed as the equivalent amount of spiral reinforcement required to develop the original capacity of the column after the shell had spalled off. To accomplish this, it was recommended that the ties formed a closed loop and had adequate anchorage. The two specimens were subjected to the same loading history shown in **Fig. 2.6** (two earthquakes in series were simulated) and their performance is shown in **Fig. 2.7**. It was seen that the specimen properly designed and detailed in the joint region could maintain the computed ultimate moment throughout the whole programmed load reversal whereas for the specimen without joint reinforcement the test was terminated after only three cycles

due to the rapid deterioration of the joint concrete. The Authors also proposed an equation to evaluate the shear strength capacity of the joint similar to the one used for the shear in the beams.

At University of Texas at Austin a research program aimed at examining experimentally the significance of several parameters on the behaviour of interior beam-column joints in planar frames was started [Jirsa, Meinheit and Woolen, 1975; Meinheit and Jirsa, 1981]. In particular, the main objective of the research was to verify the joint shear strength equation given by the current ACI recommendations and hence, the contribution of the concrete to the shear strength of the joint. For this purpose, the specimens were designed with small amounts of transverse reinforcement so as to have the concrete carrying most of the joint shear. The programmed experimental series allowed also to evaluate the influence of transverse reinforcement in joint as four identical specimens except for the amount of transverse reinforcement in the joint were considered, **Table 2.1**. The experimental results showed that while shear cracking of the concrete was not influenced by the amount of hoop reinforcement only a slight increase in the connection shear strength was noted, **Fig. 2.8**. However, this increase was not in the same ratio as indicated by the equation of the joint shear strength and hence, a modification of the equation was recommended.

Specimen	Column		Main Beam reinforcement	Connection Hoops		f'_c [MPa]	$\Sigma M_c/\Sigma M_b$
	ρ_g	σ_c [MPa]		Reinforcement	ρ_h		
II	4.3	10.6	3#10 on top; 3#8 on bottom. 5 cm. Concrete	2 #4 @ 15cm	0.011	41.80	1.72
IV	4.3	10.6		2 # 4 @ 15cm	0.011	36.10	1.18
XII	4.3	10.6		6 # 5 @ 5cm	0.052	35.2	1.63
XIII	4.3	10.6		6 # 4 @ 5cm	0.033	41.3	1.71
XIV	4.3	10.6		6 # 4 @ 5cm	0.033	33.2	1.14

ρ_g: percentage of column reinforcement; σ_c: nominal axial stress on the column; ρ_h: volumetric percentage hoop reinforcement; f'_c: concrete compressive strength; $\Sigma M_c/\Sigma M_b$ ratio of column flexural strength to beam flexural strength.

Table 2.1 Specimen details (after Meinheit and Jirsa, 1981).

Uzumeri and Seckin [1975] and Uzumeri [1977] carried out experiences with the main variables being the amount and type of joint reinforcement. Two types of joint steel were used: one exhibited a flat yield plateau and the other one did not. Interesting observations were drawn by comparing joints without and with horizontal transverse reinforcement, **Fig. 2.9**, and joints with the same amount of horizontal transverse reinforcement but having the above different steel characteristics, **Fig. 2.10**. Once again, it was confirmed the importance of providing joint reinforcement which increased the ductility of the sub-assembly several times over the unreinforced joints and this enhancement of behaviour was attributed to the capacity of the joint stirrups to confine the concrete. As to the effect of the characteristics of the stirrup steel, it appeared that the joint steel without flat yield plateau continued to confine the joint region and provided anchorage to beam steel over very large tip deflections. Different behaviour was noted for the joint steel with flat yield plateau which seemed to relax its confinement when it yielded and thus released the anchorage for the beam steel, resulting in a downward turn of the strength envelope, **Fig. 2.10**. Hence, it was first recommended that the design of joint steel should be based on the avoidance of yielding of the joint steel and then,

the use of steel as joint reinforcement that does not exhibit a flat yield plateau warranted serious consideration.

Durrani and Wight [1984, 1985] tested interior beam-column connections to study the influence of the amount of joint reinforcement and the presence of transverse beam and slab. In their experimental research programme two identical specimens except for the joint reinforcement were compared. The characteristics of the two specimens are listed in **Table 2.2** and the quasi-static loading considered is shown in **Fig. 2.11**. Furthermore, the specimens were designed according to the principle of weak beam-strong column. The specimen X1 had a lower amount of joint reinforcement given by only two layers of hoops. After the early loading cycles, the specimen began to lose its strength as a result of the spalling of the concrete between the two layers of hoops and opening of wide cracks from the hollow core area toward the corners of the joint. On the other hand, the well-confined joint core of specimen X2 helped the beam reinforcement reach strain hardening without any appreciable slippage. Only upon yielding of hoops the joint partially lost its confinement and resulted in a loss of strength, **Fig. 2.12**. These experiences allowed also noting the presence of an effect of joint confinement on the beam bars slippage. Both of the two specimens had a ratio of the total column depth to the beam bar diameter equal to 14. Due to the low value of the ratio, the slip was likely to occur. This was observed in the case of the specimen X1 whereas in the specimen X2 the beam main reinforcement experienced very little slippage.

Specimen	Connection Hoops			f'_c [MPa]	$\Sigma M_c/\Sigma M_b$
	Spacing of hoops [cm]	2 #4 @ 15cm 2 # 4 @ 15cm	ρ_h		
X1	6	2	0.76	34.31	1.50
X2	4	3	1.15	33.62	1.55

ρ_h: percentage of hoop reinforcement; f'_c: concrete compressive strength; $\Sigma M_c/\Sigma M_b$ ratio of column flexural strength to beam flexural strength.

Table 2.2 Specimen details (after Durrani and Wight, 1985).

Yunfei, Chingchang and Yufeng [1984] attempted to quantify the hoop content influence trend in their experimental results. After having described the typical joint shear failure observed in the tested specimens, in order to describe the effect of hoop content the researchers introduced the parameter α so defined:

$$\alpha=\rho_{hp}f_y/f_c \tag{2.1}$$

where:

ρ_{hp} is the volumetric hoop ratio in the joint core
f_y is the yield strength of the steel hoop
f_c is the compressive uniaxial concrete strength.

According to the values of this parameter the joint shear failure could be detected by hoop yielding or concrete crushing. The balance condition was attained when the concrete and the hoops reached their ultimate strength simultaneously. For this end, an upper limit to the hoop ratio was required as in the case of high values of the ratio α the concrete could fail before yielding of hoops.

The study of the effects of joint stirrups especially on the shear strength was the objective of the research program carried out by the New Zealand's researchers. On the basis of the behavioural model proposed by Paulay, Park and Priestley [1978], which will be illustrated in the chapter 4, the direct contribution of the joint stirrups to the shear strength was basically investigated. The tests carried out by Park and Keong [1979], Park, Gaetry and Stevenson [1980] and Park and Milburn [1983] addressed all of them at validating the above design model which implies a proportional dependence of the joint shear strength upon the joint hoop content. Furthermore, in these experiences was also confirmed the influence of the hoop yielding condition on the joint behaviour. In fact, irrespective of the direction of diagonal cracking, horizontal shear reinforcements were always subject to tension forces. Hence, the inelastic steel strains that resulted were irreversible. Consequently, during subsequent loading, stirrup ties could make a significant contribution to shear resistance only if tensile strains imposed were larger than those developed previously. This then led to drastic loss of stiffness at low shear force levels.

Kitayama, Otani and Aoyama [1988, 1991] reported the experimental results of tests carried out on three half-scale planar interior beam-column joint specimens varying reinforcement detailing and amount in a joint. The objective was to study the role of the lateral confinement, i.e. lateral reinforcement to resist shear and that to confine core concrete, in order to quantify accurately its effects and the strictly necessary amount of stirrups without resulting in undue construction difficulties. The specimen properties are listed in **Table 2.3** and **Fig 2.13** shows the different reinforcement arrangement. The specimens B1 and B2 were identical but the reinforcement detailing, whereas in the specimen B3 the amount of transverse reinforcement changed. The arrangement of the joint stirrups as legged ties in the two orthogonal directions in specimens B1 and B3 served to separate in the researcher's intention the effect of confinement from that of resisting the shear. It was assumed that the ties parallel to a loading direction would resist joint shear and confine joint core concrete to that direction, whereas transverse ties would only restrain the expansion of core concrete normal to the loading direction. It was observed that the contribution of joint lateral reinforcement to shear resistance decayed after bond deterioration along the beam longitudinal bars and the principal role of joint lateral reinforcement came to confine the cracked joint core concrete, **Fig. 2.14**. Furthermore, no appreciable difference was observed between the two specimens B1 and B3, which had different amount of reinforcement, as in both the specimens the strains did not reach the yield value before a high value of the story drift was applied, **Fig. 2.15**.

Specimen		B1/B2	B3
Beam ($200*300mm^2$)	top bars, p_t	2.05	1.68
	bottom bars p_t	2.05	1.68
	stirrups p_w	0.56	0.56
	f_y [MPa]	498	498
Column ($300*300mm^2$)	total bars, p_g	3.54	2.26
	f_y [MPa]	358	378
	hoops p_w	0.75	0.37
	f_y [MPa]	498	498
	σ_c[MPa]	2	2
Connection	p_w	0.35	0.88
	detail	Leg/closed	Leg
	f_y [MPa]	240	240
f'_c [MPa]		25	25
f_{ct} [MPa]		2.6	2.6

p_t tensile reinforcement ratio; p_g gross reinforcement ratio; p_w web reinforcement ratio; f_y yield strength; f'_c concrete compressive strength; f_{ct} concrete tensile strength.
σ_c: nominal axial stress on the column

Table 2.3 Specimen details (after Kitayama, Otani and Aoyama 1991)

Even the experiences carried out by Wong, Priestley and Park [1990] allowed confirming that the stiffening action of closed stirrups occurred not only in the direction of the load but in the perpendicular direction, as well. Two full scale beam-column joint assemblages were tested in which the closed stirrups were replaced by longitudinal beam reinforcement that was uniformly distributed along the height and anchored outside the joint. Although the joint in these specimens were able to resist the shear demanded to develop beam hinging, a rapid deterioration of joint shear resistance was observed with cycling, **Fig. 2.16**. Hence, it was emphasized the need for the presence of significant quantities of shear reinforcement in the form of conventional horizontal hoops to confine the joint core and to carry shear across the diagonal tension cracks.

In the experimental tests carried out by Fujii and Morita [1991] the effect of joint hoop reinforcement on the joint behaviour was investigated, as well. Two interior beam-column subassemblages of one way frames were tested. As opposed to the majority of the previous experimental studies, which adopted the design philosophy of weak beam and strong column, in their investigation the program was determined such that joint shear failure occurred in specimens prior to beam and column yielding. The specimen properties, which allowed comparing the effect of hoop reinforcement, are listed in **Table 2.4**. It was observed that the shear cracking was not influenced by the amount of joint hoops, whereas only 2% increase of the joint shear strength resulted from the increased amount of joint hoop from steel percentage of 0.41% to 1.1%. Furthermore, no effect of the stirrups was observed in the load deflection curves.

Specimen		A3	A4
Beam ($200*300mm^2$)	top & bottom bars, p_t	1.68	1.68
	f_y [MPa]	1069	1069
Column ($220*220mm^2$)	total bars, p_g	4.20	4.20
	f_y [MPa]	656	656
	σ_c[MPa]	10.2	10.2
Connection	p_w	0.41	1.1
	f_y [MPa]	297	297
f'_c [MPa]		41	41

p_t tensile reinforcement ratio; p_g gross reinforcement ratio; p_w web reinforcement ratio; f_y yield strength; f'_c concrete compressive strength; f_{ct} concrete tensile strength. σ_c: nominal axial stress on the column

Table 2.4 Specimen details (after Fujii and Morita, 1991)

The experimental studies carried out by Goto, Joh and Shibata [1988,1991] on half scale beam column joint specimens indicated a close interaction between bond of beam bars and shear reinforcement. The more transverse reinforcement in the joint panels was provided, the less the slippage of beam bars from the joint panel resulted. Consequently, pinch effect hardly appeared on the shear force-deflection curves of subassemblages laterally reinforced heavily in the beam-column joints, and energy dissipation ability of such subassemblages was large. Once again, it was also observed that the amount of lateral reinforcement in the joint panel did not influence to cracking stress. However, the shear stiffness of the joint panels after cracking was kept higher with the heavier lateral reinforcement. Particularly interesting was also the behaviour of one of the specimens that had been treated as to be bondless within the joint region of the beam bars. It was observed that this specimen showed low stiffness even on the elastic region of the frame response. Moreover, no shear crack occurred in the panel nor, consequently, the shear stiffness of the joint panel degraded, as shear force in the panel was transmitted mainly through a predominant compressive stress field.

2.4 Column Bars Arrangement

In the previous section the joint shear reinforcement was provided in the form of horizontal hoops to sustain basically the horizontal shear force. Regarding the joint as a beam segment it is observed that the connection must resist also to vertical shear force, hence the need for vertical shear reinforcement in the joint is recognised, as well. In most connections, the column longitudinal reinforcements serve this purpose. Their efficiency, however, cannot be compared to the stirrups as they do not bend around and bear against the beam steel, thereby provide a clamping force which improves the bond.

The importance of vertical joint shear reinforcement, in the form of intermediate column bars passing through the joint, was demonstrated experimentally by Park and Keong [1981]. They considered two series of tests. In the first one, columns with flexure reinforcement placed in the two opposite faces of the column only, close to the fibres of maximum flexural strain, were used. In spite of the use of large quantities of horizontal joint shear reinforcement, joint shear failure occurred. In the second series of tests, beam and columns, identical to those of the first series, were used except that intermediate column bars, providing vertical joint shear reinforcement, were also provided. A dramatic improvement in hysteretic response without joint failure was observed.

The positive influence on the shear strength and shear stiffness of joint due to intermediate column bars was observed as well, by Jirsa and Meinheit[1981] and by Goto et al. [1988, 1991].

2.5 Effect of Column Axial Load

Most of the experimental studies previously reported to describe the effect of the joint reinforcement addressed also to investigate the effect of the column axial load on the joint behaviour. Since the first experiences by Hanson and Connor [1967] the axial column load has always aroused suspicion of being a parameter which potentially could influence the joint shear strength. Especially when the column is subject to tensile axial load the joint becomes the weakest link of the chain and the attainment of the full resisting capacity of the beam section is jeopardised. However, the experiences carried out by Hanson and Connor [1967], Hanson [1971], Jirsa, Meinheit and Wollen [1975], Jirsa and Meinheit [1981] were not always able to show this aspect. In the experimental program carried out by Jirsa et al. [1975, 1981], five specimens were tested. These were identical except for the level of column compressive load ranging from $0.03f'_c$ to $0.39f'_c$. In each case the plastic hinges beam, which occurred at the column face, were able to attain their full strength and the shear strength of the joint was practically unaffected by the magnitude of the column compressive load. On the other hand, shear cracking of the concrete was significantly affected by the column compressive load and increased as the axial compressive load increased.

Kitayama, Otani and Aoyama [1988, 1991] drew similar conclusion. Discussing the results of experimental tests carried out in Japan and USA and reported in **Fig 2.17** as column axial stress level versus maximum joint shear stress normalised by concrete uniaxial compressive strength, they observed that the column axial load did not seem to influence the joint shear strength. However,

high axial compression load accelerated the strength decay in the diagonal compression failure of the joint core concrete after beam flexural yielding.

Yunfei, Chingchang and Yufeng [1984] obtained different type of results. Their investigations indicated that within certain range of the compression stress ratio σ/f'_c, the increase of axial compressive force did increase the shear at first cracking of the concrete in the core and also its ultimate shear strength. It was also observed that the increase of the axial force reduced the ductility of the beam column subassemblage.

All the aforementioned studies conducted on the connections shared the strong column weak beam design philosophy. This philosophy usually leads to formation of plastic hinges in beam regions adjacent to the column face. Consequently, even though it was said that the type of failure experienced by the joint was a shear failure; yielding penetration of beam bars and some amount of bond deterioration were likely to occur within the joint. As result, interaction between the two failure modes was expected, hence, the previous experiences could not be used to gauge the actual shear capacity of the connection. Starting from this observation, Fujii and Morita [1991], Agbabian, Higazy, Abdel-Ghaffa and Elnashai [1994] and Higazy, Elnashai and Agbabian [1996] adopted a non conventional design approach to ensure pure panel zone shear failure so as to ensue a realistic estimate of joint shear strength.

Fujii and Morita undertook a general research programme which aimed at evaluating the influence of different design variables. Only two specimens were tested to evaluate the effect of axial loads assumed for both the specimens as a compressive load equal to $f'_c/12$ and $f'_c/4$, respectively. Their properties are reported in **Table 2.5**. As expected, the shear cracking capacity of joint concrete was increased with the increase of column axial load whereas no appreciable effect was observed on the joint shear strength.

Specimen		A1	A3
Beam ($200*300mm^2$)	top & bottom bars, p_t	1.68	1.68
	f_y [MPa]	1069	1069
Column ($220*220mm^2$)	total bars, p_g	4.20	4.20
	f_y [MPa]	656	656
	σ_c[MPa]	3.4	10.2
Connection	p_w	0.41	0.41
	f_y [MPa]	297	297
f'_c [MPa]		41	41

p_t tensile reinforcement ratio; p_g gross reinforcement ratio; p_w web reinforcement ratio; f_y yield strength; f'_c concrete compressive strength; f_{ct} concrete tensile strength. σ_c: nominal axial stress on the column

Table 2.5 Specimen details (after Fujii and Morita, 1991)

Much more detailed experiences were reported by Agbabian et al. and by Higazi et al. The objectives were to provide a better understanding of the shear transfer mechanism in joints and quantify the effect of variation of axial column load, as an aspect of demand, on the panel zone shear strength and deformability. Identical specimens were considered and a strict quality control was imposed in order to isolate irrevocably the effect of axial column load. Details of the test models are listed in **Table 2.6**, Higazi, 1993. The experimental results indicated that the behaviour of the panel zone was affected by axial column load. It was observed that the strength capacity was sensitive to reductions of axial column compression; more so for tension application. It was also seen that a slight increase in column compression resulted in a relatively high increase in shear stiffness. Hence, a lower interstorey drift would be experienced. Conversely, introduction of a

tensile axial force of 5% of column compressive squash capacity or the absence of column compression increased substantially the panel zone shear deformation and losses of ductility and energy dissipation capacities occurred, as well. By comparing the behaviour of the specimens with no axial column compression and that with 5 per cent compressive load, considerable differences in the behaviour were noted up to the level of complete development of cracks in both specimens. Afterwards, the role of axial load in crack control diminished and the two specimens deformed identically up to failure.

Specimen		SA1	SA2	SA3
Beam ($127*203mm^2$)	top bars, p_t	0.55	0.55	0.55
	bottom bars, p_t	0.55	0.55	0.55
	f_y [MPa]	410	410	410
Column ($127*178mm^2$)	total bars, p_g	1.2	1.2	1.2
	f_y [MPa]	410	410	410
	σ_c[MPa]	1.4	0	2.8
Connection	p_w	0.71	0.71	0.71
	f_y [MPa]	410	410	410
f'_c [MPa]		28	27	28

p_t tensile reinforcement ratio; p_g gross reinforcement ratio; p_w web reinforcement ratio;
f_y yield strength; f'_c concrete compressive strength; f_{ct} concrete tensile strength.
σ_c: nominal axial compressive stress on the column

Table 2.6 Specimen details (after Higazy, 1993)

To date there are very few experiments investigating the influence of column axial force on joint beam bar conditions, despite that this effect has been considered in some bond mechanical models [Tassios, 1979; Ciampi, Eligehausen Bertero and Popov, 1981].

By interpreting results of experiences carried out in Japan and USA Kitayama, Otani and Aoyama [1991] adopted the equivalent viscous damping ratio evaluated at a story drift of 1/50 rad on hysteretic loops of beam-column connections as index to describe the effect of beam bar slippage. The results were plotted as column compressive stress normalised by the concrete compressive strength versus the equivalent viscous damping ratio as shown in **Fig. 2.18.** . It was observed that the test results were scattered widely regardless of column axial stress level, and column axial stress smaller than $0.3f'_c$ did not seem to exhibit beneficial effect on the bond resistance along the beam bar within a joint.

Morita, Fujii, Murakami and Yamada [1992] observed that the available experimental studies performed on beam-column subassemblages were generally not appropriate to focusing on the bond behaviour in joints as it was difficult to exclude the effects due to the other influencing factors from the total behaviour. Hence, they introduced a new test method aimed at reproducing the real pull-push condition of a beam bar in an interior beam-column joint under earthquake type loading. The results of their experience will be discussed in the following section so as to have an overall picture of the parameters which influence the bond conditions.

2.6 Column Depth; Bar Diameter; Ratio of Bottom to Top Steel Area Bars; Concrete and Steel Strength.

In this section will be considered the effects of the parameters referred to in the title, as their main influence is on the bond conditions through the joint. Most researchers have assessed the bond conditions by comparing an average bond demand with average bond strength. Hence, the influence

of the above parameters could be further distinguished according to the side of the equation which they influence, **Fig. 2.19**. The two terms of the equation are given by:

$$\text{Average Bond Demand} = \tau_{bad} = (F_1+F_2)/(\phi h_c) \quad (2.2)$$

$$\text{Average Bond Supply} = \tau_{bas} = f_{cb} \quad (2.3)$$

where the symbols have the following meaning:

F_1 and F_2 are the forces that act on the ends of the bar at the joint boundary.
ϕh_c is the bar surface along which the total force is transmitted to the concrete by bond stresses.
f_{cb} is the concrete bond strength.

In its simplest formulation, the total force acting on the bar is evaluated as $2f_yA_s$ which assumes that yielding occurs in compression on one side of the bar and in tension on the other side whereas the bond strength is simply assumed as a function of the square root of the concrete uniaxial compressive strength [Park and Paulay, 1975].

Given that, the condition $\tau_{bad} < \tau_{bas}$ results in an upper limit on the ratio of bar diameter to column depth, d/h_c.

The experimental research carried out by Park and Dai Ruitong [1988] can be interpreted as an attempt to a better definition of the bond demand. The two tested units differed only by the concrete strength, which were 36.0MPa in one units and 40.1MPa in the other one. Same steel Grade 275, same ratio of the bottom to top steel area equal to 0.51 and same ratio of bar diameter to column depth equal to 14.5 were assumed. Although the maximum value for the ratio d/h_c permitted by NZS 3101 was 1/25 for Grade 275 deformed bars, the performance of the two units was satisfactory. It was attributed to the ratio of bottom to top steel area. In fact, the total force acting on the bar was not $2\lambda_0 f_y A_{s,top}$, as assumed by the Code provision, but $\lambda_0 f_y(1+\beta)A_{s,top}$ with $\beta=A_{s,bot}/A_{s,top}<1$.

The experimental studies carried out by Leon [1988,1990a, 1990b] were addressed basically at giving recommendations on the allowable value of the bar diameter to column depth ratios. At this end four half scale beam column joints were tested which had identical beam sizes and beam reinforcement whereas only the column depths were varied. It was observed that a minimum anchorage of 24d was required for the beam to reach its ultimate strength and that 28d was necessary to insure that a weak girder-strong column mechanism could be maintained through a sever load history. Conversely, a large amount of shear cracking and spalling was observed in the joints with 16d and 20d, leading to a very rapid deterioration of the behaviour.

Aoyama, Otani and Kitayama [1988] introduced the bond index as measure of possibility of bond degradation along the beam reinforcement. It was defined as the ratio of the average bond stress to the square root of the concrete uniaxial compressive strength. The average bond stress was evaluated considering the simultaneous yielding of the beam reinforcement in tension and compression at the two faces of the joint. Hence,

$$\text{Bond Index} = BI = \frac{\tau_{bad}}{\sqrt{f'_c}} = \frac{2f_yA_s}{\Phi h_c\sqrt{f'_c}} = \frac{f_yd}{2h_c\sqrt{f'_c}} \quad (2.4)$$

In this way the effects of bar diameter, column depth, yield strength and concrete strength were not considered individually but globally by means of the above parameter. The assumption of $\tau_{b,d}=2\lambda_0 f_yA_s$ made loose the influence of the ratio of bottom to top reinforcement. By interpreting

experimental results on plane beam-column joints tested in Japan, they tried to establish a relationship between the bond index and the equivalent viscous damping ratio h_{eq} at a storey drift angle of 1/50, assumed as measure of the dissipative capacity of the joint. It was observed, as obvious was it, that h_{eq} values tended to decrease with an increasing bond index value. Hence, a limit on the value of the bond index was suggested as corresponding to a give limit on the value of h_{eq}, dictated by the supplied energy dissipation capacity of the structure. The nature of this condition implied that some deterioration was accepted within the joint, being not feasible to prevent it at all especially when plastic hinges were required to form adjacent to the column faces. The criteria to define the allowable bond deterioration was set accounting for the ensuing energy dissipation capacity of the joint which one meant to obtain.

Morita, Fujii, Murakani and Yamada [1992] performed comprehensive experimental parametric studies. A new test method was developed to reproduce the real pull-push condition of a beam bar in an interior beam column joint as in the available experimental studies was difficult to exclude the effects due to the other influencing factors from the total behaviour, **Fig. 2.20**. The test variables considered in this study were (1) concrete strength, f'_c, varied up to 120 MPa; (2) yield stress of bars, f'_y, up to 700 MPa; (3) bar diameter, d, up to 35mm; (4) column depth, h_c, and unit width, b, per beam bar and (5) column axial stress, $N/(h_c b)$. Fig. shows the local bond slip curves obtained at several locations within the joint region. It was observed that the condition for bond changed along the embedment length of the beam bar passing through the joint. The curves obtained within core concrete were different from that obtained at the neighbours of column faces i.e. at the cover concrete. The almost equal magnitude of local bond stress in both directions was observed within the core concrete, while in the cover concrete the low bond stress was developed in the outward direction and the extremely high bond stress were obtained in the inward direction. This characteristic performance in bond was explained as the result of crack opening and closing mechanism in the joint. **Fig. 2.21** reports the envelope of τ-s curves observed in the core region and they are grouped into three to show the influence of each main variable. It was recognised that the increase in concrete strength or column axial force gave higher local bond strength and higher rigidity of τ-s curves. **Fig. 2.21** shows that the local bond strength was increased with the increase of specimen width versus beam bar diameter ratio and that column depth was not a decisive factor for the local bond strength. By means of regression analysis of their test results, the following equation was proposed for the local average bond strength, τ_{bas}, as function of the above design variables:

$$\tau_{bas} = 2.2(0.86 + 0.84\frac{N}{bh_c f'_c})\frac{b}{d}(\frac{f'_c}{35}) \qquad \text{[MPa]} \qquad (2.5)$$

Also, to express the severity of the bond conditions they introduced the bond index defined as the ratio of the average bond stress demand, τ_{bad}, and the average bond stress supply, τ_{bas}, hence $BI=\tau_{bad}/\tau_{bas}$. In the above expression τ_{bas} was given by equation (1) whereas τ_{bad} was simply evaluated as the average bond stress required for beam bar to develop tensile yielding at the front face and compressive yielding at the far face of an interior column, thus $\tau_{bad} = 2f_y A_s/(\phi h_c)$.

For sake of completeness, it is of interest to compare the functional structure of τ_{bas} with the one obtained on the basis of the analytical model by Tassios [Penelis and Kappos, 1997] and included in EC8. The expression of τ_{bas} has been rearranged by the writer as:

$$\tau_{bas} = \frac{1}{4}(7.5 + 8.5\mu_f \frac{b_c}{b_w} \frac{N}{b_c h_c f'_c})f_{ctm} \qquad (2.6)$$

Furthermore, the analytical model of Tassios gives also a much more detailed expression for the average bond stress demand given by

$$\tau_{bad} = \frac{T_1 + C_2}{\Phi h_c} = \frac{\lambda_{Rd} f_y A_{s1} + \lambda_{Rd} f_y A_{s2} \frac{q}{q_{max}} \frac{\rho_1}{\rho_{max}}}{\pi d_1 h_c} = \lambda_{Rd} f_y \frac{d_1}{4h_c} (1 + \frac{q}{q_{max}} \frac{\rho_2}{\rho_{max}}) \quad (2.7)$$

In this way the ratio demand/supply includes all the important parameters which influence the bond conditions.

2.7 Conflicting Response Mechanisms

In this section a qualitative interpretation of the influence of axial column load and hoop reinforcement on the joint shear strength capacity is given. It is assumed that the joint experiences a pure shear failure of the panel zone whereas good bond conditions are sustained. This can be the case simulated experimentally by Fujii and Morita [1991], Algabian et al. [1994] and Higazy et al. [1996]. The first researchers concluded that column axial load did not influence the joint shear strength capacity whereas the second ones did. Before proceeding further, a fundamental result on the concrete behaviour needs to account for. This is referred to as softened concrete principal compressive strength [Vecchio and Collins, 1981; Vecchio and Collins, 1986]. In presence of biaxial stress state with tension and compression, the concrete compressive strength is lower than the uniaxial compressive strength and the reduction, expressed by the softening coefficient ζ, has been assumed as dependent on the tensile strain, ε_1, in the orthogonal direction. Vecchio and Collins [1986], for example, proposed the following relationship for the concrete principal compressive stress, σ_{c2}, which is softened in stress only [Hsu, 1993]:

$$\sigma_{c2} = \zeta \sigma'_c [2(\frac{\varepsilon_2}{\varepsilon'_c}) - (\frac{\varepsilon_2}{\varepsilon'_c})^2] \quad (2.8)$$

where

$$\zeta = \frac{\sigma_{c2max}}{\sigma'_c} = \frac{1}{0.8 - 0.34 \frac{\varepsilon_1}{\varepsilon'_c}} \quad (2.9)$$

ε'_c is the compressive strain where the stress σ_{c2} takes its peak value and is assumed equal to the uniaxial value.

Fig. 2.22 depicts the stress-strain relationship for cracked concrete in compression and the variation of the softening coefficient with the tensile strain. It is remarkable to note the strong effect of the principal tensile strain on the softening coefficient, ζ.

In the following, two identical specimens, specimen 1 and specimen 2, but with different level of axial force, N_1 and N_2 are considered. Let be $N_1 < N_2$, and σ_1 and σ_2 the corresponding average normal stresses whereas τ is the applied average shear stress.

If both specimens experience a shear failure detected by concrete crushing while hoops still remain elastic then it is expected that as τ increases the failure is detected first by the specimen 2 due to the

higher level of compressive stresses present in the specimen. However, with the usual amount of joint shear reinforcement provided, the previous failure mode is difficult to occur. Therefore, in the following will be considered the case where the joint shear failure is detected by first yielding of the hoops and then concrete crushing or reduction of the concrete strength to a given value.

Let $\tau_{cr,i}$, with i=1,2, be the average cracking shear stress. It would be better if τ_{cr} is used to denote the value of the average shear stress such that as $\tau > \tau_{cr}$ the tensile strain in the hoops, ε_t, starts to increase meaningfully. For example τ_{cr} can be the value of the average shear stress so as to have a crack crossing the stirrup. If $\sigma_1 < \sigma_2$ then is $\tau_{cr,1}<\tau_{cr,2}$ [Jirsa et al., 1981; Yunfei et al. 1984; Higazy et al., 1996].

The diagram depicted in **Fig. 2.23a** might be assumed to represent qualitatively the variation of the hoop tensile strain, ε_t, with the applied average shear stress τ for the two specimens. Up to $\tau_{cr,1}$ the strains in the hoops of the two specimens are practically equal [Kitayama, Otani and Aoyama, 1988, 1991]. When $\tau_{cr,1}<\tau<\tau_{cr,2}$ a higher increase of strains in the stirrups of the specimen 1 than those in the specimen 2 is expected. In drawing this diagram it has been assumed that the yield strain is attained in the stirrups of the specimen 1 for a value $\tau_{1,y}$ which is less than $\tau_{cr,2}$. As a result, the tensile strain in the stirrups of the specimen 1 increases further on before getting to $\tau_{cr,2}$.

Say $\sigma_{c,1}=\sigma_{c,1}(\sigma_1,\tau)$ and $\sigma_{c,2}=\sigma_{c,2}(\sigma_2,\tau)$ the principal compressive stresses in the specimens 1 and 2, respectively. For the given τ, if is $N_1<N_2$ then is $\sigma_{c,1} < \sigma_{c,2}$, **Fig. 2.23b** . Further, let $\varepsilon_{t,i}$ be the tensile principal strain present in the specimen i and $\sigma_{cu,i}$ the effective compressive strength of the specimen i which is a function of $\varepsilon_{t,i}$.

In **Fig. 2.23a** is $\varepsilon_{t,2}<\varepsilon_{t,1}$, consequently is $\sigma_{cu,1}< \sigma_{cu,2}$.

It is assumed that the failure condition for the specimen *i* is attained when $\sigma_{c,i}$ is equal to $\sigma_{cu,i}$. Hence, as the shear stress τ increases is not possible to say a priori which is the specimen to meet first the failure condition. If as τ increases, is first $\sigma_{c,1}=\sigma_{cu,1}$ then this is a case where $N_1<N_2$ and $V_1<V_2$. The shear strength is increased as the axial force is increased. If as τ increases, is first $\sigma_{c,2}=\sigma_{cu,2}$ then this is a case where $N_1<N_2$ and $V_2<V_1$. The shear strength is increased as the axial force is decreased. The occurrence of a case rather than the other one can be related to the occurrence of $V_{1,y}$ before or after $V_{cr,2}$ which in turn can be assumed dependent on the reinforcement ratio.

The above considerations rely on the assumption that the influence of hoop ratio and axial load play in a different way according to their influence on the hoop tensile strain, which is assumed to influence the compressive constitutive law [Stevens, Uzumeri, Collins and Will, 1991a; Stevens, Uzumeri and Collins, 1991b]. If this effect is not taken into account, once the hoops start yielding, no influence of hoop strain on the concrete strength is observed, hence an overestimation of the shear strength is obtained and apparent contradictions of experimental results cannot be explained.

2.8 Concluding Remarks

The experiments reported in literature have revealed that the joint response to cyclic loads is influenced by hoop reinforcement and steel characteristics, axial column load, concrete strength and ratio of top to bottom steel area bars. The available experimental knowledge, however, has not always been capable of clarifying the influence of each of the above design variables on the

possible joint failure modes because of the variety of objectives which each experimental program intended to pursue. Tests could be seen either as an attempt to cause failure in the joint so that its full behaviour would be observed, or as proof that certain joint design met a stated objective, such as sustaining beam hinging. Furthermore, the conclusions drawn from the experimental tests should be related to the preferences given in the design approaches. For example, to suggest by experiment that transverse reinforcement is more important for confinement than for resisting shear, it would only be necessary to test a specimen with excessive demand for bond through the joint. But even when the objective of the experimental investigation seemed to pursue the same objective, such as in the tests carried out by Fujii et al. [1991], Algabian et al. [1994] and Higazy et al. [1996] that enforced a pure shear failure of the panel zone, different type of influence of the design variables on strength capacity was observed. On the other hand, conclusions of this type from comparing different experimental investigations, without making clear the way by which the imposed shear failure is detected are too simplistic and misleading. Similar situation occurs, for example, even in a flexural failure where the tensile reinforcement ratio plays a different role on the flexural strength depending on what the flexural failure is detected. Furthermore, it is not always feasible to expect to describe the joint behaviour by means of physical models. The definition of a physical model would require a huge database and, consequently, appropriate definition of characteristic indices to enter it and characteristic indices to describe the joint response, and even more the necessity to consider the type of loading.

By relying on general accepted aspects of concrete behaviour it has been shown how some experimental results can be interpreted adopting the usual tools of the continuum mechanics. An important role has been seen to play by the hoop strain conditions in relation with the deterioration of the concrete compressive strength as a function of the coexisting principal tensile strain. This deterioration becomes especially significant to the joint behaviour under reversed cyclic shear because, if cycling is done at levels causing repeated yielding of the steel, then the principal tensile strain will continue to increase with each cycle. This means that the concrete compressive strength will decrease with each cycle until eventually failure occurs by concrete crushing. Therefore, enough cyclic of shear stress at any level above yield will cause failure of the joint [Stevens, Uzumeri and Collins, 1991b].

All the above considerations indicate clearly that the future research effort should aim at a better understanding of the joint inner working and carry out experimental investigation for this end rather than as attempt to validate or justify code recommendations.

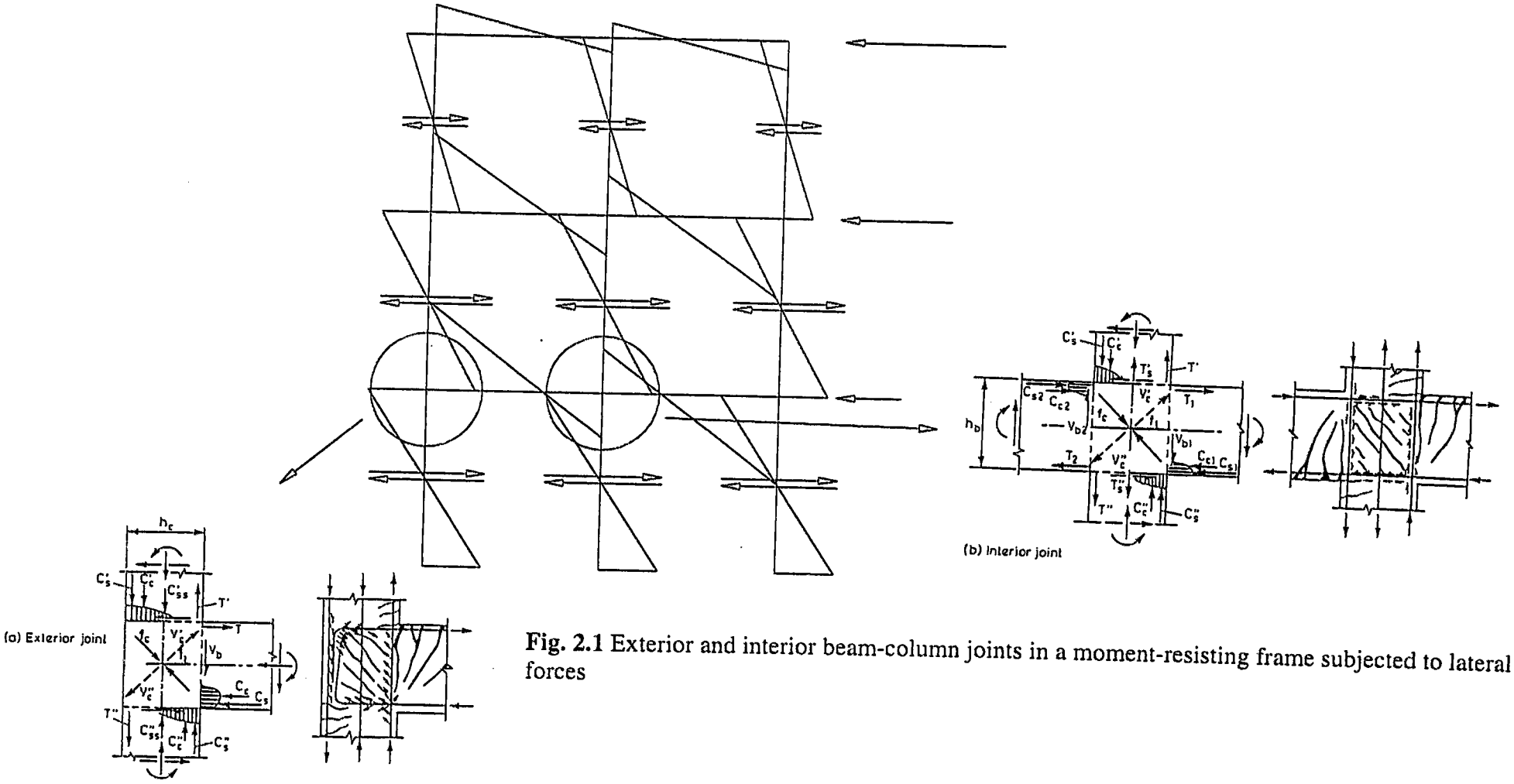

Fig. 2.1 Exterior and interior beam-column joints in a moment-resisting frame subjected to lateral forces

Fig. 2.2 Diagonal tension failure of a beam-column joint during an experimental test

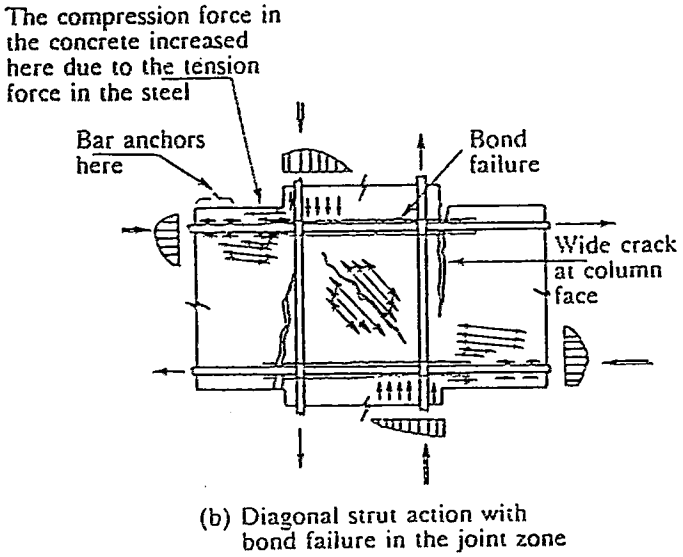

(b) Diagonal strut action with bond failure in the joint zone

Fig. 2.3 Resisting mechanisms within the joint upon bond failure of beam bar reinforcement

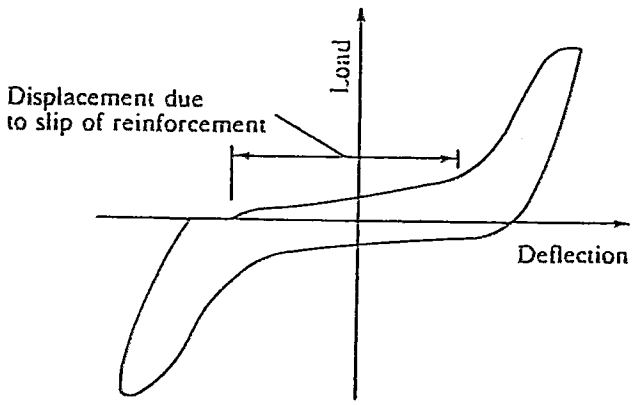

Fig. 2.4 Load deflection diagram for joint zone after bond failure of beam reinforcement

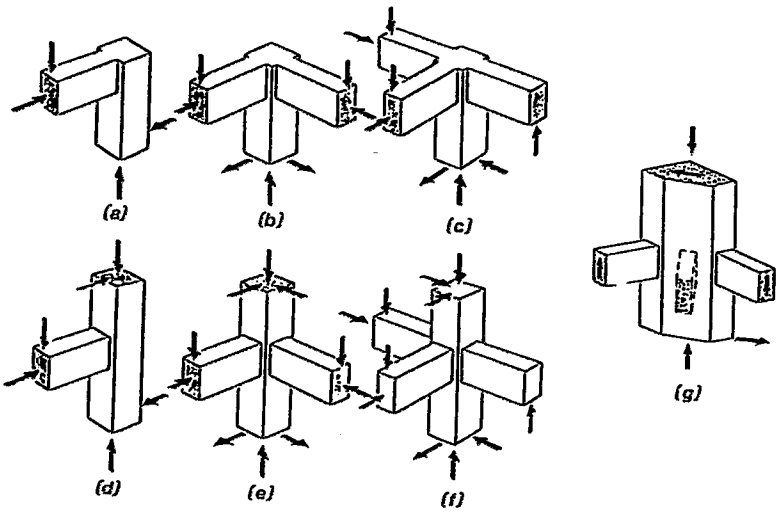

Exterior beam–column joints.

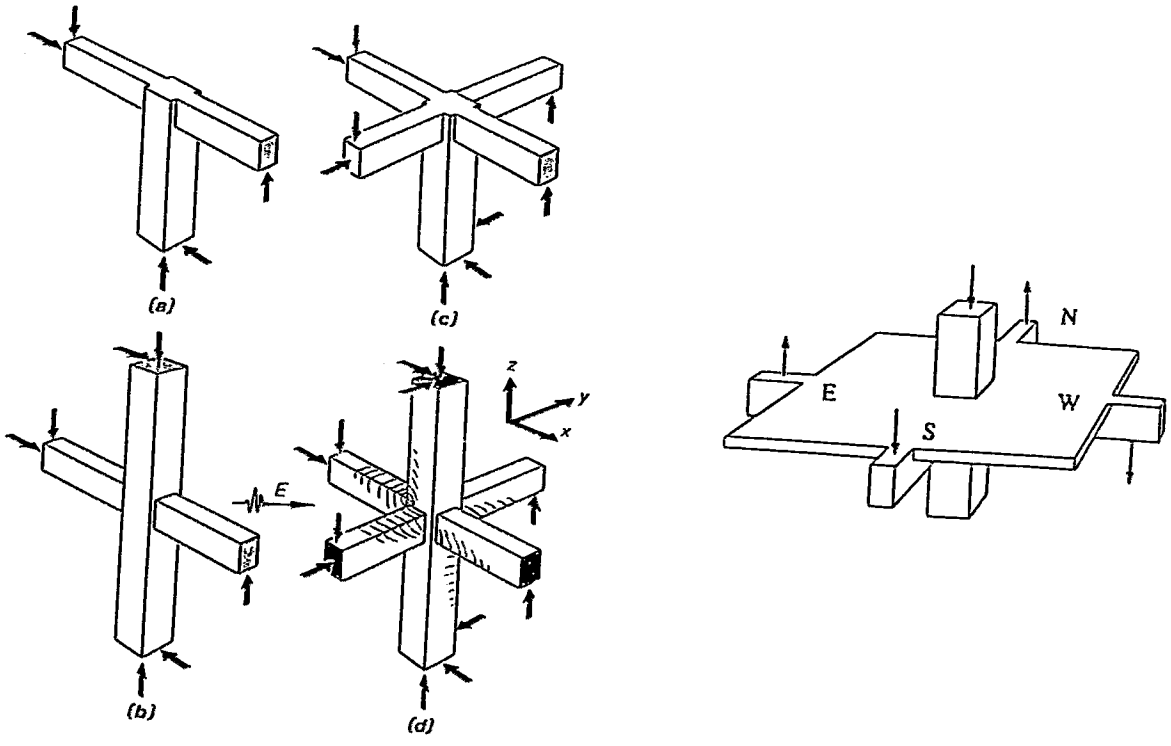

Interior beam–column joints.

Fig. 2.5 Possible beam-column joint configurations in a typical 3-D framed structure

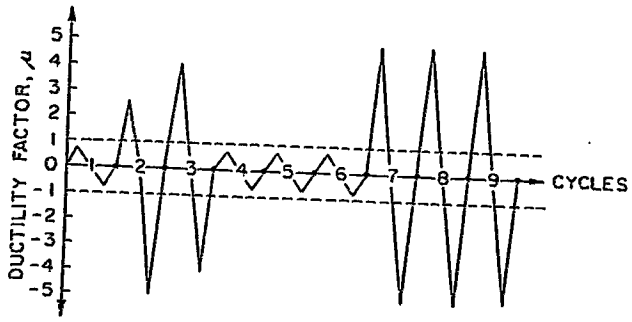

Fig. 2.6 Earthquake representation in the experimental tests carried out by Hanson et al, 1967. The loading cycles represent the effect of two major earthquakes

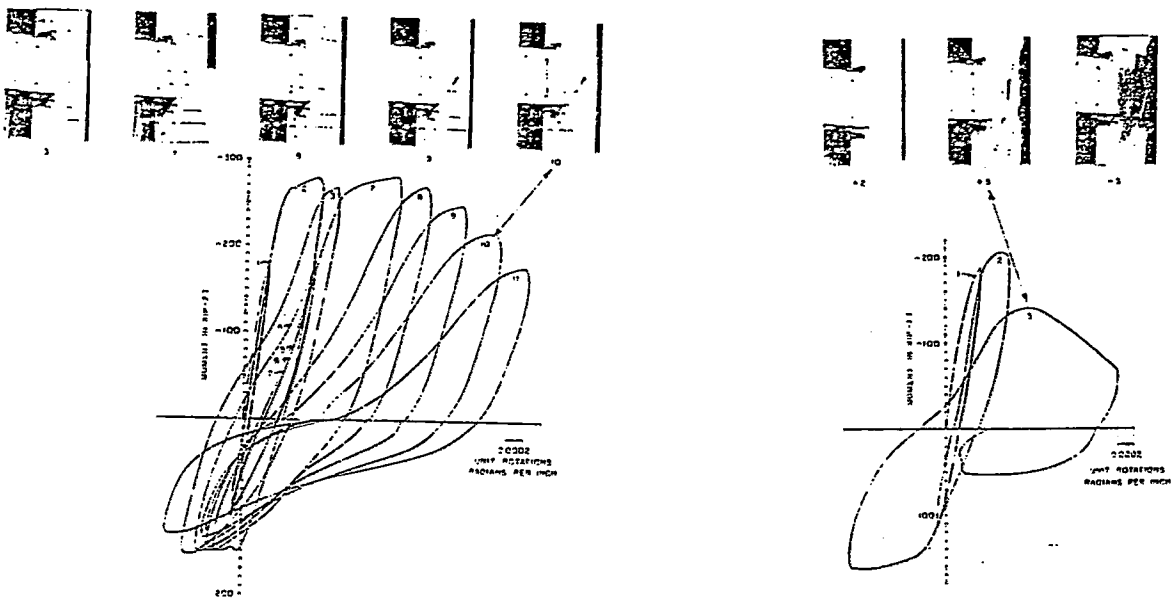

Fig. 2.7 Moment-rotation curves. The specimens on the left has joint reinforcement whereas the specimen on the right have no shear reinforcement within the joint

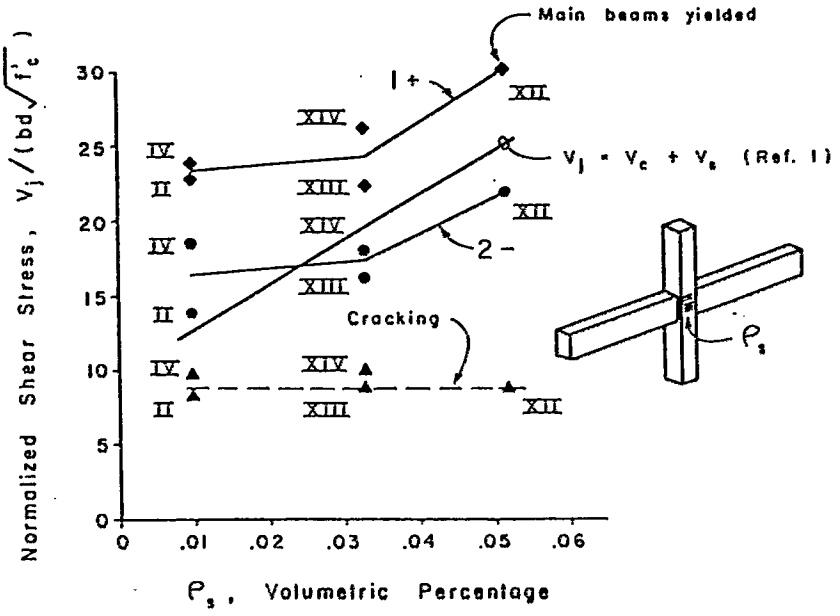

Fig. 2.8 Effect of joint reinforcement, Meinheit et al.

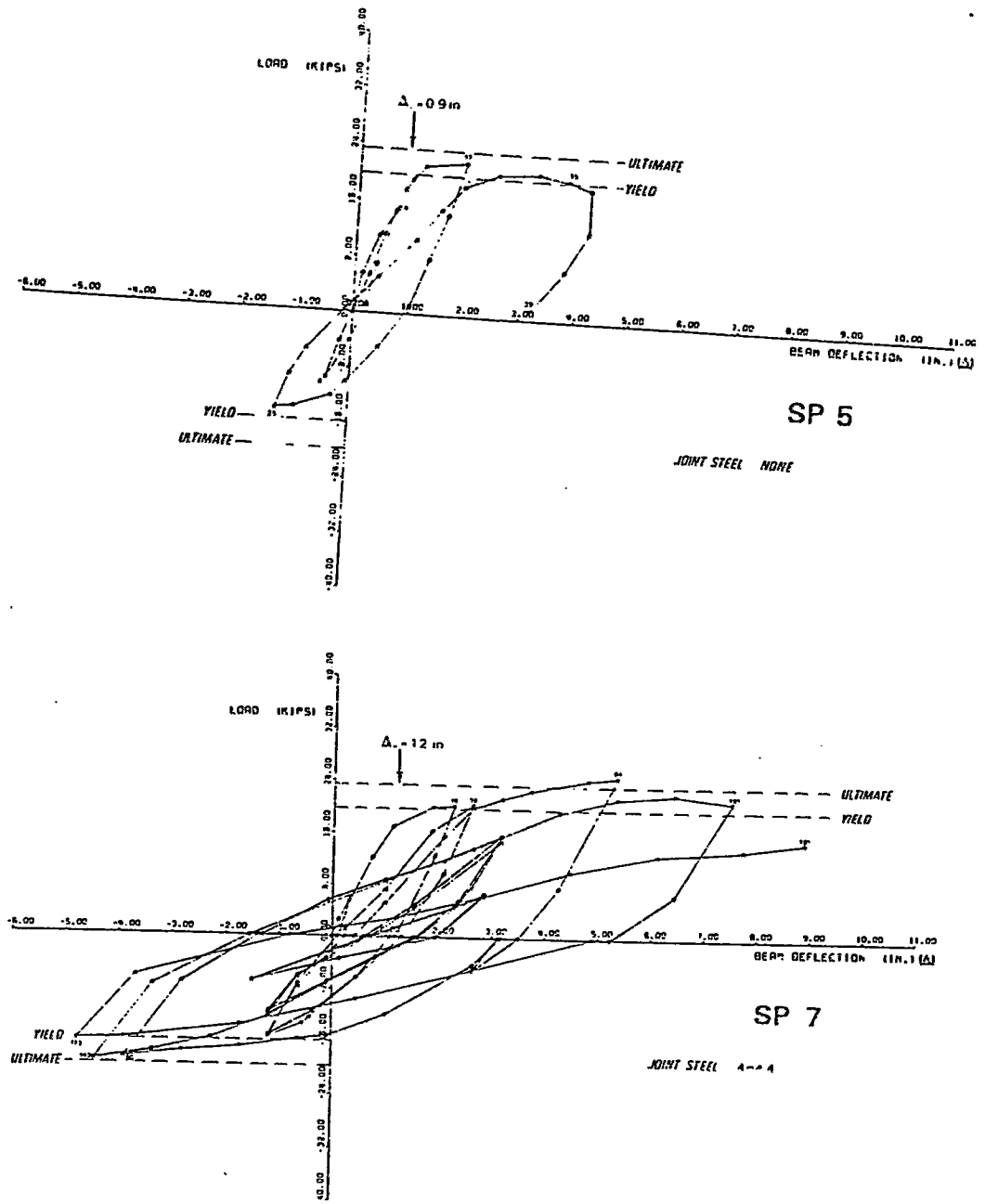

Fig. 2.9 Beam tip load versus beam tip deflection; specimen 5 has no shear joint reinforcement whereas specimen 7 has been reinforced with 4#4 closed hoops spaced at 3.0 inches apart

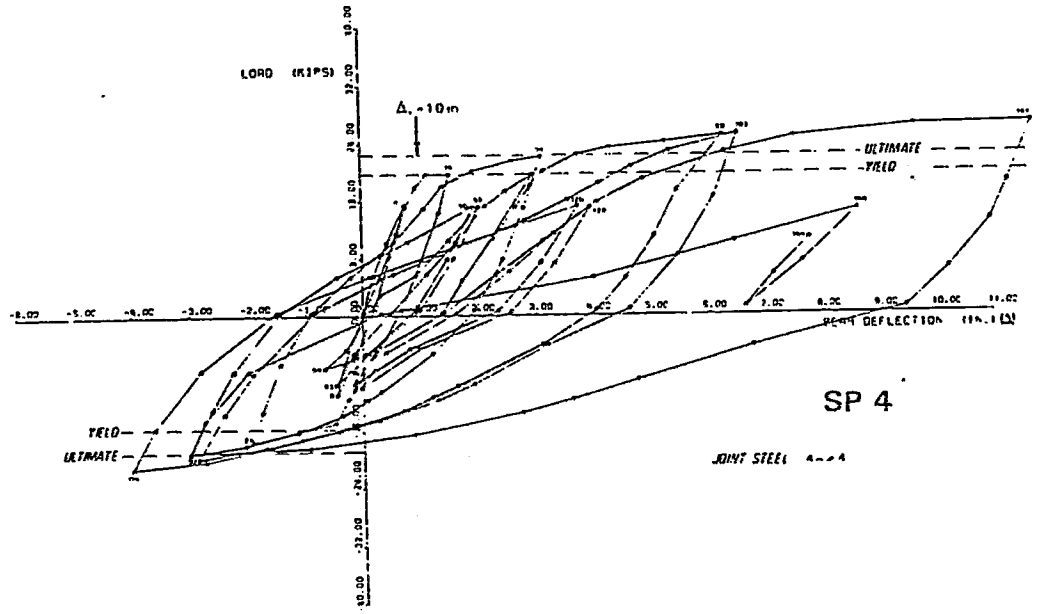

Fig. 2.10 Joint steel in the specimen 4 does not exhibit a flat yield plateau as opposed to the joint steel in the specimen 7

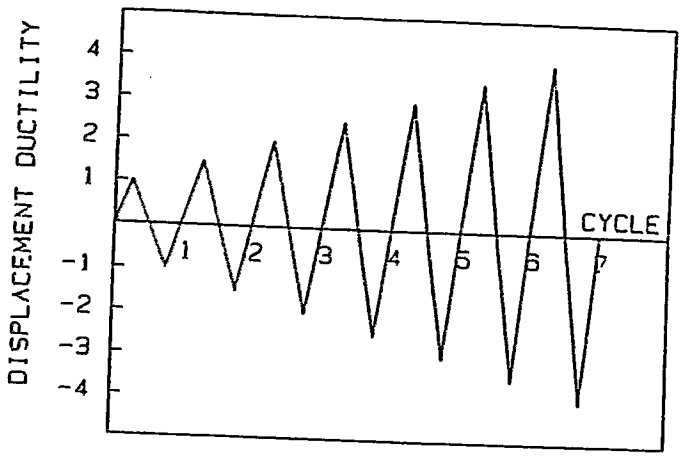

Fig. 2.11 Quasi-static loading assumed in the experimental tests carried out by Durrani et al., 1985

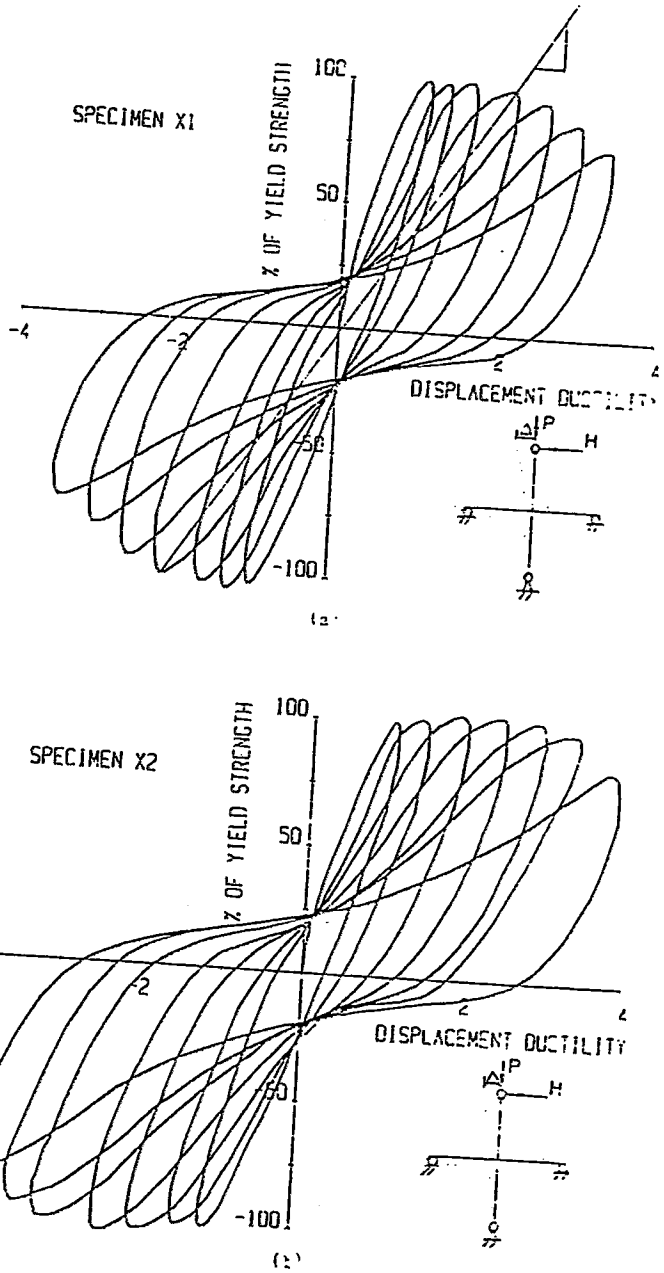

Fig. 2.12 Lateral force-displacement curves for specimen X1 and X2 with different ratio of joint reinforcement

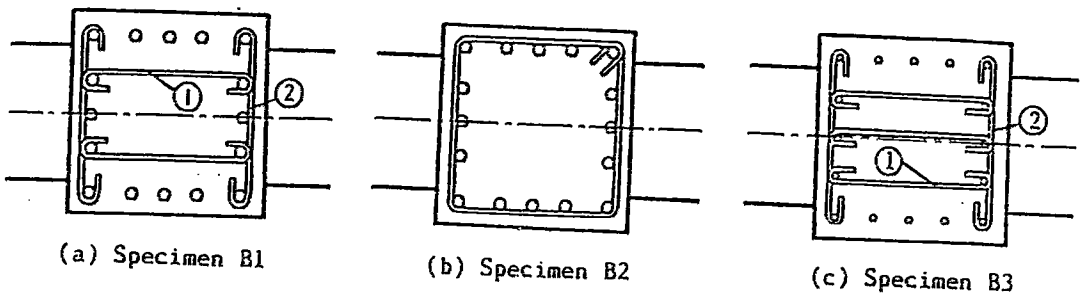

Fig. 2.13 Detail in joint lateral reinforcement

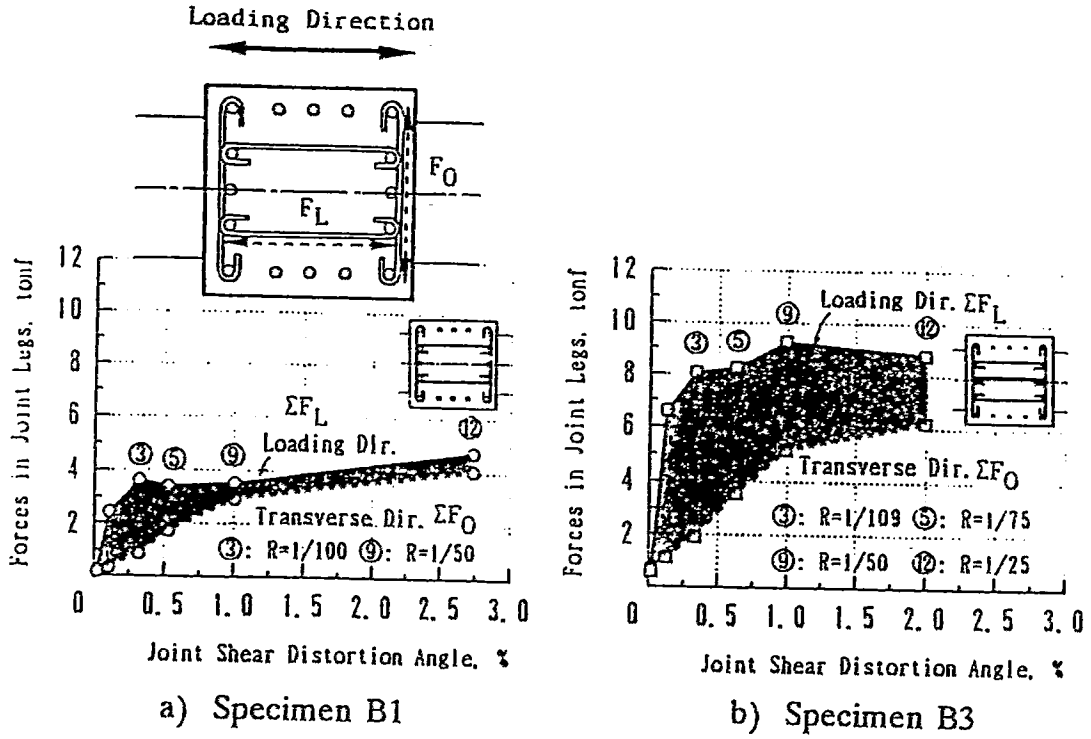

Fig. 2.14 Total tensile forces in joint ties

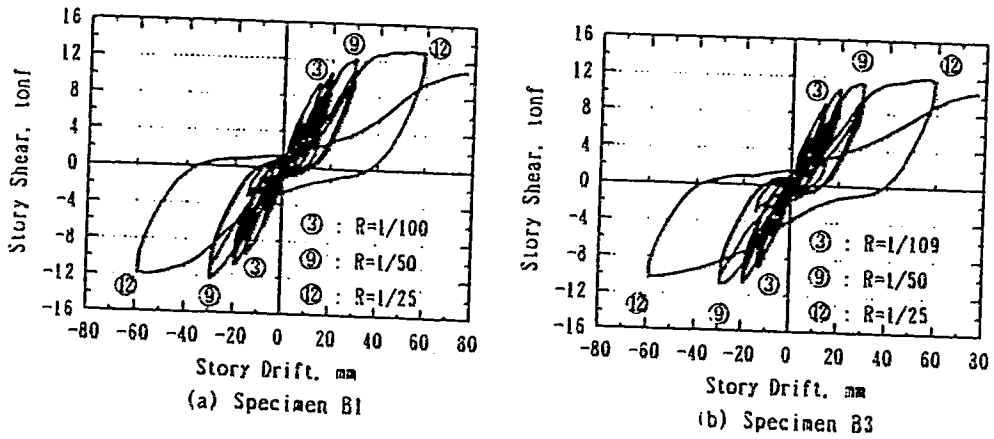

Fig. 2.15 Story shear – story drift relations

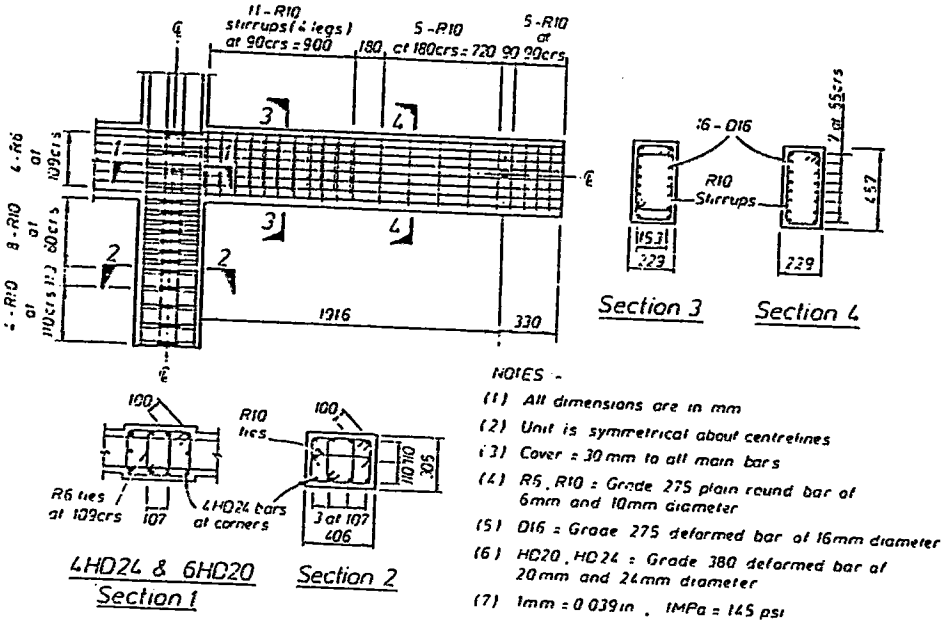

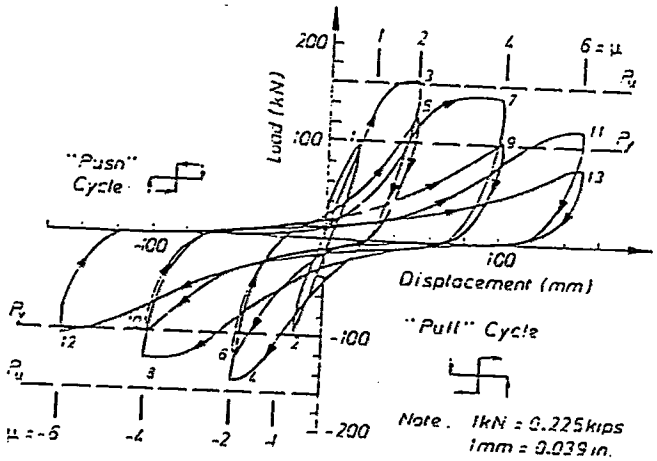

Fig. 2.16 Measured hysteresis loops for horizontal load vs. displacement at top of column

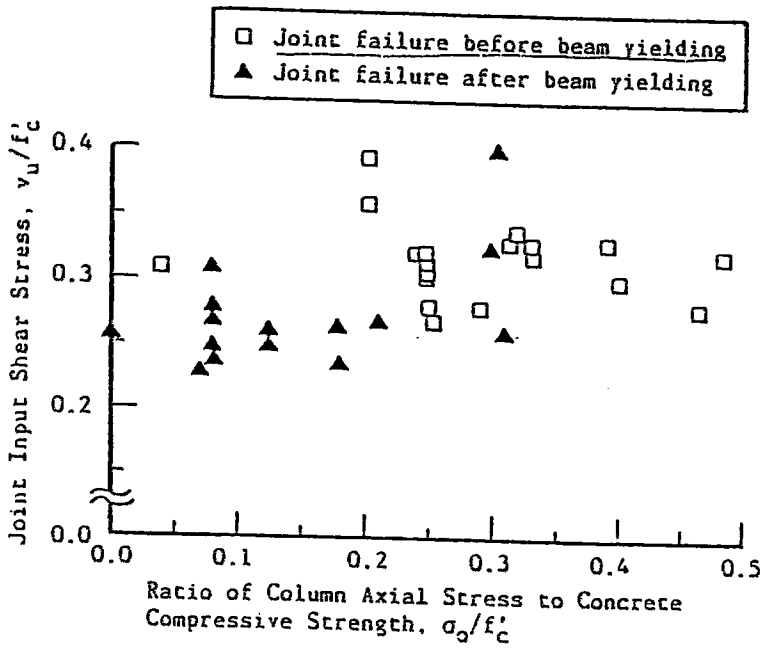

Fig. 2.17 Effect of column axial load on joint shear strength

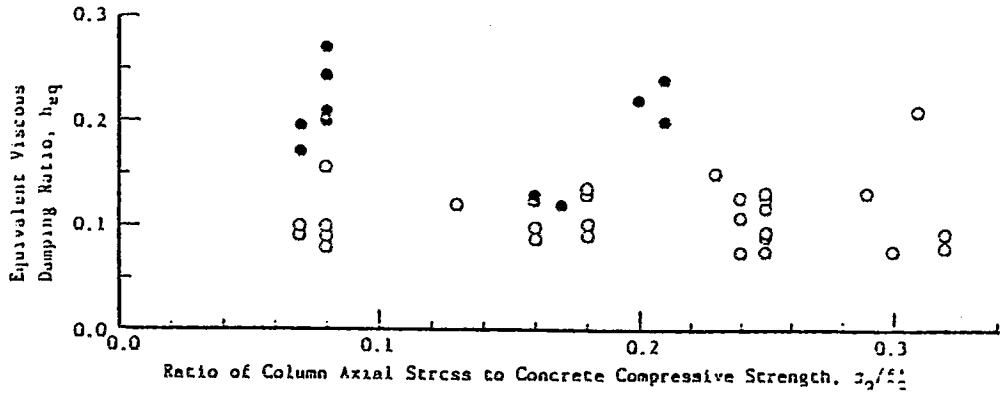

Fig. 2.18 Effect of column axial load on beam reinforcement bond condition

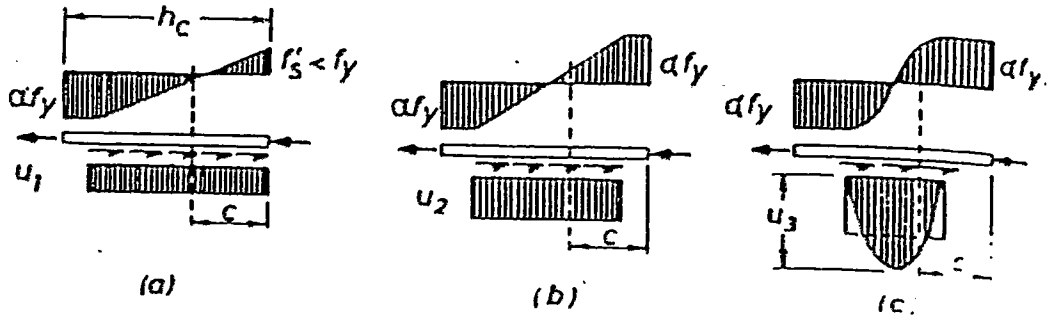

Fig. 2.19 Probable steel and bond stress distributions in joint core

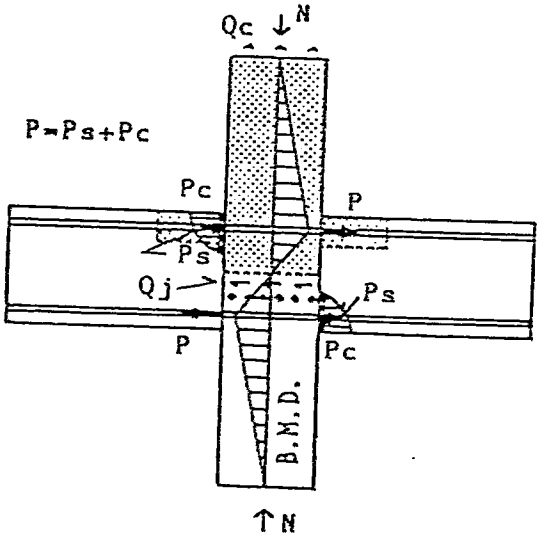

Fig. 2.20 Novel test method for bond in beam column joint

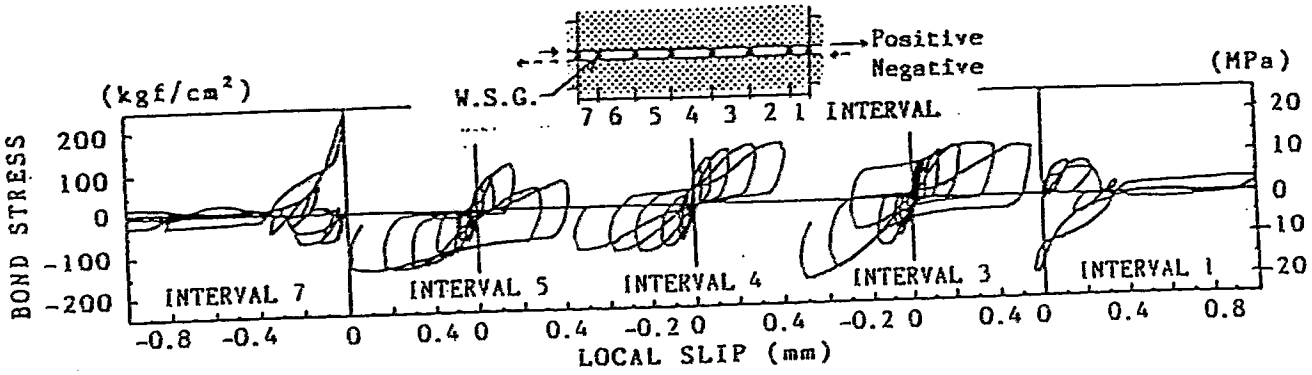

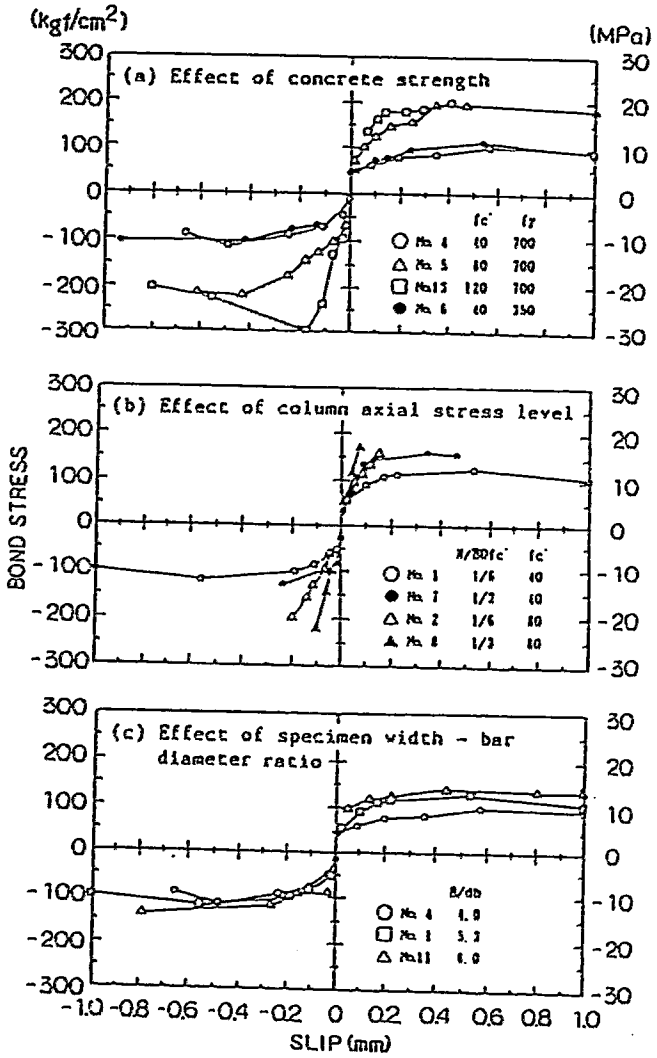

Fig. 2.21 Envelope of local bond stress - slip curves in core region

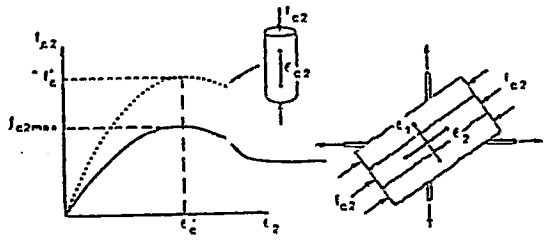

(a) Stress-Strain Relationship for Cracked Concrete in Compression

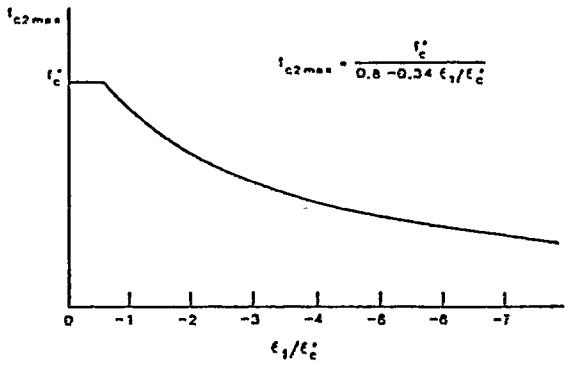

(b) Proposed Relationship for Maximum Compressive Stress

Fig. 2.22 Collins – Vecchio concrete constitutive model

hoop tensile strain

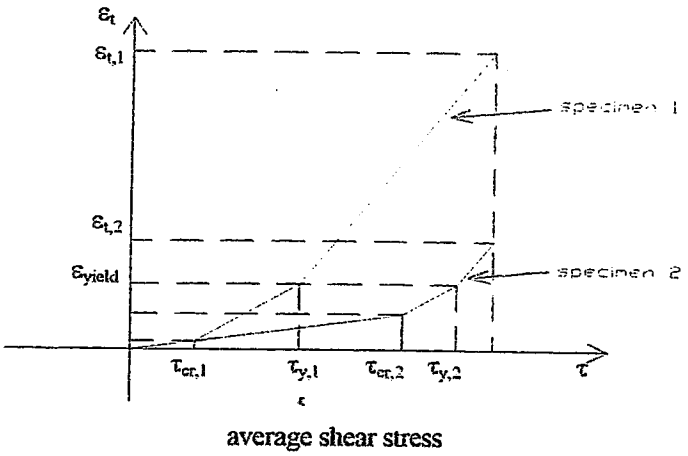

average shear stress

Fig. 2.23a Variation of the hoop tensile strain with the average shear stress

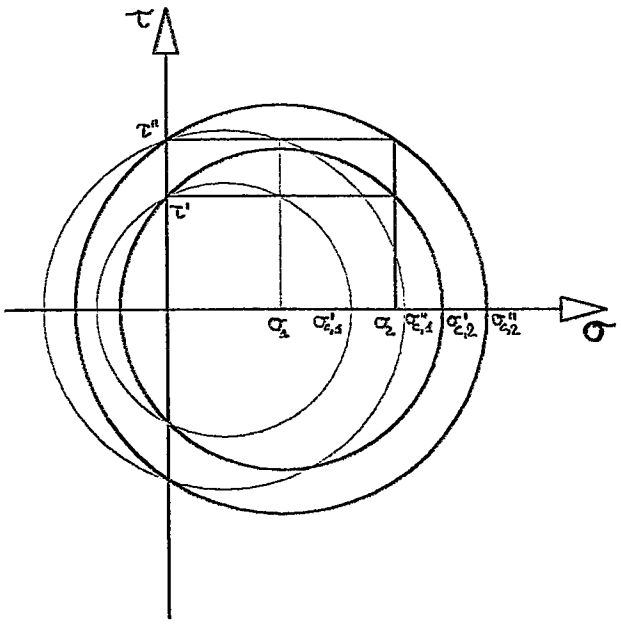

Fig. 2.23b Mohr's circle for stress

CHAPTER 3

ANALYTICAL MODELS

3.1 Introduction

In conventional analysis and design of reinforced concrete frames, beam-column connections are assumed to behave as rigid. Although the above assumption simplifies significantly analysis and design procedures, in practice the predicted frame response may not be realistic. Experimental investigations and on situ observation show that the joint has its own deformability and strength characteristics. The sources of flexibility present in the connection, due to shear deformation and reinforcing bar slippage, can contribute up to 50% to overall deflections of beam-column subassemblages after yielding of the reinforcement [Solemani, Popov and Bertero, 1979]. On the other hand, the loss of joint shear capacity can be detrimental for the overall stability of the structure, and bond deterioration can jeopardise the attainment of hysteretic stable cycles in the adjacent critical regions which are meant to dissipate the seismic energy input.

Experimental hysteretic loops of subassemblages generally show the characteristic pinched shape during reloading. This aspect is especially characteristic of force-deformation relationship of subassemblages where shear cracking and bond slippage are involved. The dissipation of energy is reduced as much of the deformation occurs with small forces before the cracked surfaces come in full contact, **Fig. 3.1**. Hence, an accurate joint model must be capable of describing these features if consideration of the actual energy dissipation mechanism along with strength and stiffness deterioration in a reinforced concrete structure under earthquake loading is sought.

Several attempts to derive hysteretic joint models to account explicitly for the contribution of the joint behaviour to the non-linear earthquake response of reinforced concrete structures have been reported. The available analytical models may be classified according to their theoretical basis into the following categories:

- Global Models
- Finite Element Beam-Column Models

As the connection in the steel structures, the global models describe the joint hysteretic behaviour by means of a moment-rotation and/or force-displacement relationship. These functions can be obtained either by fitting mathematical expressions to experimentally obtained data for full or reduced scale beam-column joints subjected to cyclic excitations or by predefined hysteretic models which are typically characterised by control parameters that have to be calibrated from observed experimental testing. According to the mechanical models used to idealize the single members of a frame system, the above relationships may be assigned to concentrated springs located at the ends of the member or to components which the member is assumed to be made up.

Finally, modelling by finite element allows quite satisfactory simulation of test results for many different situations and may simulate all the source of flexibility present in the joint. Given the large size of the problem in terms of degree of freedom and the complexity of the models required to carry out the analysis, its use is usually conceived to clarify the basic joint response mechanisms and to derive from these studies simplified models for more common design applications.

3.1 Global Models

The development of these models to describe the effect of the joint behaviour must be related to the type of idealisation adopted for reinforced concrete members. Hysteretic models are used to describe the hysteretic characteristics of reinforced concrete elements. These models are then assigned to mechanical member models which simulate member response. According to the member modelling and how the non-linear behaviour is taken into account, the level of accuracy varies.

To describe the behaviour of reinforced concrete joints phenomenological models of hysteretic behaviour are typically used. Such models can be obtained either by fitting them to experimental data or by considering predefined functions which simulate the degradation and deterioration aspects of the mechanisms governing the joint response. The predefined hysteretic models range from the simple bilinear model (elastic-perfectly plastic model), **Fig. 3.2a**, through the Clough degrading stiffness model, **Fig. 3.2b**, to the most complex, such as the Takeda model, **Fig. 3.2c**. Consequently, even the number of parameters needed to describe the hysteretic behaviour increases as the complexity of the model increases. Furthermore, the parameters are typically established from a limited set of experimental data.

The basic features of the hysteretic curves are reported by Sozen [1974], whilst Otani [1980] summarizes the curve shapes on the basis of those pertinent to flexural characteristics, shear characteristics, and bar slip and bond deterioration. A critical and detail discussion of the several hysteretic models can be found in Cosenza and Manfredi [1994].

The simplest way to model structural members in a reinforced concrete frame is to idealise each member as a linearly elastic element with one equivalent non-linear rotational spring attached at each end, **Fig. 3.3**. All the inelastic deformations of the member and adjacent joints may be lumped into the rotations at these two inelastic end springs, or point plastic hinges. This model is referred to as single-component single-spring model and its first introduction is attributed to Giberson [1967]. The moment rotation loading history of the two non-linear rotational springs are specified by hysteretic models, as said previously.

The multicomponent member model, **Fig. 3.4**, represents another approach to the member modelling. In its simplest application the element is divided into two imaginary subelements which are connected at their ends so that the two elements have the same member end deformation. Each of the subelements is then described by a different constitutive relationship to take into account the contribution of the different mechanisms on the response of the member.

In the following, is reported how the effects of the joint behaviour have been taken into account in the different member modelling.

The single component member model can have more than one spring at each end, where each spring represents separate deformation component. **Fig. 3.5** illustrates the single component member model with two rotational springs in series adopted by Solemani, Popov and Bertero [1979]. One spring was meant to simulate the contribution of the fixed-end rotations due to the bond deterioration in the joint whereas the other one described the spread of non-linear flexural curvature along the end regions of the beam. For both the springs the moment-rotation relationship was assumed to follow the stiffness degrading bilinear Clough hysteretic rule, **Fig. 3.2b**.

Townsend and Hanson [1973] proposed a set of quadratic equations which fit experimental data from testing of twenty-two beam-column connections. The hysteresis loops were expressed in terms of the parameters which were considered to be the most important in describing the non-linear behaviour, such as displacement level, column axial loads and number of inelastic cycles of displacement, **Fig. 3.6**.

Banon, Biggs and Irvine [1981] also considered a single-component member multi-spring model. At each end of member three springs acting in series and independently were placed, **Fig. 3.7a**. These springs were meant to simulate the inelastic flexural deformation and shear deformation within the length of the member and the slippage of the main longitudinal reinforcement at the joint interface. The flexural deformations at each hinge were assumed to follow a modified version of the Takeda model. After having observed that the mechanisms of energy dissipation were the same for shear and slippage, the same hysteretic model defined by a set of seven rules was proposed to describe both the inelastic shear deformations and the effects of bar slippage, **Fig. 3.7b**.

In the multicomponent member model proposed by Otani [1974] each frame member was considered to consist of two parallel flexible linear elements (linearly elastic and inelastic), two inelastic rotational springs at the ends of the flexible linear elements, and two rigid linear elements outside of the rotational springs, **Fig. 3.8a**. Once the flexibility characteristics for the four constituent elements of a member were given, the overall member stiffness could be determined. The presence of the springs allowed the bond deterioration mechanism within the joint core to be simulated. Owing to the lack of knowledge about bond deterioration in the joint core upon load reversals, the Author assumed a simplified Takeda model to describe the moment-rotation relationship of the springs, **Fig. 3.8b**.

Reviewing the results of four sets of beam-column connection tests, Anderson and Townsend [1977] recognised the importance of an improved hysteretic model to describe the inelastic behaviour at the ends of the members. At this purpose, adopting the dual component member model for the member modelling, **Fig. 3.4**, the Authors discussed the effect of four different hysteretic models on the dynamic response of reinforced concrete frames. The adopted models were a bilinear elastic-plastic strain hardening model, a degrading bilinear model with equal unloading and reloading stiffness, a degrading trilinear model with different stiffness for unloading and reloading (DTL) and the degrading trilinear connection model (DTLC), introduced by the same Authors, **Fig.3.9**. In DTLC model, the behaviour of the joint was explicitly taken into account. In fact, the inelastic subelement was subdivided in three parts. The central part was described by the DTL model previously mentioned whereas the two small end elements were described by a DTL model, as well, but with a reduction of the initial loading branch stiffness and subsequent unloading branch stiffness. In this way, the loss of stiffness produced by concrete cracking in the beam and joints rotations generated by bond failure around the longitudinal beam steel were modelled and pinched effect in the force-displacement diagram was simulated. The results of their numerical analysis showed that the DTLC model was the most promising one as the reduction of stiffness occurred in the short elements which were representative of the connection test specimens.

In the above studies global moment fixed-end rotation relations were given to describe the joint behaviour. Such relations were defined by a set of rules matching a particular set of experimental results. Furthermore, the behaviour of the joint was modelled by assigning a moment-rotation relationship on each face of the joint with no interaction between the two joint end sections. Owing to the experimentally observed slip-through of reinforcing bars in interior joints, no unique moment relationship could be derived for one end, unless the actions at the other end of the joint are accounted for. Starting from this observation, Filippou, Popov and Bertero [1983] proposed an analytical model which accounted for the cyclic bond deterioration along anchored bars and the associated relative slippage between bars and surrounding concrete. The model was obtained considering the local behaviour at discrete points along the reinforcing bar as governed by equilibrium, geometry and constitutive models for cyclic bond and steel behaviour. By integrating the response of top and bottom reinforcing layers the moment fixed-end rotation relation at the joint end sections was established, **Fig. 3.10**. The model seems to have all the characteristics of a predictive model. It defines the cyclic joint behaviour only on the basis of the geometry, material properties and reinforcement layout of the connection but it does not take into account the influence of the joint shear reinforcement on the bond deterioration. As the model is eventually the result of the solution of the set of differential equations governing the response of a bar under generalised excitation with a given bond stress-slip relationship, the variables which influence the joint hysteretic model are the same that influence the adopted bond stress-slip relation. Furthermore, the geometric quantities present in the model stem from the integration over each side of the joint to determine the applied moments. In the model the influence of the deterioration due to shear of the panel zone is not taken into account, as well.

Filippou and Issa [1990] gave an example of application of the previous model within the framework of an inelastic analysis of reinforced concrete frames. Adopting an approach similar to the model proposed by Otani [1974], each frame member was decomposed into several subelements as shown in **Fig. 3.11**. Such subelements were meant to model the different sources of flexibility. At this end, the Authors distinguished the following elements: an elastic beam subelement to represent the behaviour of the member before yielding of the reinforcement; a plastic subelement with plastic hinges at the ends to represent the behaviour of the element in the post yielding range; a joint subelement to account for the fixed-end rotation at the beam-column interface and finally, a shear subelement to account for the shear distorsion in the critical regions of the member and the shear sliding at the beam-column connection. The joint subelement consisted of a rotational spring and its moment-rotation relationship was derived using the above model.

3.3 Finite Element Beam-Column Models

Representation of the connection behaviour by finite elements can produce useful information on the two basic mechanisms, shear and bond, which are so important in determining the mechanical characteristics of the reinforced concrete beam-column joint.

Owing to the accuracy of the models adopted to describe the single materials and their interaction, the method has been used both to investigate experimental results and to clarify specific problems of the connection through feedback between experiments and analysis.

The first and detailed study making use of non linear finite elements is attributed to Noguchi (1981) who analised the inelastic response of plane interior beam-column joints under monotonic loads and

adopted discrete crack approach. In 1984 first Naganuma and Noguchi, and then Noguchi and Watanabe [1988], considered the same problem under static load reversals. The finite element mesh consisted of triangular plane-stress elements simulating plain concrete, bar elements to model reinforcement, bond link elements to model the steel-to-concrete interaction, and crack-link elements to model the stress release occurring in directions normal to the crack upon crack opening, **Fig. 3.12a**. An orthotropic non-linear material model with the biaxial failure criterion by Kupfer and Gerstle [1973] was adopted to model the constitutive behaviour of plain concrete. Reinforcing steel characteristics were represented with a simple bilinear model. The bond-link element modelled the bond-slip of the beam longitudinal bars according to a given relationship. The crack-line elements were placed at the potential crack surfaces, which were predetermined based on experimental evidence. A number of specimens were selected as case studies for the analytical investigation. Specimens with good bond conditions, quite perfect bond conditions and poor bond conditions were considered. The analysis showed a good agreement with the experimental results. Also, the results indicated that deterioration of hysteretic characteristic was influenced by shear failure and slippage of the beam main bar in the joint, **Fig. 3.12b**.

Even in the study carried out by Kwak and Filippou [1992, 1997] the behaviour of reinforced concrete beam-column joints was described by a plane stress field, i.e. the actual three-dimensional behaviour was not included in the model. Really, the main concern of their study was not the analysis of the mechanics of the joint but the finite element analysis of monotonic behaviour of reinforced concrete structures. Using the rotating crack model among the smeared crack model [Rots and Baauwendraad, 1989], a new finite element concrete model was proposed based on an improved cracking criterion which was derived from fracture mechanical principles, and a new discrete reinforcing steel model which included the bond-slip deformation. In the steel model the reinforcing bar was modelled by a truss element embedded inside the concrete element and the relative slip between reinforcing steel and concrete was explicitly taken into account, **Fig. 3.13**. In order to assess the ability of the proposed finite elements to simulate the behaviour of beam-column subassemblages, a previous experimental study case was compared with the analytical results. Concrete elements were modelled by eight-node isoparametric elements whereas longitudinal bars and transverse reinforcements were modelled by two-node truss elements. The bond-slip effect was included in the analysis with bond link elements. **Fig. 3.14** compares the analytical results with the measured load-displacement response of the subassemblage. With the effects of tension stiffening and the bond slip, the analysis showed excellent agreement with the experimental results.

The finite element model adopted by Pantazopoulou and Bonacci [1994] was a two dimensional idealisation of beam column connections and the monotonic behaviour was analised, as well. Two-noded, nonlinear truss elements were used to model beam, column and joint reinforcement. Plain concrete was modelled using four-noded, plane stress elements. Inelastic concrete behaviour was defined internally, along the principal axes, assuming that the directions of principal stress and principal strain are coincident. Relations between the two measures were based on the tension-softened stress-strain laws for concrete under two-dimensional states of stress, proposed by Vecchio and Collins [1986], **Fig. 3.15**. Bond conditions at concrete-reinforcement interfaces were modelled using springs elements with direction along the bars. Two types of relationships were considered for the spring simulating favourable and unfavourable bond conditions, respectively, **Fig. 3.16**. The objective of their analysis was to study the parametric dependence of beam-column connection behaviour. The most notable conclusion drawn from the computed results was that participation of hoops in joint shear resistance typically increased with the intensity of imposed lateral storey drift; however, joint hoops became fully engaged only in a limited number of cases. These cases were characterised by favourable bond conditions and either a large joint shear input or, alternatively, very small amounts of joint hoops.

3.4 Concluding Remarks

In the previous section existing analytical models for the prediction of the cyclic joint behaviour were presented. Herein the two groups of models are compared and their merits are discussed.

Although global models can fit closely virtually any shape of the moment-rotation curve, they suffer from the disadvantage that they cannot be extended outside the range of calibration data. Unlike the Filippou et al. model, elegant from the rational point of view but not easy to implement in a frame analysis program, a unique global moment-rotation curve is used to describe the behaviour of the joint. Such an approach is in contradiction with the actual behaviour as the moments on each face of the joint are generally different and the behaviour of the sections on each side of the central core are interdependent through the behaviour of the steel-concrete bond in each reinforcement layer. Additionally, the global models are unable to predict substantially different behaviour due to possible change of failure mode, when the joint boundary conditions change. Nevertheless, most of the presently available connection models belong to this category as they have the doubtless advantage of capturing global behaviour in an equivalent sense (usually the equivalence should be established in terms of dissipated energy) without resorting to the most complex finite element model.

From the theoretical standpoint the Finite Element Method would be the most appropriate method of analysis to predict the response of a beam-column joint. The separate modelling of concrete, steel and bond would allow it to represent in great detail the global behaviour of the connection. Such a possibility for Finite Element analyses is its strong point over the global analyses. Nevertheless, it is also its weakness as the terms of the problem have been simply moved from the macroscopic level to the microscopic one. In fact, there are two new aspects to account for. One is related to the constitutive material laws and the other one is the role of such type of analysis within the routine design applications. The current state of the art in computational modelling and material interaction is either inadequate or prohibitive to permit a complete three-dimensional non-linear finite element analysis of a structural system. This is particularly true of a highly non-linear material like reinforced concrete where system characteristics are continually being altered by either degradation of strength and stiffness or apparent pinching of loops resulting from repeated opening and closing of cracks. In fact, in the concrete modelling one of the main concern is how to model the cracks and their influence on the bond characteristics, especially under the actions of multi stress state. For a critique analysis of the numerical tools to simulate cracking in concrete, the reader can refer to Rots and Blaauwendraad [1989] and to Crisfiel and Wills [1987, 1989] as for the use of different models within the smeared crack approach to study reinforced concrete panels.

The above considerations show that, albeit the theoretical potentiality of the Finite Element Method, the results from such analysis should be considered in a qualitative light and for comparative interpretations. Bearing this in mind and the limits implied by the material models adopted, the method can be used as a necessary complement to large scale structural testing, both as an economical means of extending test results and a tool for understanding complex behaviour.

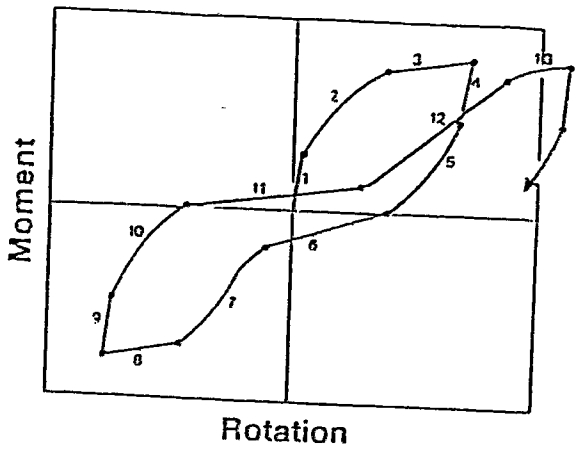

Fig. 3.1 Stage of behaviour for atypical inelastic cycle

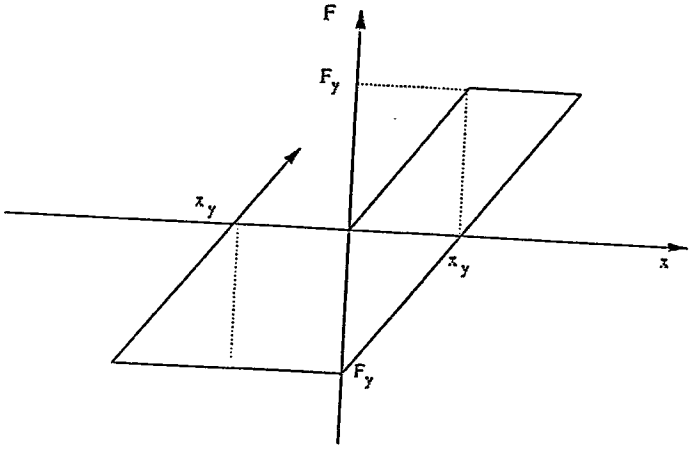

(a) Elasto-plastic Model

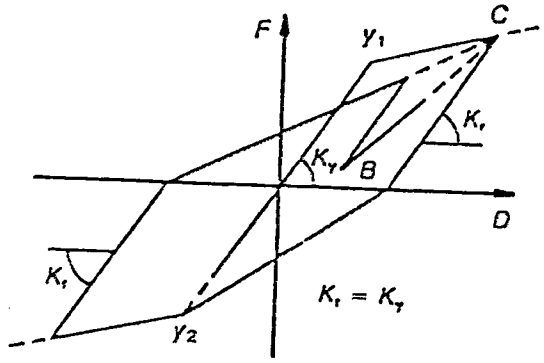

(b) Clough-Johnson Model

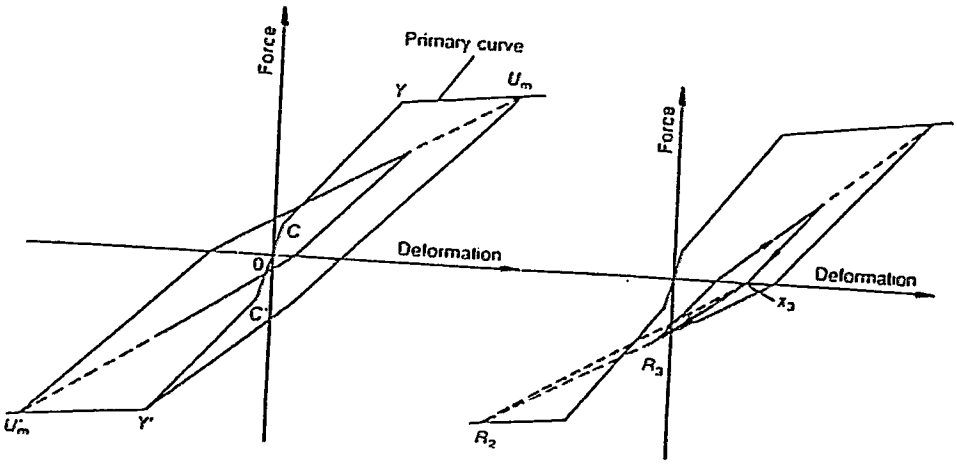

(c) Takeda Model

Fig. 3.2 Hysteresis Models

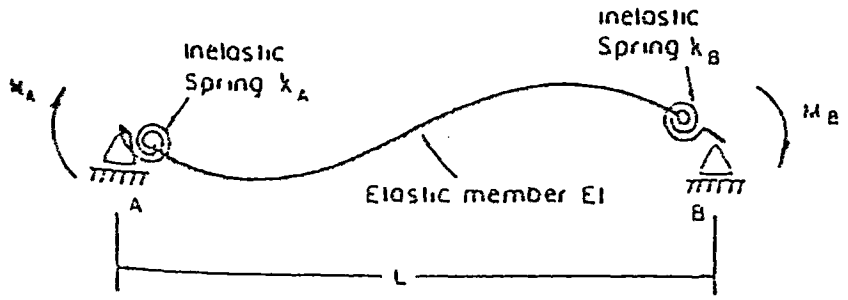

Fig. 3.3 One component member model

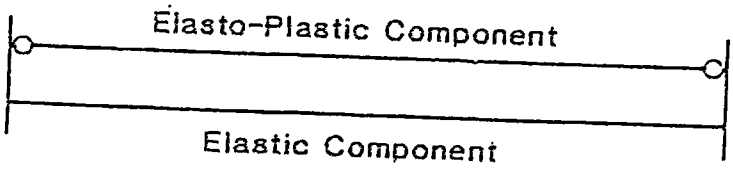

Fig. 3.4 Dual component model

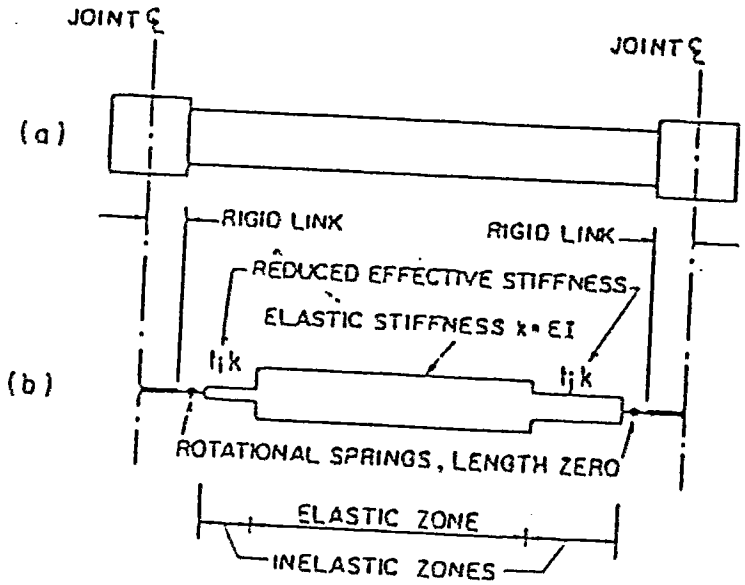

Fig. 3.5 One component member model adopted by Solemani et al., 1979

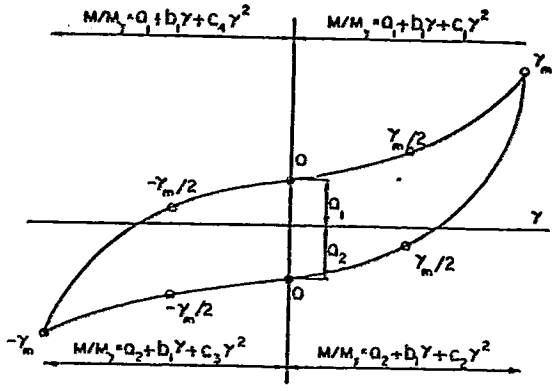

Fig. 3.6 Parabola in a hysteresis loop adopted by Townsend et al., 1973

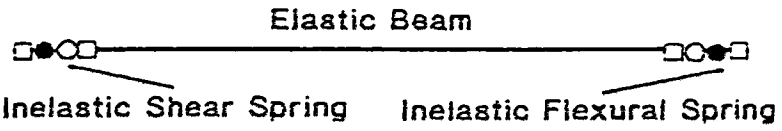

(a) One component member model with flexural and shear springs

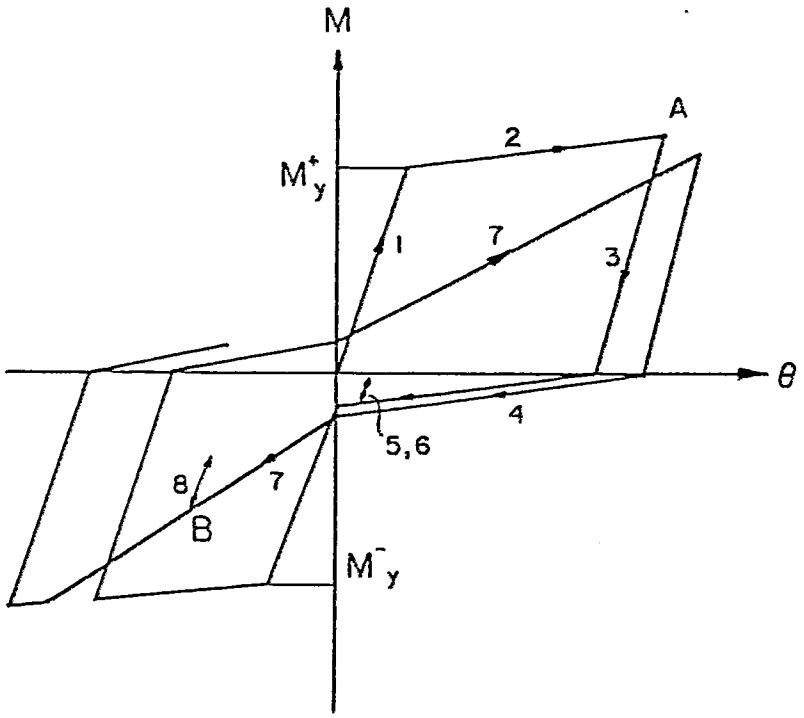

(b) Moment - Rotation hysteresis model with flexural and shear springs

Fig. 3.7 Beam element model as adopted by Banon et al., 1981

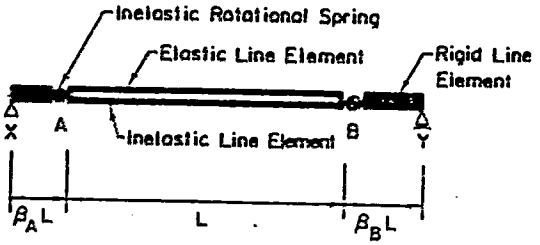

(a) Multicomponent member model

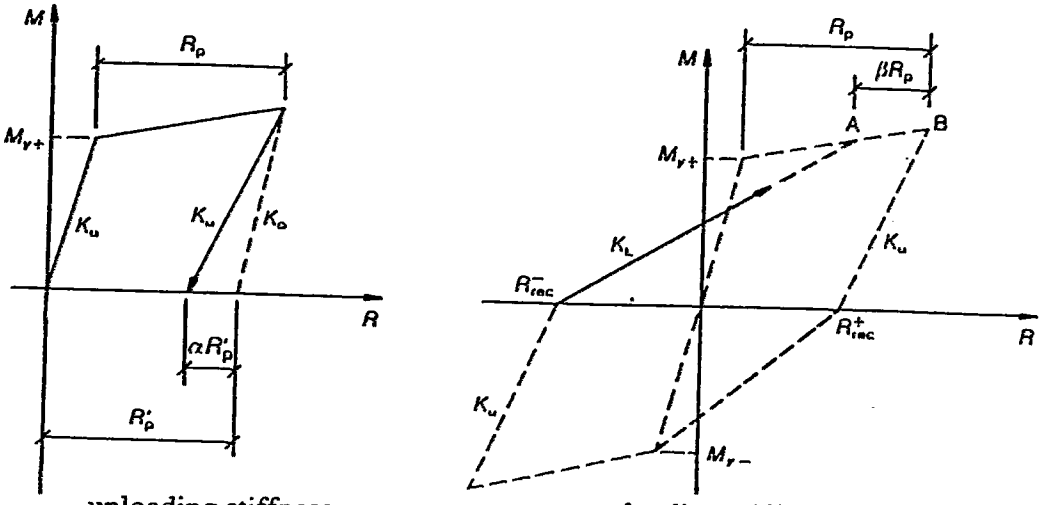

(b) Takeda model as modified by Otani

Fig. 3.8 Beam element model as adopted by Otani, 1974

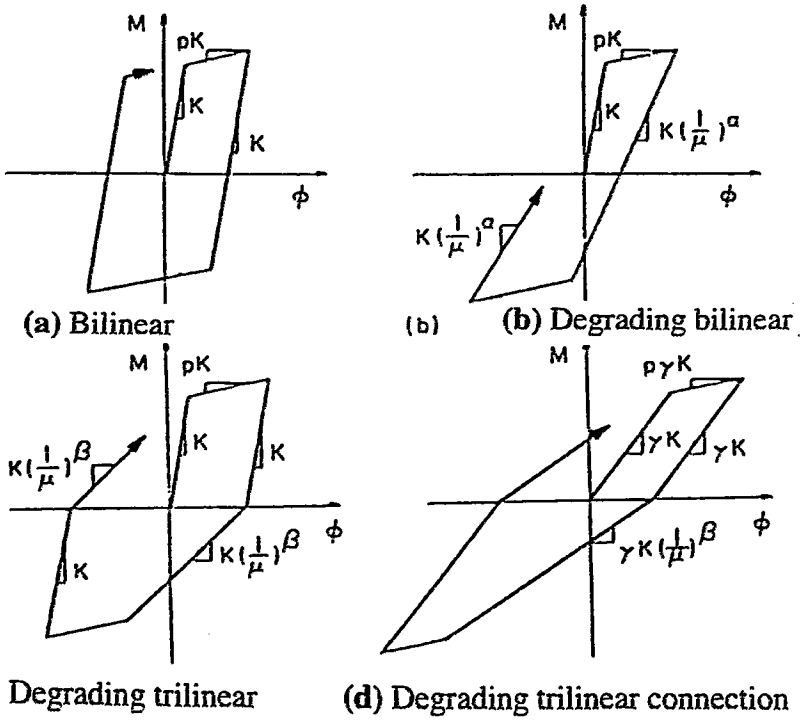

Fig. 3.9 Hysteresis models for reinforced concrete members considered by Anderson et al., 1977

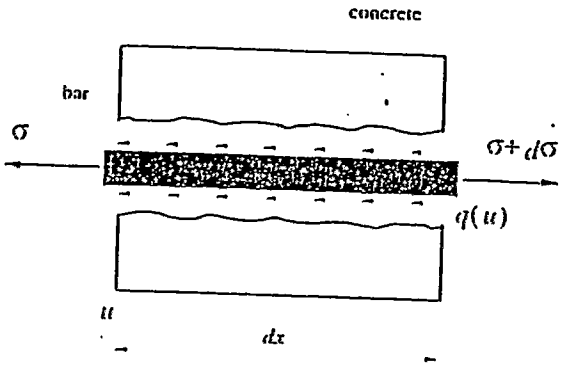

(a) Forces acting on infinitesimal segment of anchored reinforcing bar

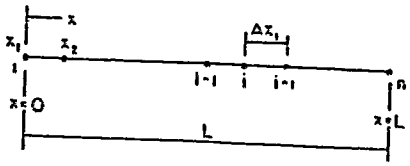

(b) Discretization along reinforcing bar

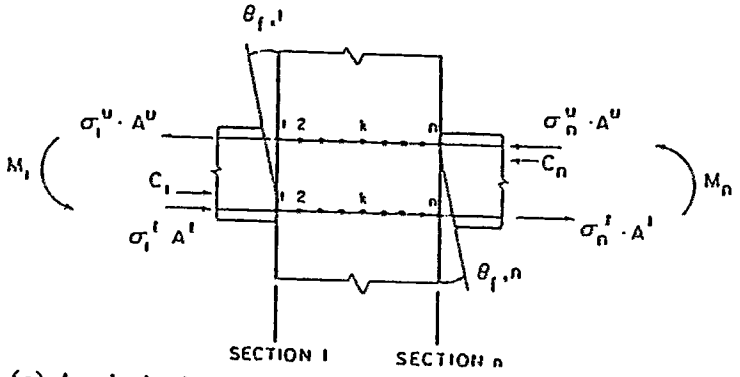

(c) Analytical model for interior beam-column joint

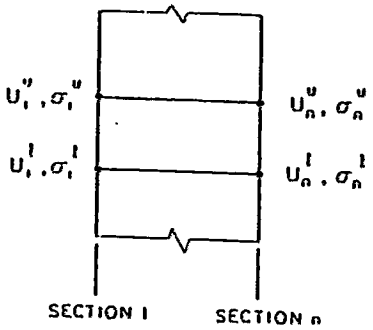

(d) Unknown variables at joint end section

Fig. 3.10 Joint finite element model proposed by Fillipou et al., 1983

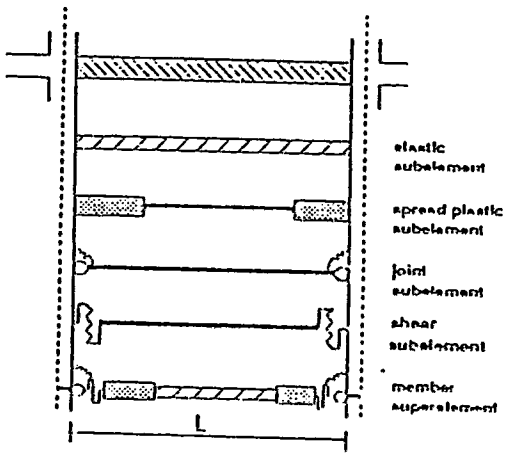

Fig. 3.11 Decomposition of abeam into differnt subelements, Filippou et al., 1990

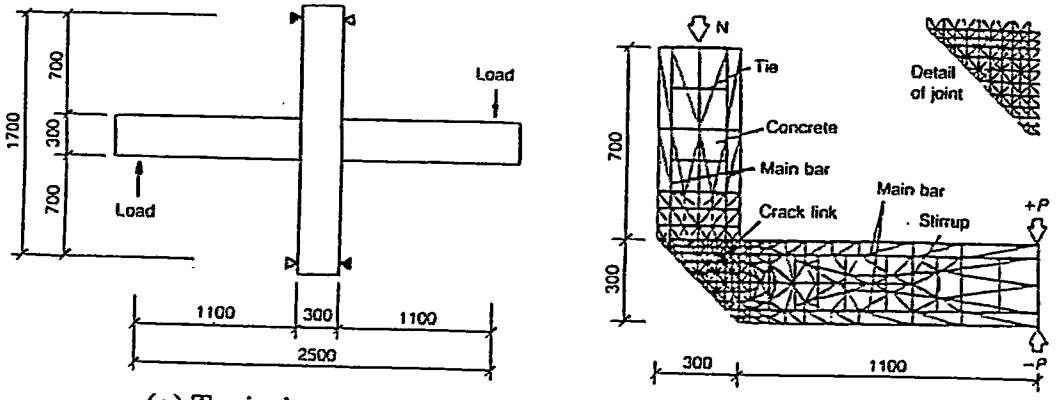

(a) Typical connection analysed, and finite element mesh

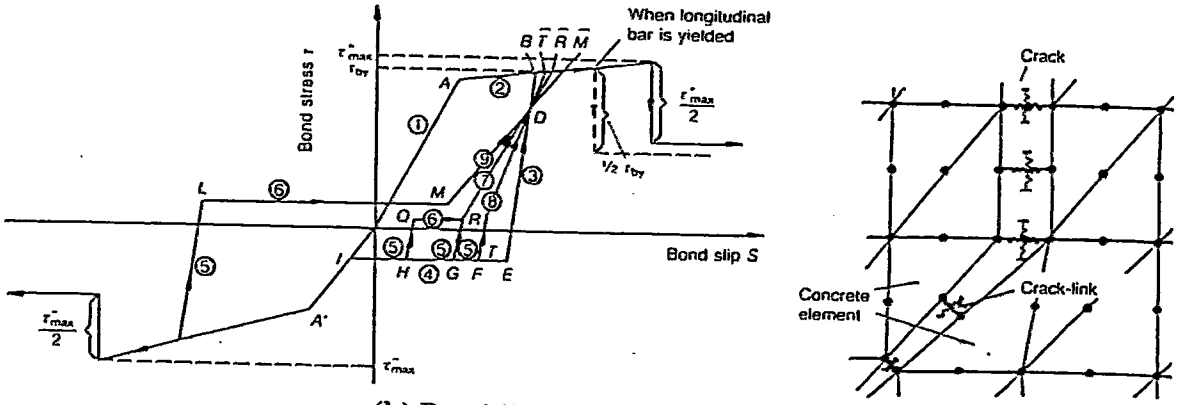

(b) Bond-link element properties

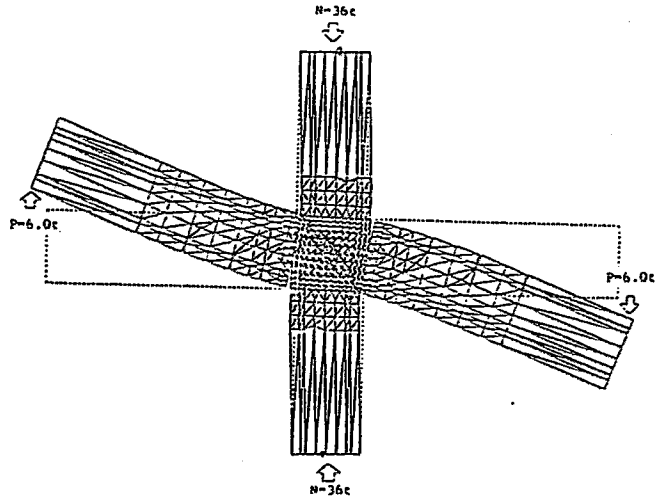

(c) Crack propagation

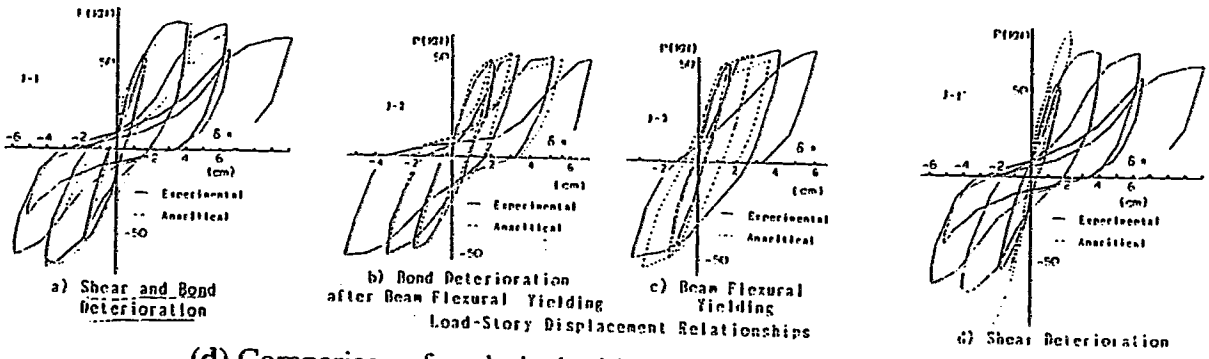

(d) Comparison of analytical with experimental results

Fig. 3.12 Discrete finite elemnt beam-column model studied by Noguchi, 1981

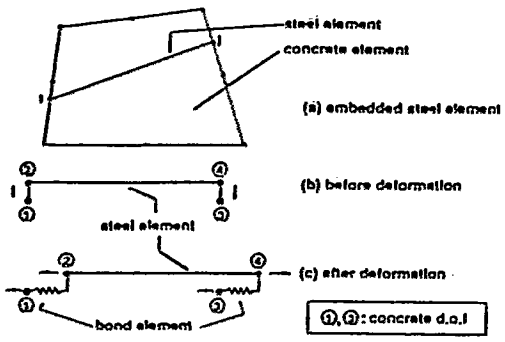

Fig. 3.13 Reinforcing steel element with bond-slip implemented by Kwak et al, 1990

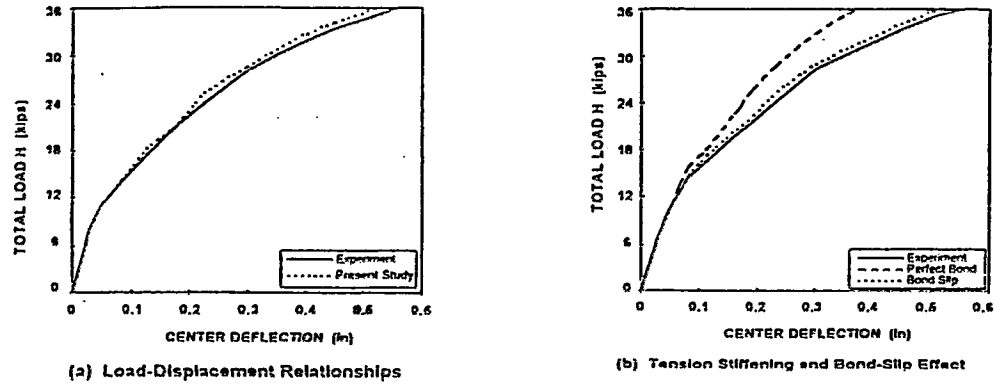

Fig. 3.14 Load displacement response of beam-column subassembly

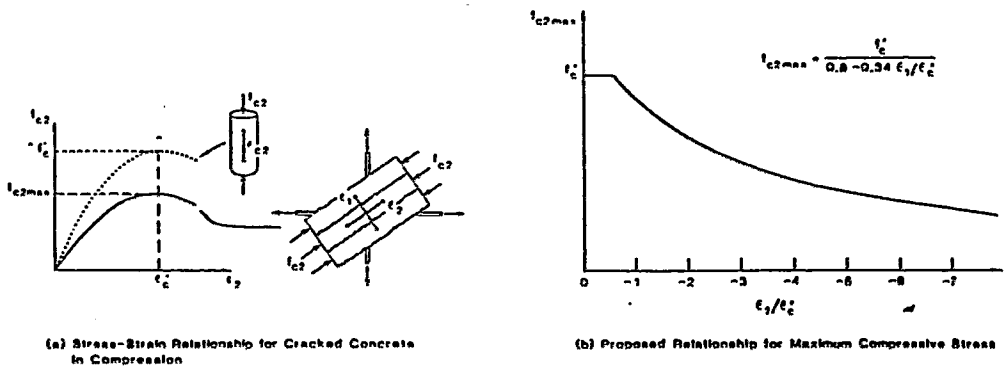

Fig. 3.15 Concrete model used by Pantazopoulou et al., 1994

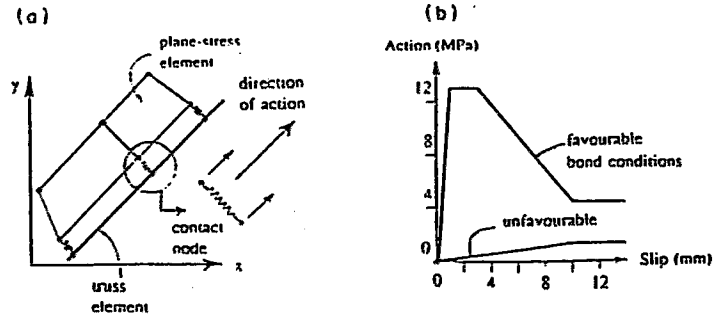

Fig. 3.16 Contact element modeling reinforcement to concret interface (a) element; (b) action-deformation relationship

CHAPTER 4

BEHAVIOURAL MODELS

4.1 Introduction

Beam column connections are considered as 'disturbed' regions of a structural system and are often referred to as D regions [Hsu, 1996]. Stresses and strains are so irregular that they are not amenable to mathematical solution. In particular, equilibrium and compatibility conditions are difficult to apply. Moreover, owing to the above irregularity and the brittle nature of concrete under shear stresses, the joint exhibits poor hysteretic properties. The main concern of the designer, then, is to warranty that the joint has an overall strength which is higher than the other structural elements where dissipation of energy are considered to take place. For this reason, among others, increasing attention has been given to the application of limit analysis method to the design of reinforced concrete joints. Especially the static method has been applied because it provides a possible equilibrium system of internal forces throughout the joint at the ultimate load stage and thus it indicates the required strengths of both concrete and reinforcement [Marti, 1985a and 1985b]. A clear visualization of statically stress fields is obtained with strut and tie models. These models provide a clear concept of the stress flows within the joint and allow evaluating quite simply the corresponding global force in equilibrium on the joint boundary, **Fig. 4.1**.

Since the introduction of the strut and tie model due to Paulay, Park and Priestley [1978], many other models have been proposed in literature. They range from the simplest one proposed by Zhang and Jirsa [1982], **Fig. 4.2**, that postulates the occurrence of an inclined compression strut, to the complex one introduced by Ichinose [1987, 1988] that assumes the joint shear strength as contribution of three different shear resisting mechanisms, **Fig. 4.3**. These models are different one from each other for the type of external actions to be equilibrated, the role assigned to the joint reinforcement and the postulated stress field within the joint which equilibrates the joint boundary forces. In the following, the basic concepts of the strut and tie models are given. Thereafter, the behavioural joint model introduced by Pantazopoulou and Bonacci [1992] is described. The latter does not belong to the family of strut and tie models but is a global model which, on the basis of some assumptions, allows to describe the primary response of the joint under increasing monotonically loads.

4.2 Strut and Tie Models

The essential features of a strut and tie model of joint behaviour may be understood with reference to **Fig. 4.1**, which shows a joint of frame subject to lateral loading, with clockwise moments from the beams equilibrated by counter-clockwise moments from the columns [Paulay and Park, 1992]. The forces introduced to the joint by adjacent members are assumed to be equilibrated by a

combination of two mechanisms, as shown in **Fig. 4.4**. The first is a large strut formed between the opposite corners of the joint in compression, and the second is a panel truss mechanism formed by the intermediate joint ties acting as tension members and smaller inclined concrete struts acting in compression. Hence, even in the second mechanism a diagonal compression field is developed. The above two mechanisms may be assumed as two extremes of joint behaviour and the importance of one with respect to the other one depends on how the forces are introduced to the joint. In the first mechanism compression and shear forces transferred to the joint by means of concrete stresses, along with bond forces from beam and column bars developing within the compression zone of the joint, are assumed to be equilibrated by a single diagonal strut [Paulay, Park and Priestley, 1978; Fenwick, 1981]. Hence, the strut mechanism requires the existence of the transfer compressive stress concrete area and can exist without any bond stress transfer along the beam and column reinforcement within the joint. On the other hand, the panel truss action is associated to the remainder of the joint shear forces, introduced solely by steel forces by means of bond. Hence, this mechanism can develop only when good bond conditions are realised along beam and column reinforcement within the joint.

At the initial load stage, both the strut and the truss mechanism contribute to the joint shear resistance [Paulay, Park and Priestley, 1978]. The strut mechanism contributes more because a significant amount of forces can be transmitted through the non-cracked part of the section whereas large strains are required to activate the tension members in the panel truss. As the load increases two paths are possible, depending on the bond conditions and the cracking pattern at the joint edges. If full vertical depth crack occurs against the joint faces because of residual strain due to large inelastic deformation reversals, shear forces cannot be transferred to the joint by internal concrete forces. Consequently, the contribution to shear strength by the main diagonal concrete strut in the joint core deteriorates. If good bond conditions are present in the joint, all the forces are transferred by bond stresses and are resisted by the truss mechanism. To sustain this type of behaviour through a severe load history, a large amount of transverse joint reinforcement is required. The cracking pattern shown by the joint in this case is given by diffuse cracks all over the joint as a result of the numerous developing diagonal struts, **Fig. 4.5**. On the other hand, if poor bond conditions are present, caused by progressive yield penetration into the joint core or because of the use of large diameter bars, the joint shear forces cannot be transferred to the joint by bond stresses. Hence, the truss mechanism cannot be activated. In this case, the strut mechanism must resist dominant part of the joint shear. The beam bars are then anchored in the beam at the opposite side of the joint, increasing the size of the compressive blocks on the beams and thus increasing the effectiveness of the strut mechanism [Leon, 1990a]. The joint corner are better confined and the strut mechanism is more effective, **Fig. 4.6a**. Theoretically, no stirrups are required for shear resistance [Blakeley, 1977]. However, some steel must be provided to the joint zone to control the width of the diagonal cracks and tensile strains. In fact, diagonal compression forces creates a splitting force perpendicular to it [Fenwick and Irvine, 1977] and the compressive strength of the diagonal strut is reduced by the increasing tensile strain perpendicular to the main diagonal strut. Hence, the principal role of the lateral reinforcement is to confine the cracked joint core concrete in order to maintain its integrity [Kitayama, Otani and Aoyama, 1991]. The cracking pattern shown by the joint in this case is given by a main corner to corner tension diagonal failure as depicted in **Fig. 4.6b**.

Strut and tie models proposed in literature are obtained in general by a superposition of the two above mechanisms by quantifying the contribution of each of them to the joint shear strength. In the model conceived by Paulay, Park and Priestley [1978], for example, the joint shear strength is assumed as given by:

$$V_{jh}=V_{ch}+V_{sh} \quad (4.1)$$

$$V_{jv}=V_{cv}+V_{sv} \quad (4.2)$$

where the subscripts *c* and *s* refer to the contribution of the concrete strut and the truss mechanism, respectively, Fig. 4.4. From equilibrium arguments, the term V_{ch}, in turn, consists of:

$$V_{ch} = C'_c + \Delta T'_c - V_{col} \tag{4.3}$$

where C'_c is the concrete compression force; $\Delta T'_c$ is the force transmitted by means of bond to the strut approximately over the depth c of the flexural compression zone in the column and V_{col} is the shear force from the column, **Fig. 4.4.** Hence, the definition of V_{ch} is turn out to do a realistic estimate with respect to the concrete stress and bond stress distribution to evaluate C'_c and $\Delta T'_c$, respectively. Once V_{ch} has been determined V_{sh} is obtained by the (1) after evaluating the joint shear demand, V_{jh}. The value of V_{sh} so determined is used to evaluate the horizontal joint shear reinforcement. Furthermore, in the model the effect of the column axial compressive force on the shear strength is taken into account, as well. Increases of the compressive force produce an increase of the compressive zone of the column and make the contribution of the strut mechanism more important. The details of the formulation of the model, however, can be found in Paulay and Priestley [1992]. This model has also been assumed as background of the joint design recommendations in the New Zealand Earthquake Resistant Design Code.

The model proposed by Zhang and Jirsa [1982] assumes only the diagonal strut mechanism to govern the joint shear resistance, **Fig. 4.2.** The entire joint shear is carried by joint concrete and hence, the strength of the diagonal compression field will control the strength of the joint [Kurose, 1993]. Furthermore, a significant amount of joint reinforcement can be omitted, as said previously, and reduced to that which is necessary to confine the concrete properly [Leon, 1990a]. For these reasons, the joint provisions that rely on this model, such as the ACI recommendations on the earthquake resistant joint design [Durrani and Wight, 1984; Ehsani and Wight, 1985], require a minimum amount of joint shear reinforcement be provided and establish an upper limit for joint shear stress. The code provisions do require no fraction of the joint shear demand be apportioned to the shear joint reinforcement. It is of interest to note that the specification on the maximum input shear stress is given also by recommendations that rely on other models. In fact, the essence of this limit is to safeguard the core concrete against excessive diagonal compressive stresses. The limit-input shear stress is usually expressed simply as function of the uniaxial compressive strength.

As conclusion of this section, it is of interest to mention the background of the recommendations on the joint design given in EC8. It is assumed that under the column and beam axial forces, acting on the core concrete of the joint, as well as due to some dilatancy produced from shear slip along diagonal cracks, horizontal and vertical expansion of the concrete of the core occurs. Due to this effect, both the horizontal and vertical reinforcement of the joint (stirrups of the column and intermediate longitudinal bars of the column respectively) are mobilised, contributing to the confinement of the concrete in the joint. On the basis of these considerations, the forces acting on the joint core concrete are determined and consequently the corresponding average stress state described by (σ_{cv} , σ_{ch}, τ_{cvh}). In this model, the core of the joint is considered safe, even after a limited cracking of concrete has occurred, provided that this cracking is not generalised. Hence, a tensile stress is allowed to develop in the concrete of the core. The tensile principal stress, σ_{ct} is obtained by the Mohr's stress circle as:

$$\sigma_{ct} = \sqrt{\left(\frac{\sigma_{cv} - \sigma_{ch}}{2}\right)^2 + \tau_{cvh}^2} - \frac{\sigma_{cv} + \sigma_{ch}}{2} \tag{4.4}$$

and the condition that $\sigma_{ct} \leq \sigma_{ct,suppl}$ is used to evaluate the necessary joint shear reinforcement [Tassios, 1988; Penelis and Kappos, 1997].

4.3 Two Dimensional Panel Models

Strut and ties models are based only on presumed equilibrium states and aim at evaluating the ultimate strength capacity by applying the concepts of limit analysis. Hence, they are not capable of predicting the response through the full range of loading, from zero loads to failure.

By adopting the same approach used by Collins [1978] and Vecchio and Collins [1986] in developing the Modified Compression Field theory, Pantazopoulou and Bonacci [1992] developed a global mode to describe the joint behaviour. The model permitted the determination of the magnitude and direction of principal stresses and strains in a manner that depended only on design parameters [CEB No 231, 1996].

In this model, the panel zone was assimilated to a reinforced concrete membrane and treated as a continuous material with 'smeared cracks' allowing the application of the principle of mechanics of materials [Hsu and Zang, 1997]. Hence, stresses and strains averaged over the dimensions of the entire joint were introduced to describe the concrete and steel behaviour.

In the following, the analytical formulation of the model is presented in a slightly different form from the original paper and a simpler and clearer algorithm to solve the final non-linear system of equations is given. The latter has been obtained adapting to the problem in hand the algorithm proposed by Hsu [1991] to solve the softened truss model for membrane elements.

The reinforced concrete panel zone is viewed as composed of a concrete element and steel reinforcement as shown in **Fig. 4.7**. The three stress components σ_l, σ_t and τ_{lt} denote the global stresses applied on the reinforced concrete element viewed as a whole. The stresses on the concrete itself are denoted as σ_{cl}, σ_{ct} and τ_{ctl} and are shown in **Fig. 4.7b**. The longitudinal and transverse steel provide the smeared stresses of $\rho_l f_l$ and $\rho_t f_t$ as shown in Fig. **4.7c** [Hsu, 1991]. The principal stresses for σ_{lc}, σ_{tc} and τ_{ltc} are defined as σ_d and σ_r based on the *d-r* axes shown in **Fig. 4.7b**. It is worth noting that the principal axis *d* and *r* are different in general from the principal axis of the global stress state described by the stresses σ_l, σ_t and τ_{lt} [Hsu and Zang, 1997]. Referring to **Fig. 4.7**, the overall equilibrium of the reinforced concrete element yields the following equation:

$$\sigma_l = \sigma_{lc} + \rho_l f_l \tag{4.5}$$

$$\sigma_t = \sigma_{tc} + \rho_t f_t \tag{4.6}$$

$$\tau_{lt} = \tau_{ltc} \tag{4.7}$$

In summing the concrete stresses and the steel stresses in the *l* and *t* directions, it is assumed that steel reinforcement can take only axial stresses. Any possible dowel action is neglected. However, this assumption implies no considerable approximation of the joint behaviour as shear displacements necessary to mobilize the above mechanism would have to be substantial and cannot develop [Paulay, Park and Priestley, 1978]. Since the concrete stresses will be related to strains only trough the principal directions, it is necessary to express the concrete stresses σ_{lc}, σ_{tc}, and τ_{ltc} in terms of the principal stresses σ_d, σ_r and the angle α, **Fig. 4.7**. This can be done through a transformation of stresses from the *l-t* co-ordinates to the principal *d-r* co-ordinates according to the following equations:

$$\sigma_{lc} = \sigma_d \cos^2\alpha + \sigma_r \sin^2\alpha \tag{4.8}$$

$$\sigma_{tc} = \sigma_d \sin^2\alpha + \sigma_r \cos^2\alpha \tag{4.9}$$

$$\tau_{ltc} = (-\sigma_d + \sigma_r)\sin\alpha\cos\alpha \tag{4.10}$$

which, replaced in the equations (4.5), (4.6) and (4.7), yield

$$\sigma_l = \sigma_d \cos^2\alpha + \sigma_r \sin^2\alpha + \rho_l f_l \quad (4.11)$$
$$\sigma_t = \sigma_d \sin^2\alpha + \sigma_r \cos^2\alpha + \rho_t f_t \quad (4.12)$$
$$\tau_{lt} = (-\sigma_d + \sigma_r)\sin\alpha\cos\alpha \quad (4.13)$$

As to the strain conditions, it is assumed that concrete and reinforcing bars are perfectly bonded at the boundaries of the joint. Hence, compatibility conditions require that any deformation experienced by the concrete must be matched by an identical deformation of the reinforcement. Any change in concrete strain will be accompanied by an equal change in steel strain and therefore, the following equations hold [Vecchio and Collins, 1986]:

$$\varepsilon_l = \varepsilon_{lc} = \varepsilon_{ls} \quad (4.14)$$
$$\varepsilon_t = \varepsilon_{tc} = \varepsilon_{ts} \quad (4.15)$$
$$\gamma_{lt} = \gamma_{ltc} \quad (4.16)$$

Bond deterioration is taken into account by Pantazopoulou and Bonacci [1992] for the effect that produces on the stress distribution along the height of the joint. Hence, the transverse reinforcement is assumed as

$$\rho_t = \rho_s + \beta\rho_b \quad (4.17)$$

where

ρ_s is the stirrup reinforcement ratio
ρ_b is the longitudinal beam bars ratio
β relates the magnitude of stresses in the longitudinal beam reinforcement to the average stirrup stresses. For perfect bond, β is assumed equal to zero whereas for negligible bond resistance, β is taken as equal to 1.

Owing to the above assumption the behaviour of the joint panel can be described as a reinforced concrete membrane with perfect bond and transverse and longitudinal reinforcement ratio given by ρ_t and ρ_l, respectively.

Strain principal directions are assumed coincident with stress principal directions in the concrete element, hence α is also the angle that the first principal strain direction forms with the axis *l*. The strain transformation which relates the strains in the two systems, (*l*, *t*) and (*d*, *r*) is the following:

$$\varepsilon_l = \varepsilon_d \cos^2\alpha + \varepsilon_r \sin^2\alpha \quad (4.18)$$
$$\varepsilon_t = \varepsilon_d \sin^2\alpha + \varepsilon_r \cos^2\alpha \quad (4.19)$$
$$\gamma_{lt} = 2(-\varepsilon_d + \varepsilon_r)\sin\alpha\cos\alpha \quad (4.20)$$

The constitutive laws of the materials complete the above equilibrium and compatibility equations. In more recent studies on concrete modelling under plane stress states [Vecchio and Collins, 1981, 1986; Belarbi and Hsu 1995] the constitutive law of the concrete is expressed by means of the following system of equations:

$$\sigma_d = = f_1(\varepsilon_d, \zeta) \quad (4.21)$$
$$\zeta = = f_2(\varepsilon_r, \varepsilon_d) \quad (4.22)$$

$$\sigma_r = = f_1(\varepsilon_r, \zeta) \tag{4.23}$$

where it is assumed that the compressive stress-strain curve of concrete is a function of the peak softening ζ, which in turn, is assumed as a function of the tensile and compression strains of concrete, ε_r and ε_d [Hsu, 1993], **Fig. 4.8.**

The constitutive laws for the steel are given in general by the equations:

$$f_l = f_3(\varepsilon_r, \zeta) \tag{4.24}$$
$$f_t = f_4(\varepsilon_r, \zeta) \tag{4.25}$$

Note that in the formulation of the model it is assumed that there is only a unique stress state corresponding to the given strain state [Pantazopoulou and Bonacci, 1992].

A simplification of the above relationships refers to the constitutive laws of the concrete in tension and the steel. The tensile strength of the concrete is neglected whereas an elastic perfectly plastic model is assumed for steel behaviour.

Finally, the system of equations to be solved is the following:

$$\sigma_l = \sigma_d \cos^2\alpha + \sigma_r \sin^2\alpha + \rho_l f_l \tag{4.11}$$
$$\sigma_t = \sigma_d \sin^2\alpha + \sigma_r \cos^2\alpha + \rho_t f_t \tag{4.12}$$
$$\tau_{lt} = (-\sigma_d + \sigma_r)\sin\alpha\cos\alpha \tag{4.13}$$
$$\varepsilon_l = \varepsilon_d \cos^2\alpha + \varepsilon_r \sin^2\alpha \tag{4.18}$$
$$\varepsilon_t = \varepsilon_d \sin^2\alpha + \varepsilon_r \cos^2\alpha \tag{4.19}$$
$$\gamma_{lt} = 2(-\varepsilon_d + \varepsilon_r)\sin\alpha\cos\alpha \tag{4.20}$$
$$\sigma_d = f_1(\varepsilon_d, \zeta) \tag{4.21}$$
$$\zeta = f_2(\varepsilon_r, \varepsilon_d) \tag{4.22}$$
$$\sigma_r = f_3(\varepsilon_r, \zeta) \tag{4.23}$$
$$f_l = f_4(\varepsilon_l) \tag{4.24}$$
$$f_t = f_5(\varepsilon_t) \tag{4.25}$$

In this system there are 11 equations and 14 unknown variables. The unknown variables include 7 stresses (σ_l, σ_t, τ_{lt}, σ_d, σ_r, f_l, f_t) and 5 strains (ε_l, ε_t, γ_{lt}, ε_d, ε_r), as well as the angle α and the softening coefficient ζ. If 3 unknown variables are given, then the remaining 11 unknown variables can be solved using the 11 equations [Hsu, 1991]. Usually the joint behaviour is described by reporting the variation of the external shear stress τ_{lt} versus the shear strain γ_{lt}. In this case, then, the applied normal stresses σ_l and σ_t are given as constants, whereas the shear stress τ_{lt} is the variable to be solved. In fact, it is convenient to give as third variable the concrete compressive strain ε_d so as to have the concrete described in different stages.

Hsu [1991] proposed an efficient algorithm of solution of the above system of equations which avoided to have the angle α in the iteration process as opposed to the procedure proposed by Pantazopoulou and Bonacci [1992]. By combining compatibility and equilibrium equations, the following additional equations can be considered:

$$\varepsilon_r = \varepsilon_l + \varepsilon_t - \varepsilon_d \tag{4.26}$$

$$\varepsilon_l = \varepsilon_r + \frac{\varepsilon_r - \varepsilon_d}{\sigma_r - \sigma_d}(\sigma_l - \sigma_r - \rho_l f_l) \tag{4.27}$$

$$\varepsilon_t = \varepsilon_r + \frac{\varepsilon_r - \varepsilon_d}{\sigma_r - \sigma_d}(\sigma_t - \sigma_r - \rho_t f_t) \tag{4.28}$$

$$\tan^2\alpha = \left(\frac{\varepsilon_l - \varepsilon_d}{\varepsilon_t - \varepsilon_d}\right) \tag{4.29}$$

The algorithm is shown in the flow chart depicted in **Fig. 9** and is performed through the following steps:

Step 1 Select a value of strain in the *d* direction, ε_d.
Step 2 Assume a value of strain in the *r* direction, ε_r.
Step 3 Calculate the softened coefficient ζ and the concrete stresses σ_d and σ_r from Eqs. (27), (21) and (23), respectively.
Step 4 Solve the strains and the stresses in the longitudinal steel (ε_l and f_l) from Eqs. (27) and (24), and those in the transverse steel (ε_t and f_t) from Eqs. (28) and (25).
Step 5 Calculate the strain $\varepsilon_r = \varepsilon_l + \varepsilon_t - \varepsilon_d$ from Eq. (26). If ε_r is the same as assumed, the values obtained for all the strains are correct. If ε_r is not the same as assumed, then another value of ε_r is assumed and Steps 3 to 5 are repeated.
Step 6 Calculate the angle α, the shear stress τ_{lt}, and the shear strain γ_{lt} from Eqs. (29), (13) and (20), respectively. This will provide one point on the τ_{lt} versus γ_{lt} curve.
Step 7 Select another value of ε_d and repeat Steps 2 to 6. Calculation for a series of ε_d values will provide the whole τ_{lt} versus γ_{lt} curve.

Note that in the step 4, combining the Eqs. (24) with (18), and (12) with (19) a fix point equation for ε_l and ε_t is obtained, respectively. The solution of each of these equations requires, in turn, an iterative procedure.

The implementation of the above algorithm on a computer allows the response history of the joint to be traced and the maximum shear sustained by the joint to be located. The sequence of significant features in joint behaviour can be detected. The steel may yield before the crushing of the concrete or the concrete may crush before the yielding of the steel. Depending on the ratio of the percentages of steel in the two directions, yielding of steel may first occur in the longitudinal bars or in the transverse bars. A joint designed in different ways will behave very differently. Depending on the percentages of steel in the longitudinal and the transverse directions, a joint shear failure may appear in one of the following four modes:

1. **Under-reinforced element**: Both the longitudinal steel and the transverse steel yield before the crushing of concrete.
2. **Element partially under-reinforced in *l* direction**: Longitudinal steel yields before the crushing of concrete; Transverse steel does not yield.
3. **Element partially under-reinforced in *t* direction**: Transverse steel yields before the crushing of concrete; Longitudinal steel does not yield.
4. **Over-reinforced element**: Concrete crushes before the yielding of steel in both directions.

The expression for the shear stress corresponding to the first three failure modes can be obtained very easily. They are given by, respectively:

$$\tau_{lt} = \sqrt{(\rho_l f_{ly} - \sigma_l)(\rho_t f_{ty} - \sigma_t)} \tag{4.30}$$

$$\tau_{lt} = \sqrt{(-\sigma_{dmax} + \rho_l f_{ly} + \sigma_l)(\sigma_l - \rho_l f_{ly})} \tag{4.31}$$

$$\tau_{lt} = \sqrt{(-\sigma_{dmax} + \rho_t f_{ty} + \sigma_t)(\sigma_t - \rho_t f_{ty})} \tag{4.32}$$

Here, it is of interest to note that the equation (30) can be solved for the limiting shear stress. This expression can also be obtained by applying the equilibrium plasticity truss model [Hsu, 1993] as it is derived by only equilibrium and yielding conditions of the materials. Equations (31) and (32) include the evaluation of σ_{dmax} which depends on the tensile strain ε_r at the onset of the failure. Hence, the last two equations can be evaluated only after having traced the whole path or having estimated ε_r.

In appendix is given the list of the Fortran program which implements the above algorithm. The Vecchio-Collins model for concrete in biaxial tension-compression state is adopted, **Fig. 4.8**. Also, the tensile concrete strength has been neglected and an elastic perfectly plastic model has been used to describe the steel. **Fig. 4.10** depicts the shear stress-shear strain relationship for the three specimens with the properties reported in **Table 4.1**.

specimen	f_y MPa	E_s MPa	f'_c MPa	ε_{co}	ε_{cmax}	ρ_l	ρ_t	σ_l MPa	σ_t MPa	Maximum value of shear stress MPa	Note
A	300	200000	-34.5	-0.002	-0.0035	0.04	0.01	-3.45	0.1725	5.433	SY+CC
B	300	200000	-51.75	-0.002	-0.0035	0.025	0.01	-3.45	0.1725	5.564	SY+CRLY+CC
C	300	200000	-34.5	-0.002	-0.0035	0.06	0.06	-3.45	0.1725	12.156	CC

SY+CC: stirrup yielding+concrete crushing; SY+CRLY+CC: stirrup yielding+column longitudinal reinforcement yielding+concrete crushing; CC: concrete crushing;

Table 4.1: Design parameters for analised specimens and corresponding value of the maximum shear stress and type of failure experienced according to the model proposed.

In **Table 4.2** the solution of the above system is given for values of ε_d where the most meaningful characters of the reinforced concrete panel behaviour have been detected.

The diagrams reported in **Fig. 4.10** are described up to crushing of the concrete. This condition is defined when $\sigma_d=\sigma_{dmax}$. It is remarkable to note the change of slope in correspondence of the reinforcement yielding. In the specimen A concrete crushing occurs after yielding of transverse; in the specimen B concrete crushing occurs after yielding of both transverse and longitudinal reinforcement whereas in the specimen C the concrete crushing occurs before any yielding of the reinforceemnt as a result of high values of the reinforcement ratio along longitudinal and transversal diresction which delay the yielding of the reinforcement and make concrete crush earlier.

In **Table 4.2** it is of interest to note that despite the application of a compressive stress along the *l*-direction, the solution of the system gives a corresponding tensile strain as ε_l. Consider the case of a membrane loaded as depicted in **Fig. 4.11**, where a biaxial tension-compression external load is given and let σ_l and σ_t denote the total external stresses. The assumption that concrete has no tensile strength implies that the normal stresses acting on the concrete are all compressive stresses. Hence, the Mohr's circle develops only on the compressive side and is tangent to the τ-axis. When no shear stress is applied ε_l is negative and ε_t is positive, consistently to the total loads applied as the principal stresses directions of the concrete coincide with that of the total stresses. When a shear stress is applied, it is expected that σ_d increases. An increase of σ_d implies an increases of σ_{lc}, as

well. The Mohr's circle increases its size and the point with co-ordinate σ_{lc} must lie beyond the centre of the circle. Hence, if σ_{lc} increases f_l decreases as the external total stress applied σ_l is constant Eq. (5). But if f_l decreases then also ε_l decreases because of the assumption of perfect bond $\varepsilon_l=\varepsilon_{ls}$ and of $\varepsilon_{ls}=f_l/E_s$. Therefore, as the shear stress increases it is expected to have a situation where ε_l changes sign. This occurs when the increases of τ is such that the increases of σ_d implies a value for σ_{lc} that is greater than the total stress applied, σ_l. In **Fig. 4.11** the line of equation $\sigma=\sigma_l$ has been reported, as well, hence when the Mohr's cirle size increases such that σ_{lc} crosses this line, then a change in the value of ε_l will be inevitable.

The diagrams shown in **Fig. 4.12**, taken from a study carried out by Pantazopoulou and Bonacci [1992], report the variation of the shear stress capacity as determined by the equations (19) and (21) with the hoop ratio. The two diagrams refer to the specimens A and B with the properties listed in **Table 4.3**. Also, it is reported the value of $20(\sigma'_c)^{1/2}$ recommended by the ACI -ASCI Committee 352 [1985] for a similar connection type. The equations suggest that the strength of the joint A is limited by concrete crushing after hoops yield, while for joint B crushing is less likely than yielding of vertical reinforcement. The shifting of failure modes has been obtained by increasing σ'_c and decreasing ρ_l for the joint B. In this way, the concrete crushing is delayed and yielding column reinforcement is accelerated. Furthermore, in the case of the joint B it is observed a range of values for the hoop ratio in which the ACI-ASCE recommendations would give a higher value of the strength capacity than what effectively the joint could sustain.

4.4 Concluding Remarks

Strut and ties models are obtained applying the static method of the limit analysis to the reinforced concrete. Stress paths in equilibrium under the action of external loading are postulated. Hence, only equilibrium conditions are used whereas compatibility conditions are neglected. As a result, there is not unique solution and several models developed in literature reflect this indeterminacy.

The process of laying out struts and ties should prescribe the anticipated directions of principal stresses [CEB No. 231, 1994]. These are defined on the basis of the actions anticipated on the joint boundary upon cyclic loading. From a theoretical point of view, these actions should be compressive concrete block stress of the intact sections and bond stresses along longitudinal and transverse reinforcement. The consideration of one type of action instead of another, the assumption on the bond conditions and type of bond stress distribution, the type of function attributed to the transverse reinforcement, are all important factors to take into account in defining a strut and tie model.

Generally, the development of strut and ties models is guided by what is observed in experiments. As the flow of forces through the joint can be constrained by experimental technique, it should not be expected that a model developed from observations in one set or family of tests will explain the behaviour of other specimens designed with dissimilar philosophy [Bonacci and Pantazopoulou, 1993]. Furthermore, missing links in such modelling, especially when the contribution of each mechanism is to be quantified, are often derived from empirical arguments, supported by test results.

Also, it has been argued that the application of limit analysis methods to reinforced concrete is questionable because of the concrete softening. However, the theory has been applied with a certain

success in the case of under reinforced elements where the strength was essentially determined by the yield strength of the reinforcement. In the case of over reinforced elements, such as is the case of joints, for sake of rigour the application of the limit analysis is not correct. Nevertheless, detailed comparisons with experiments have shown that if an appropriate estimation of the effective concrete compressive strength is done an accurate strength prediction can be obtained [Marti, 1985].

The global mechanical model developed by Pantazopoulou and Bonacci, which basically applies the concepts of the softened truss model for membrane elements to the joint panel zone, has the value of following the joint behaviour from zero load to failure. Also, the model is defined in terms of only the properties of the joint. Nevertheless, some improvements are still necessary such as the consideration of bond deterioration and up to what point is possible to analise the joint behaviour by means of average entities.

Specimen A	Yielding stirrup	concrete crushing
ε_d selected	-.00036000	-0.002
ε_r assumed	.00226049	.01097153
σ_{dmax}	-29.13152	**-12.94481**
σ_d	-9.543487	**-12.94481**
σ_r	0	0
ε_l	.00041079	.00083341
ε_t	**.00148974**	.00813819
ε_r calculated	.00226054	.01097160
α	32.8433	27.86349
τ_{lt}	4.348523	5.348561
γ_{lt}	.00238811	.01071926
σ_{lc}	-6.736401	-10.11726
σ_{tc}	-2.807086	-2.827555

(a)

Specimen B	yielding stirrup	Yielding column Longitudinal reinforcement	concrete crushing
ε_d selected	-.00022	-.0009	-.002
ε_r assumed	.00227624	.01073911	.01738893
σ_{dmax}	-43.59874	-19.70942	**-13.77752**
σ_d	-9.064178	-13.74732	**-13.77752**
σ_r	0	0	0
ε_l	.0005579	**.00149395**	.00197913
ε_t	**.00149843**	.00834522	.01340983
ε_r calculated	.00227633	.01073917	.01738896
α	33.93335	26.96975	26.93758000
τ_{lt}	4.198118	5.556638	5.56428800
γ_{lt}	.00231237	.00940905	.01566113
σ_{lc}	-6.23961	-10.91976	-10.9500
σ_{tc}	-2.824567	-2.827555	-2.8275

(b)

Specimen C	Concrete crushing
ε_d selected	-.002
ε_r assumed	.00373130
σ_{dmax}	**-24.0532**
σ_d	**-24.0532**
σ_r	0
ε_l	.00075383
ε_t	.00097748
ε_r calculated	.00373131
α	43.88178
τ_{lt}	12.01744
γ_{lt}	.00572694
σ_{lc}	-12.49592
σ_{tc}	-11.55728

(c)

Table 4.2: Iteration calculation for different values of ε_d.

specimen	f_y MPa	f'_c MPa	ρ_l	ρ_t	σ_l MPa	σ_t MPa
A	414	-34.5	0.04	varies	-3.45	0.1725
B	414	-51.75	0.025	varies	-3.45	0.1725

Table 4.3: Summary of design parameters for sample joints (after Pantazopoulou and Bonacci, 1992)

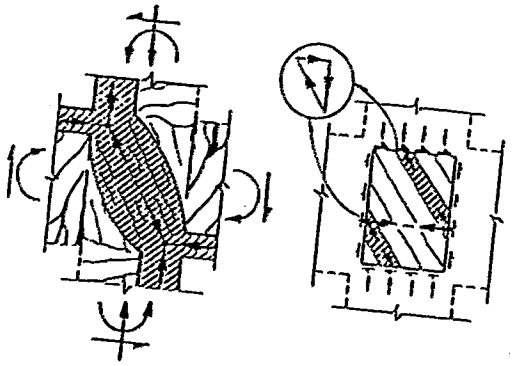

Fig. 4.1 Mechanism of shear transfer at an interior joint

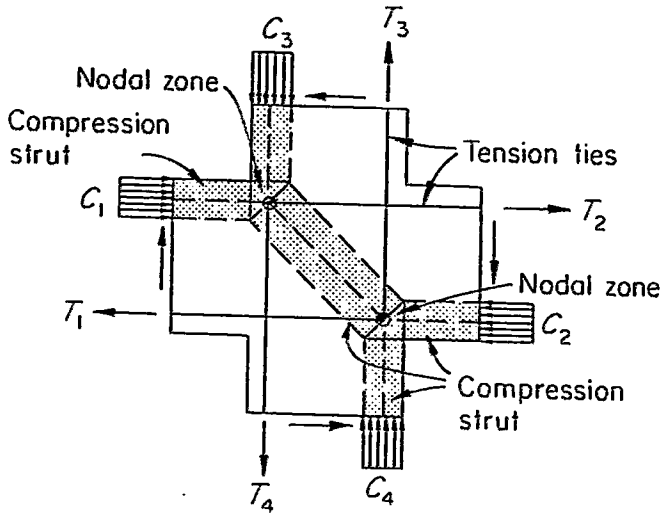

Fig. 4.2 Strut and Tie model proposed by Zhang and Jirsa, 1982

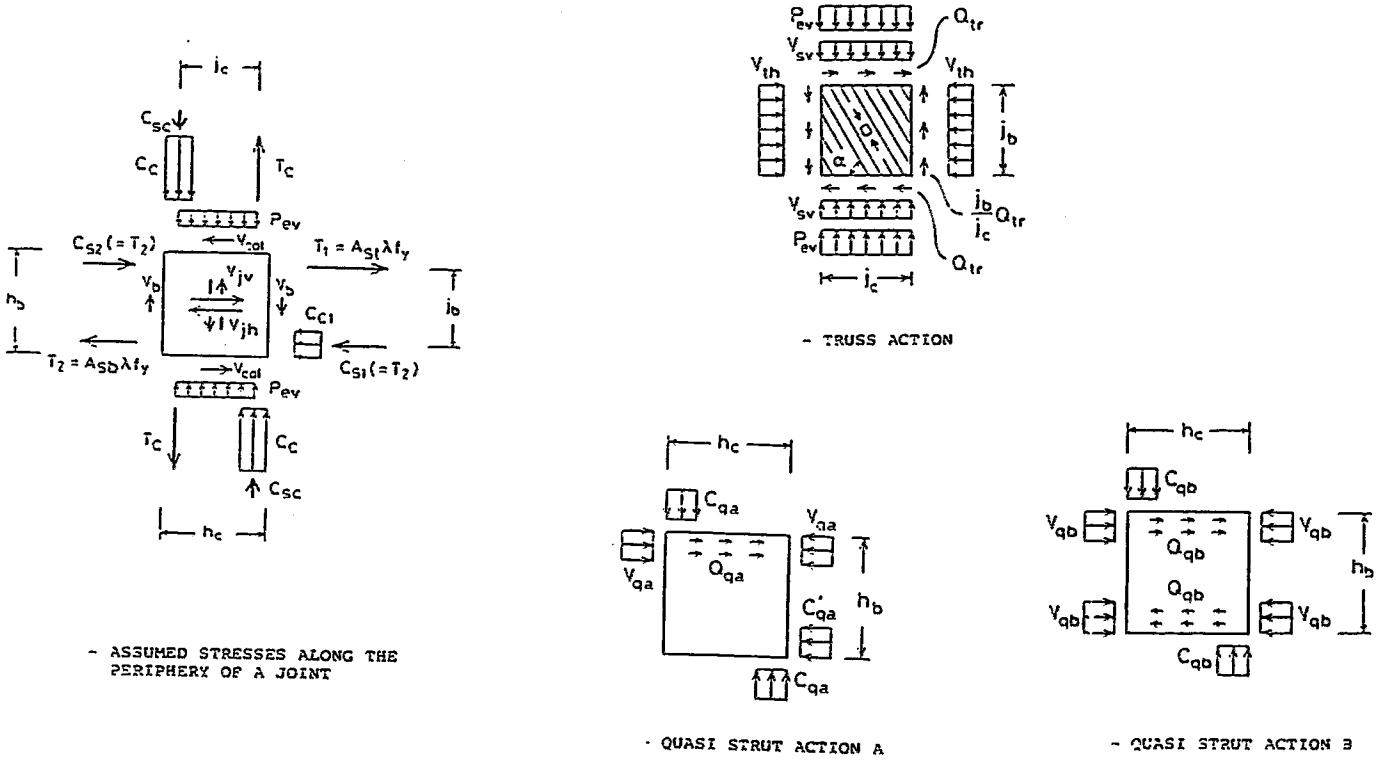

Fig. 4.3 Strut and Tie model introduced by Ichinose, 1989

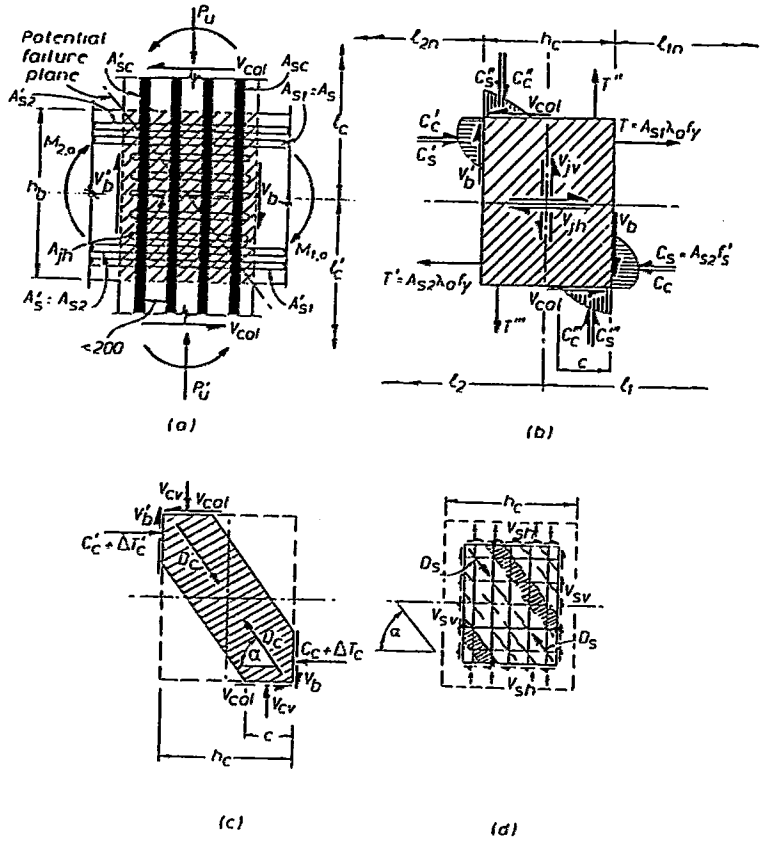

Fig. 4.4 External actions and internal stress resultants at an interior joint

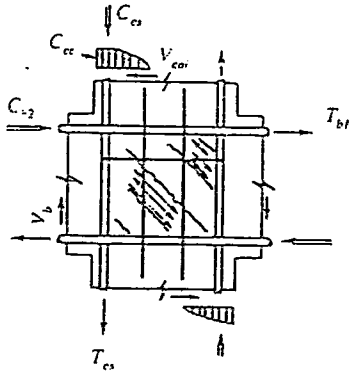

Fig. 4.5 Panel truss action in beam-column joints

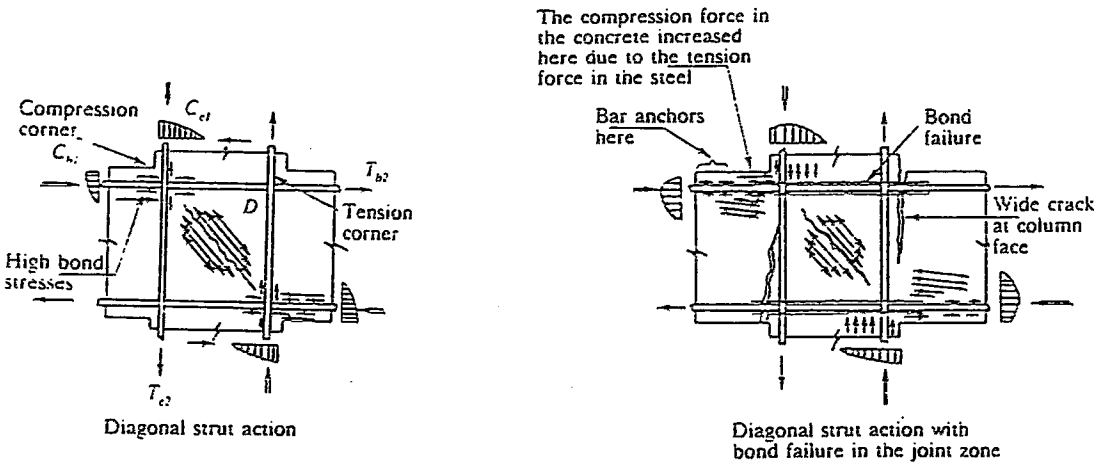

Fig. 4.6 Diagonal strut action in beam-column joints

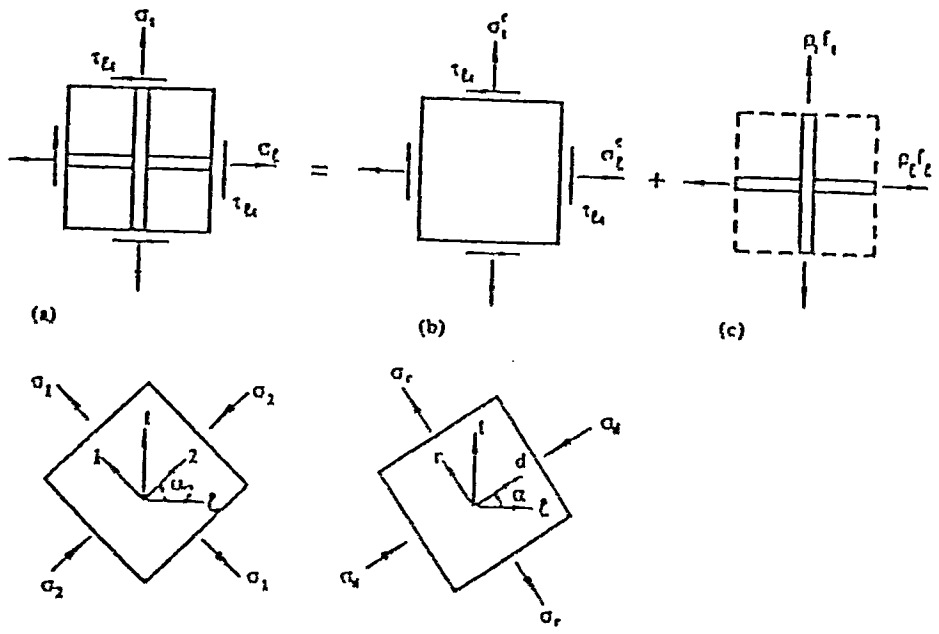

Fig. 4.7 Reinforced concrete membrane element under shear and axial stresses

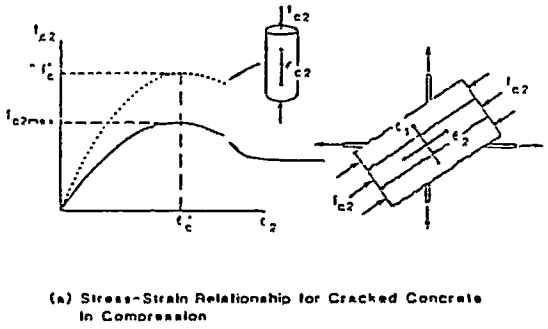

(a) Stress-Strain Relationship for Cracked Concrete in Compression

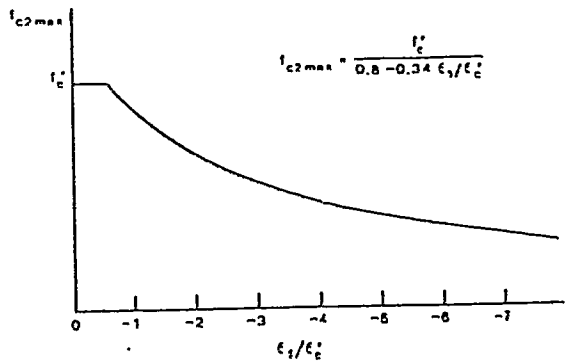

(b) Proposed Relationship for Maximum Compressive Stress

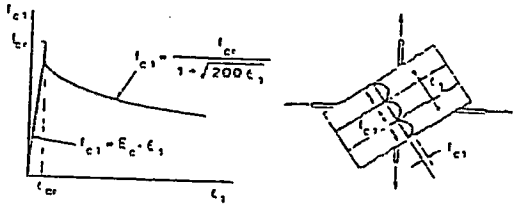

(c) Average Stress-Strain Relationship for Cracked Concrete in Tension

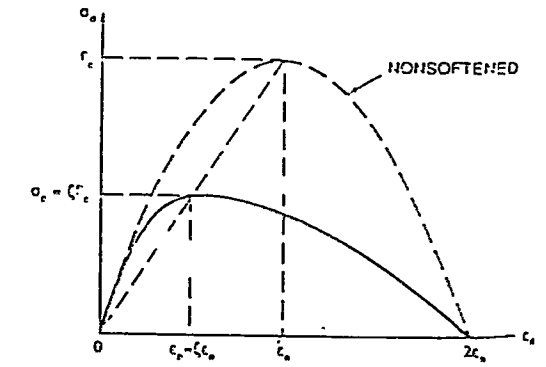

PROPORTIONAL SOFTENING OF STRESS AND STRAIN

Softened Stress-Strain Curve of Concrete in Compression

Fig. 4.8 Concrete constitutive law, Vecchio et al., 1986

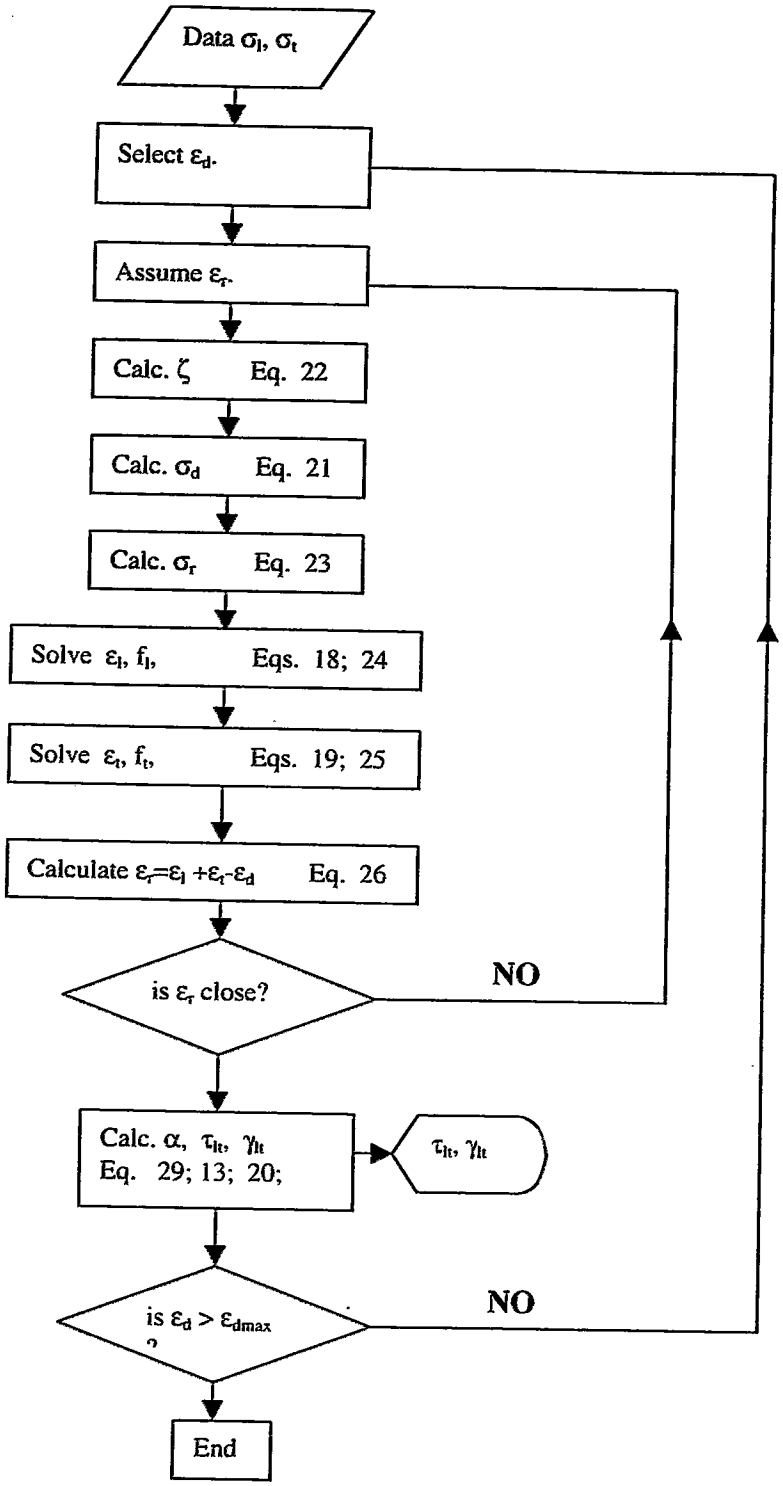

Fig. 4.9 Flow chart showing an efficient algorithm to determine the shear stress-shear strain relationships

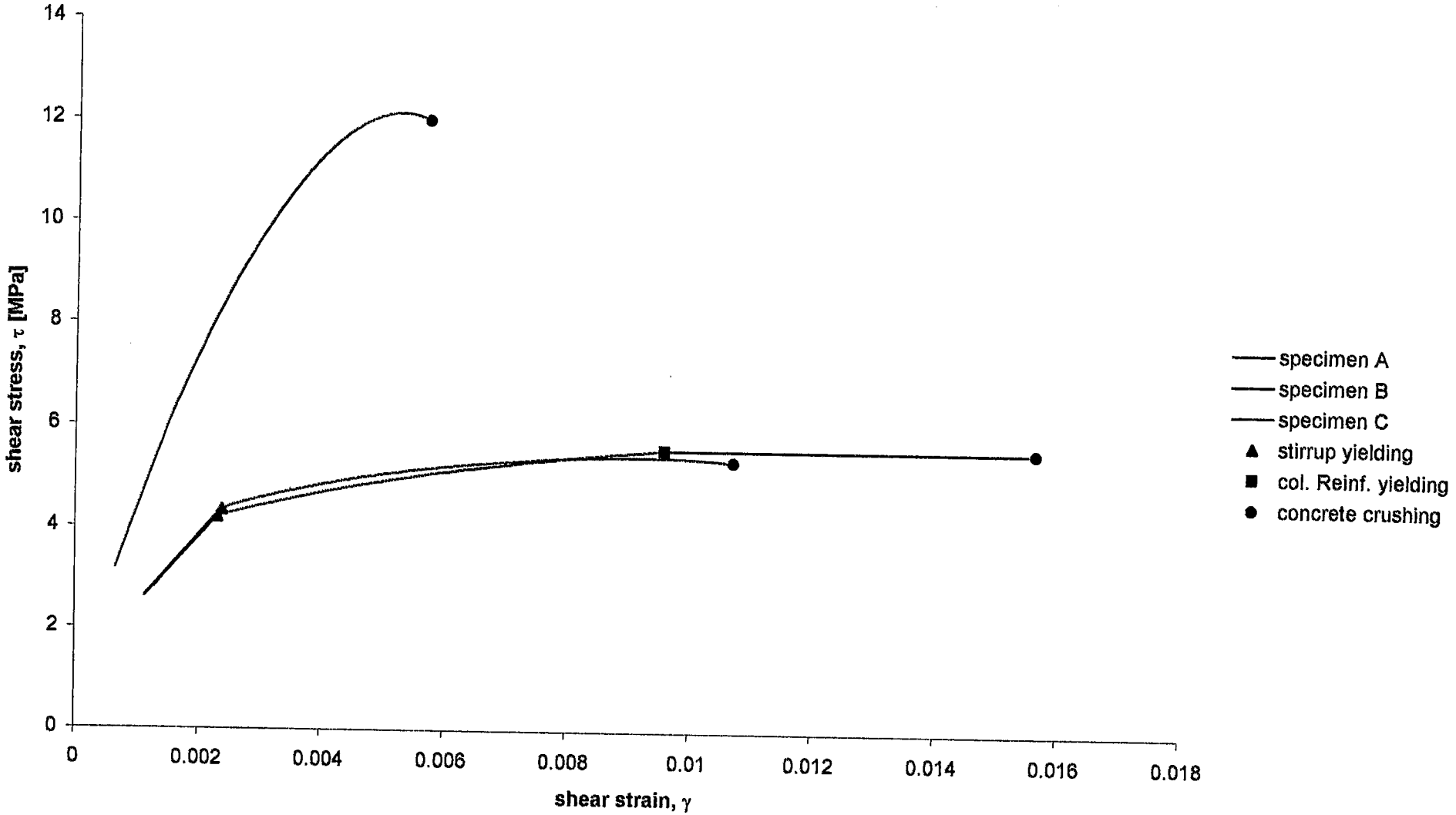

Fig. 4.10 shear stress-shear strain relationship, Vecchio-Collins Model, 1986

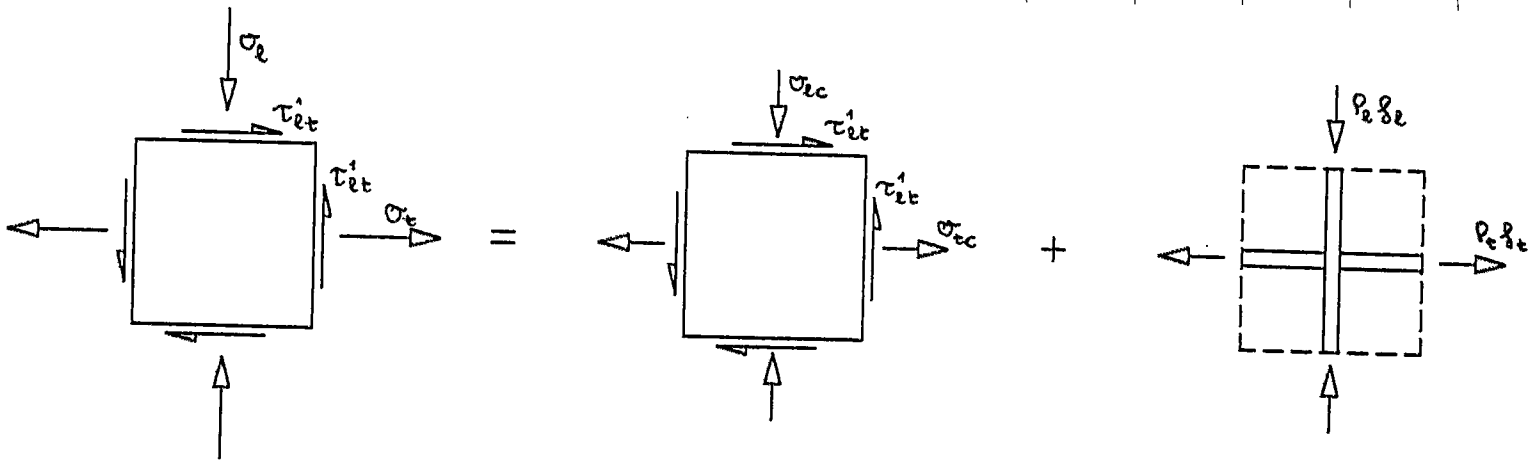

$$\tau_{lt} - \gamma_{lt}$$

$$\sigma_l = \sigma_{lc} + \rho_l f_l$$

$$\varepsilon_l = \varepsilon_{lc} = \varepsilon_{ls}$$

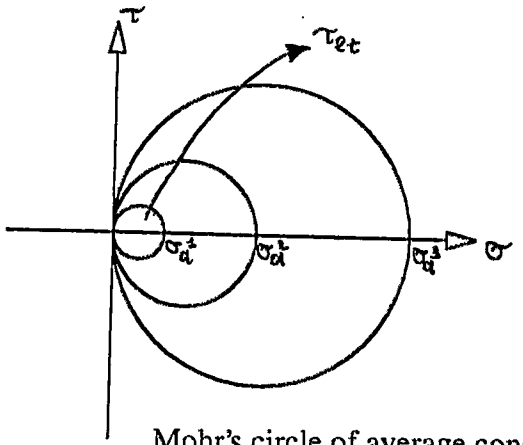

Mohr's circle of average concrete stresses

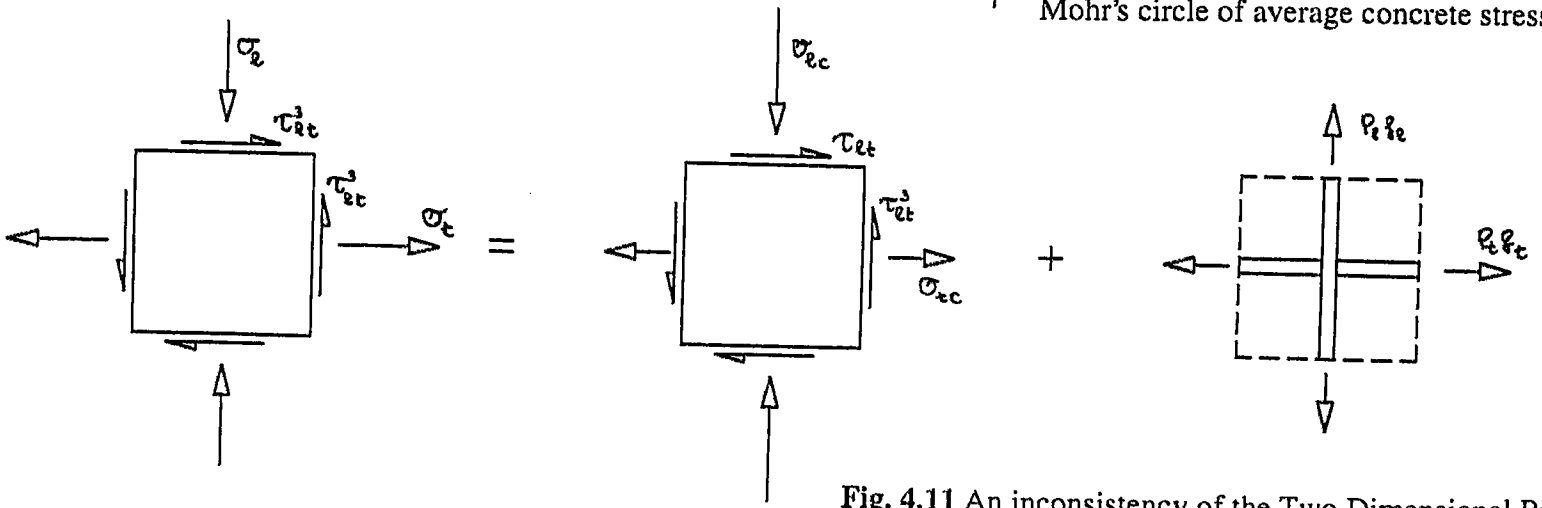

Fig. 4.11 An inconsistency of the Two Dimensional Panel Global Model

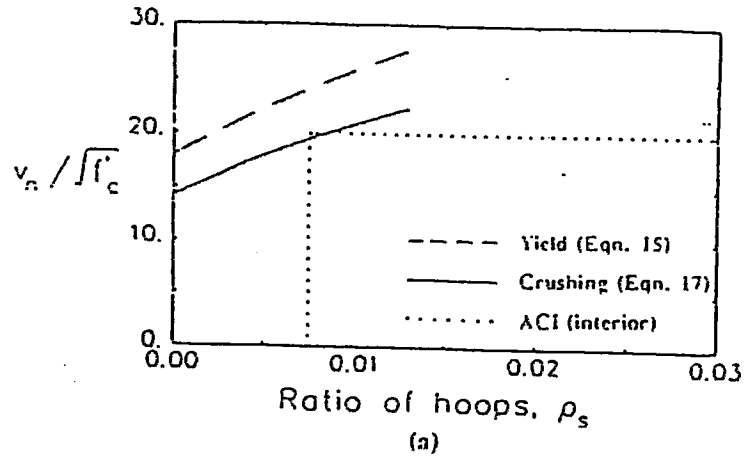

(a)

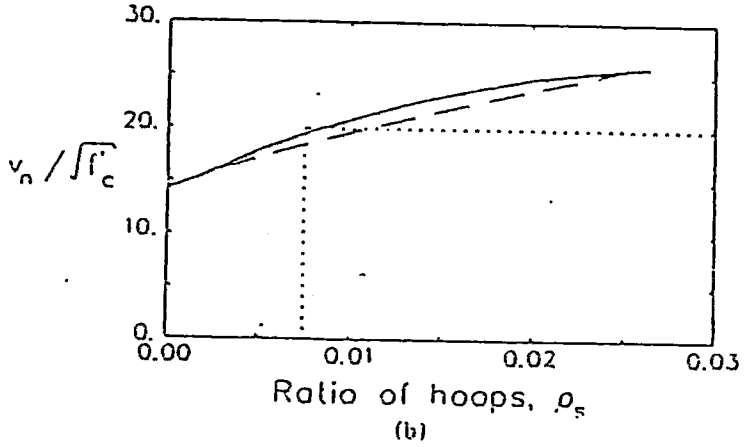

(b)

Fig. 4.12 Design shear stress

CHAPTER 5

ANALYTICAL MODELLING AND ANALYSIS

5.1 Introduction

During recent years, interest in non-linear analysis of reinforced concrete beam-column connection has increased steadily as a result of the gained importance of the joint deformation on the frame response and of the development of relatively powerful finite element procedures [Crisfield, 1997].

Understanding the pattern and magnitude of deformation within the joint upon external actions is necessary premise to discern the individual sources of flexibility of the connection and their interaction. Once this is achieved, the next step is to devise analytical models of the above mentioned sources of flexibility by means of simple mechanical elements. The aim is to have the overall connection response to be described as assemblage of the single element contributions. Hence, this process should lead to an overall model of the connection which is capable of predicting the variation of failure modes due to change in the connection geometrical and material properties, as well as loading conditions. Furthermore, the complete success of the idealisation should result in the implementation of the model into frame analysis programs.

This chapter is concerned mainly with the first part of the above study. Therefore, hereafter special emphasis will be given only to the deformational aspects of the joint behaviour. Given the complexity of the structural response of the concrete material and the objectives of the analytical investigation, a non-linear finite element analysis of complete beam-column connection has been carried out adopting the general purpose finite element program ABAQUS release 5.3 by Hibbitt, Karlsson and Sorensen [1995].

The adoption of numerical simulation techniques especially to analise non-linear problems is always done with sense of deep respect and fear. The full confidence in handling linear problems vanishes quite suddenly with the occurrence of non-linear aspects in the behaviour of a material. This is particularly true for the concrete with its various important non-linearities; namely, a non-linear stress-strain behaviour, tensile cracking and compression crushing material failures. Furthermore, constitutive properties of concrete have not as yet been identified completely and there is still no generally accepted material law available to model concrete behaviour especially in plane and triaxial stress-state. All that contribute to increase even more the doubt of reliability on the use of such techniques. These observations require the analyst to evaluate finite element analytical models and to be familiar with the underlying material models before their appropriate use [Elnashai, 1996]. For all these reasons, in the following the results of the finite element beam-column model will be preceded by an overview of the concrete model implemented in ABAQUS.

5.2 Reinforced Concrete Modelling in ABAQUS

In ABAQUS non-linear finite element modelling of reinforced concrete is accomplished by combining plain concrete model with bar elements. The program allows embedded and discrete representation of the reinforcement. In the discrete modelling of single bars one-dimensional truss elements are used. These elements are typically two-noded, but if compatibility of displacement with higher order concrete elements is desired, higher-order one-dimensional elements may be used for the steel bars. On the other hand, uniform density distributions of the reinforcement may be modelled with two-dimensional or three-dimensional elements in two-dimensional or three-dimensional analyses, respectively. In both the above representations, reinforcement elements are superimposed on the mesh of plain concrete elements, and are used with standard metal plasticity models that describe the behaviour of the steel. This modelling approach allows the concrete behaviour to be considered independently of the reinforcement. In the following, special attention will be paid to only the concrete model, as the plasticity metal models implemented by ABAQUS have been verified by many successful applications of the program in mechanical and aeronautical engineering problems.

The behaviour of plain concrete under predominantly compressive stresses exhibits fundamental differences from that under predominantly tensile ones [Elnashai, 1996]. When stresses approach and reach the failure surface, the failure mode, and more importantly, the post failure behaviour differ significantly: under predominantly tensile loading, attainment of the failure criterion leads to cracking and localisation of extensional deformations along a well defined crack plane. From then on the behaviour becomes strongly anisotropic: normal to the crack plane the material strain-soften, whereas parallel to the crack plane the behaviour is essentially that of uncracked concrete with the dimensionality of the problem reduced by one. On the contrary, under predominantly compressive stresses, the post failure behaviour is less anisotropic, with the material exhibiting gradual strain softening in all three directions, until a certain ultimate-deformation, at which the material crushes in all three directions, releasing its stresses. Such post failure behaviour corresponds to the progressive shrinkage of the failure surface in stress space, and then its sudden collapse, to the zero stress point [CEB, 1991].

These two different aspects of the concrete behaviour are modelled in ABAQUS by means of two models: a crack model which is valid for loading combinations which are assumed to be dominantly tensile, and an elastic-plasticity model for describing the behaviour of concrete under dominantly compressive stress states.

ABAQUS adopts the classical concepts of the elastic-plastic theory. The material behaviour is assumed to be linearly elastic up to the attainment of the initial discontinuous surface (analogous to the yield surface for metal plasticity) [Elnashai, 1996]. Hence, the criterion adopted to distinguish when the concrete is under a predominantly compressive or tensile behaviour is based on the location in the stress space of the point where the failure surface is reached. Cracking is assumed to occur when the stresses reach the fracture surface named as crack detection surface, whereas in the other cases the concrete is considered to be under a dominant compressive state.

In the crack model, the crack detection surface is taken to be a simple Coloumb line written in terms of the effective pressure stress, p, and of the second stress invariant of the deviatoric stress components, q, **Fig. 5.1** [Hibbitt, Karlsson and Sorensen, 1995]. As the smeared approach is adopted, the cracked solid is imagined to be a continuum where the notions of stress and strain still remain valid throughout the solid. Hence, the behaviour of the cracked concrete is still described in terms of stress-strain relations and the effect of cracking is taken into account by replacing the

initial isotropic stress-strain relation with an orthotropic stress-strain relation where the axes of othotropy are determined according to the condition of crack initiation. At an integration point, where the constitutive calculations are performed, the first crack is assumed to occur normal to the direction of the maximum principal tensile stress of concrete, σ_{c1}. Then stress-induced anisotropy is introduced in the model, with the behaviour in direction 1, normal to the crack, considered to be fundamentally different than the one in the orthogonal direction parallel to it. A damaged elasticity is used to model the failed material. The material stiffness matrix is obtained by assigning the descending branch of the stress-strain relationships of the concrete in uniaxial tension, which describes the effect referred to as tension stiffening by ABAQUS, and the shear retention factor. With regard to this aspect, ABAQUS has two options to model the descending branch of the uniaxial tensile stress-strain. In one the descending branch is controlled by fracture considerations, **Fig. 5.2**, whereas in the other one by the presence of reinforcing steel, **Fig. 5.3**. Both the modes are input means of the same data block, which is referred to as TENSION STIFFENING, despite the fact that they refer to two different phenomena, the tension softening and the properly called tension stiffening. The first is a local material softening observed during strain controlled experiments. It is a property of plain concrete and refers to the concrete softening behaviour within the fracture zone [Hillerborg, 1984]. The second one, that is the tension stiffening, is a global property of reinforced concrete even though it manifests itself as a softening phenomenon. It is a consequence of the presence of the steel within the concrete and the fact that average material properties over a finite domain are used to establish the stiffness characteristics of that domain [Schnobrich, 1986].

The smeared crack model adopted by ABAQUS is a fixed one. Hence, the orientation of the crack is fixed during the entire computational process. Let *n,s,t* denote the axes of orthotropy, where *n* refers to the direction normal to the crack and *s,t* refers to the direction tangential to the crack. In defining the damaged matrix with respect to these axes the model does not take into account the Poisson's effect after cracking, which has been recognised to be important by Bazant and Oh [1983]. Moreover, the model is based on a total strain concept in the sense that a one-to-one relation is assumed between the stress σ and the total strain ε. Finally, cracking is assumed to be irrecoverable in the sense that, once a crack has occurred at a point, it remains throughout the rest of the calculation. Hence, the model is not suitable to describe concrete behaviour under reversal loading.

The numerical implementation of concrete model to describe its behaviour under predominantly compressive stresses does not present particularly problems as the concrete is assumed to behave as an elastic-plastic material with isotropic hardening and associate flow. The shape of the failure surface is shown in **Fig. 5.1** and the definition of the loading surfaces is determined by assigning the stress-strain relationship under uniaxial compressive stress state. The model does not assume crushing and once the residual strength is attained, a perfectly plastic behaviour is assumed.

5.3 Finite Element Beam-Column Model

The finite element model studied in this section is a two-dimensional idealisation of beam-column connection with geometry similar to the subassemblage tested by Park and Milburn [1983]. The unit was designed according to the criteria of strong column and weak-beam. Very strict limits on the ratio of the beam bar diameter to the column depth were met in order to keep bond stresses to an acceptable level and single out the behaviour of the panel zone under shear stresses. The layout of

the connection along with the experimental setup is shown in **Fig. 5.4** whereas **Fig. 5.5a** depicts the corresponding finite element model.

Four-noded plane stress elements with full integration referred to as CPS4 element by ABAQUS were used to describe the behaviour of the concrete, **Fig. 5.5b**, whereas a discrete representation with two-noded linear plane truss elements referred to as T2D2 element was adopted to model beam, column and joint longitudinal and transverse reinforcement, **Fig. 5.5c**. The choice of the discrete representation of the reinforcing bars was suggested by the need to model in a following study the effect of bond by introducing bond-link elements defined by dimensionless springs. This consideration together with the one of having at least two concrete elements layers between two consecutive stirrups in order to represent accurately their effect, determined the mesh size adopted in the model. In a similar study Pantazopoulou and Bonacci [1994] suggested that if smooth-bond stress variation in between nodes was to be modelled the mesh size should be comparable to the diameter of the reinforcing bar in order to alleviate mesh sensitivity from the results. However, in the present study, as first stage of a following thorough analysis, the assumption of perfect bond is adopted and hence, the degrees of freedom of steel and concrete elements are slaved together.

Three finite element beam-column connection models, referred to as *bcjel*, *bcjnl-l* and *bcjnl*, were analysed and are shown in **Fig. 5.6**. They differentiate each other for the material behaviour assigned to the elements. The model *bcjel* has all the elements with elastic linear behaviour. In the model *bcjnl-l*, non-linear behaviour was assumed for concrete and bar elements belonging to the joint and also for bar elements belonging to beam and column regions adjacent to the joint for a length equal to the height of the respective cross section. Finally, in the model *bcjnl* the non linear behaviour was extended also to the concrete elements belonging to the above beam and column regions. The linear model was meant basivcally to check the reliability of the model by means of simple manual calculations. The other two, instead, purported to study the influence of the joint boundary conditions on the joint resisting mechanisms.

The non linear behaviour of the concrete elements was defined by the material model described in the previous section. **Table 1** reports the properties used to define the model. For the uniaxial compressive stress-strain relationship a tri-linear representation was used with departure from the linear path at $0.7f'_c$ whereas a residual strength equal to $0.8f'_c$ was assumed. The descending branch of the uniaxial tensile stress-strain relationship was modelled linearly and the maximum tensile strain was assumed equal to the yield strain of the reinforcement [Elnashai, 1996]. As to the reinforcing steel, an elastic-plastic model with strain hardening was assumed and defined by the properties reported in **Table 2**.

The boundary conditions used in the model are shown in **Fig. 5.5a** and resemble the one adopted in the experimental setup, **Fig. 5.4**. Both the column ends were assumed hinged, whereas displacement control was applied to the beam ends. Hence, effects of the column axial load on the deformation of the subassemblage were unaccounted for in the analysis. The preference for direct displacement control to load control was due to the following twofold consideration: the tangent stiffness matrix is better conditioned and does not become singular at a limit point in the load-deflection diagram [Bicanic et al., 1992].

The analysis was subdivided in two steps: in the first one a column axial load equal to $0.10f'_cA_c$ was applied in full magnitude whereas in the following step the beam ends were displaced monotonically and incrementally. The total displacement applied in the second step was expressed as multiple of the yielding displacement, $\Delta_{y,fix}$, of the beam of the subassemblage. The latter was evaluated assuming the beam fully fix at the joint interface. In this way, no deformability of the subassemblage was taken into account in $\Delta_{y,fix}$, hence the actual value of the beam-end displacement

which produced yielding of the beam bars at the joint interface was expected to be greater. The evaluation of $\Delta_{y,fix}$ is reported in Appendix B.

The numerical strategy adopted to solve the non-linear system of equations was an incremental-iterative procedure which used the Newton-Raphson procedure in each increment [Izzuddin, 1996]. The size of the increments was selected automatically by the program on the basis of the number of iterations employed to get the convergence in the previous increment. To measure the convergence of the iteration, two solution variables were used: the incremental displacements and the out-of-balance forces, hence the corresponding criteria were adopted to establish when the iteration process could be terminated.

5.4 Analysis Results and Interpretations

As stated in the previous section, all the three models were loaded subject to displacement control with a total beam-end displacement assumed equal to $5\Delta_{y,fix}$. Only for the linear model, *bcjel*, it was possible to apply completely the above displacement whereas for the models, *bcjnl* and *bcjnl-l*, the analyses stopped to run at an earlier stage which was different for each of the two models. The cause of the interruption was denounced by ABAQUS simply as a convergence failure of the plasticity algorithm without giving any indication on the points where such numerical failure occurred. As the criteria which controlled the convergence of the iterations in the previous increments was the one on the out of balance forces and the use of displacement control allows path with negative slope in load-displacement diagram to be described, it was suspected that the convergence failure was due to the occurrence of a snap-back phenomenon [Crisfield, 1982; de Borst and Nauta, 1985; Crisfield and Wills, 1988]. In a first instance, then, the analysis was restarted with a big value of the tolerance for the out of balance force, but only after one increment the analyses stopped again. Thereafter, it was attempted first to decrease the size of the elements around the joint corners and then to use a trick which is considered to be helpful with a softening or fracturing material such as concrete. The trick involved superimposing on the model of the structure another linear elastic structure (with the same nodes and elements) with a very small elastic stiffness. The latter was meant to stop the model structure falling 'totally apart' [Crisfiel, 1997], but also in these circumstances no improvement was observed for the progress of the solution. Hence, the above difficulties in getting at least a convergent solution were attributed to the specific numerical implementation of the concrete non-linearities in ABAQUS. Nevertheless, given the objectives this study purported to address, also the results obtained for the models *bcjnl* and *bcjnl-l*, allowed some considerations to be drawn as they described, however, situations which were beyond the first cracking.

Particularly interesting is to compare the stress paths in the joint of the three models at different values of the applied end beam displacement and observe how the stresses redistribute within the joint. **Fig. 5.7** gives an overview of the stresses in the complete subassemblage in the case of the linear model whereas **Fig. 5.8** gives some idea of the stresses in the joint for different values of the displacement applied. The external loads applied to the joint panel zone were resisted by stress states in which both tensile and compressive components were present. Completely different picture appeared in the case of the models *bcjnl* and *bcjnl-l* where non-linearity of the concrete was taken into account. Further to the application of the first displacement increments both the two models behaved linearly as the maximum induced tensile stress was less then σ_{ct}. First cracks, which the model assumes occurring when the principal tensile stress is equal to the tensile strength, were

computed in the two models at the same value of the applied load. At this stage the stress path in teh joint was more or less the same whereas it started to be different as the displacements were increased. **Fig. 5.9** depicts the principal stress distribution within the connection of the model *bcjnl* at two different values of the displacement applied. It was noted that the contribution of the tensile side of the beam adjacent to the joint decreased as the displacement increased due to the progression of the cracking. This aspect is much more clear from **Fig. 5.10** where normal stress distributions in the beam concrete elements at the joint interface for the two levels of displacements were compared. As the displacement applied increased and cracking progressed, the size of the compressive strut was reduced due to the reduction of the intact compressive concrete side at the joint boundary. In the model *bcjnl-l* a greater size of the compressive strut was observed than the one present in the model *bcjnl*, **Fig. 5.11**. Even in the model *bcjnl-l* the external loads applied to the joint boundary had to be equilibrated by stress states which were dominantly compressive as the joint was modelled with non-linear behaviour. The difference from the model *bcjnl* arose from the load distribution on the joint boundary. **Fig. 5.12** reports normal stress distribution on the joint boundary in the model *bcjnl-l*. It is noted that the compressive side is greater than the one present in the model *bcjnl*, **Fig. 5.10**, despite a lower average compressive stress. The previous figures depicting the internal stress flow within the joint visualize clearly that at the considered stages there is a main compressive stress state which is formed basically along the diagonal line of the connection. It can be said for grant that under monotonic loading such pattern of the principal compressive stresses will persist throughout the whole lateral displacement history. In fact, the strut mechanism can be made ineffective only if compressive actions on the joint boundary are reduced. This situation may occur for example if a full vertical depth crack forms along the joint boundary. Prerequisite for the occurrence of a such crack is to subject the subassemblage under intense cyclic loading. As a result, the reinforcement will go well within the inelastic range so as not to have the closure of the crack upon reversal of the loading. Hence, this behaviour cannot be detected under monotonic loading as it is a typical situation which is related to severe cyclic loading. A joint stress state picture which would indicate the importance of other mechanisms other than the strut one would have been shown up with a much more diffuse compressive stress state over the whole panel zone rather than concentrated along its diagonal.

Fig. 5.13 reports the computed load-deflection curve for the three models. Upon the application of the first increments of the load the three models exhibited same behaviour. As soon as the load applied was increased, the model *bcjnl* showed major deformability due to the presence of the non-linear elements in the beam and column regions adjacent to the joint where most of the cracking concentrated. The behaviour of the model *bcjnl-l* started to depart from the model *bcjnl* when cracking in the joint began to be important and spread over the panel zone.

In general, beam end displacement of a subassemblage loaded as shown in **Fig. 5.4** arises from the contribution of different mechanisms which are depicted in **Fig. 5.14**. **Fig. 5.14a** refers to the contribution of elastic and inelastic deformation along the length of the members of the subassemblage. In an elastic system, symmetric about the axis x and y, for example, the displacement of the beam-end would be given by:

$$\Delta = \frac{FL_b^3}{3EI_b}(1+\alpha) \tag{5.1}$$

where

$$\alpha = \frac{I_b L_c}{I_c L_b} \tag{5.2}$$

is an amplification term which accounts for the relative elastic stiffness among the members of the subassemblage. **Fig. 5.14b** refers to the effect known as fixed-end rotations. When the end moment

in the beam and/or column produces advanced cracking of the concrete , the bar, subjected to tension, undergoes slip depending on both the intensity of the moment and the deterioration of the bond caused by load reversals. This slippage localises at the beam-column interface where the above concentrated rotation occurs [Filippou, 1986; Russo, Zingone and Romano, 1990]. Finally, **Fig. 5.14c** refers to the shear deformation of the panel zone. As result of the shear distorsion of the concrete core, the faces of the joint are not more mutually orthogonal but a relative rotation will occur. Hence, if γ denotes such rotation, the contribution to the beam-end displacement can be estimated as given by:

$$\Delta_{s,j} = \gamma L_b \tag{5.3}$$

Owing to the assumptions built in to the analytical models of the present study, the contribution of the mechanism due to bond deterioration depicted in **Fig. 5.14b**, was not accounted for. Hence, it was possible to evaluate the importance of the deformation of the panel zone. As said previously, this is assimilated to a pure shear deformation described by an average shear strain. **Fig. 5.15** reports such contribution in the case of the model *bcjnl*. As was expected, the contribution to the overall displacement increased as the displacement increased.

The importance of the shear deformation of the panel zone in the case of a reinforced concrete connection can be appreciated if, once again, the internal stress flows are evaluated critically and assumed as starting point to estimate the deformation induced in the panel zone. On the premise that in the following only general ideas are given, it is assumed that the compressive strut is the only element to control the deformation of the panel. Due to the axial rigidity of the column, the deformation of the panel zone is shown in **Fig. 5.16a** whereas **Fig. 5.16b** depicts the simple mechanical model assumed to describe the panel deformation. The following assumptions are made:

1. Plane section remains plane at each joint face, and
2. Uniform distribution of the shear stress in the central core.

Referring to **Fig. 5.16b**, simple geometrical considerations lead to the following relation:

$$\gamma = \frac{\sigma_{av}}{E \sin\theta} \tag{5.4}$$

where

γ is the shear strain given by the variation of the angle between the two initially orthogonal faces of the joint,
θ is the inclination of the compressive strut on the horizontal
σ_{av} is the average compressive principal stress induced in the compressive strut.

In turn, σ_{av} can be related to the forces which are equilibrated by the compressive strut. If D_c denotes the axial force in the compressive strut and V_{ch} the horizontal shear force which is equilibrated by the compressive strut, then

$$\sigma_{av} = \frac{D_c}{A_{av}} \tag{5.5}$$

where

$$D_c = \frac{V_{ch}}{\cos\theta} \tag{5.6}$$

V_{ch} depends on the internal compressive concrete stresses and the bond stresses transferred within the compressive zone of the joint. Further to simple assumptions on the bond distributions, one can think of expressing the above fraction of the bond stresses in terms of the total force T_s+C_s applied to the bar, which in turn is function of the moment applied on the faces of the joint, M. Moreover, V_{ch} depends also on the shear stresses applied on the intact concrete, hence at the end a relation between γ, M and V would be expected.

In conclusion, it is of interest to observe that even in a linear model the above considerations can be applied and evaluate the assumption of joint rigidity. In this case, the simple mechanical model presents both the diagonals as resisting elements. One is the compressive strut whereas the other one is the tensile tie. Furthermore, their resisting size is also greater as the material is fully resisting. Therefore, the rigidity of the truss is big and the assumption of rigidity of the joint can be considered not producing appreciable approximations. This is no more true in the case of a reinforced concrete panel for a twofold consideration: firstly, there is no more the presence of the tensile tie and, secondly, as the cracking progresses at the beam-column interface, the strut size decreases, the average stress in the strut increases and hence an overall increases of the deformability of the panel zone is observed.

Concrete Properties	
Young Modulus, E_c	30000 MPa
Poisson's ratio	0.18
Compressive characteristics	
Compressive strength, σ_{cmax}	40 Mpa
$\sigma_{1c}=(0.7*\sigma_{cmax})$	28 Mpa
$\sigma_{cu}=\sigma_{2c}$ $(0.8*\sigma_{cmax})$	32 Mpa
ε_0	0.002
ε_u	0.003
$\varepsilon_{p0}=\varepsilon_0-\sigma_{cmax}/E$	0.00067
$\varepsilon_{pu}=\varepsilon_u-\sigma_{cu}/E$	0.00193
$\varepsilon^{p0}=\log(1+\varepsilon_{p0})$	0.00067
$\varepsilon^{pu}=\log(1+\varepsilon_{pu})$	0.00193
Tensile characteristics	
Tensile strength, σs_{ct}	3.6 MPa
ε_{ct}	0.00012
ε_{cts}	0.002
$\varepsilon_{ct}=\varepsilon_{ct}+\varepsilon_{cts}$	0.00212

Table 1 Concrete Properties adopted in the FE model

Steel Properties	
Young Modulus, E_s	200000 MPa
Poisson's ratio	0.20
Yield Stress, f_y	320
Ultimate Stress, f_u	430
Hardening Modulus, H_s $(0.04*E_s)$	8000
ε_y	0.0016
ε_u	0.0154
$\varepsilon_{pu}=\varepsilon_u-f_u/E_s$	0.0132
$\varepsilon^{pu}=\log(1+\varepsilon_{pu})$	0.0131

Table 2 Steel Properties adopted in the FE model

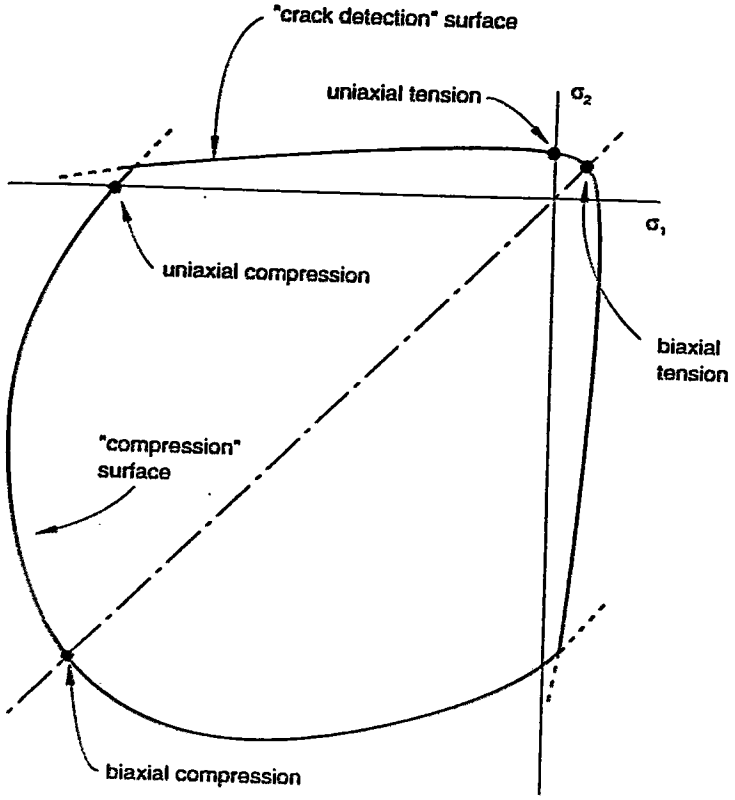

Fig. 5.1 Concrete failure surfaces in plane stress

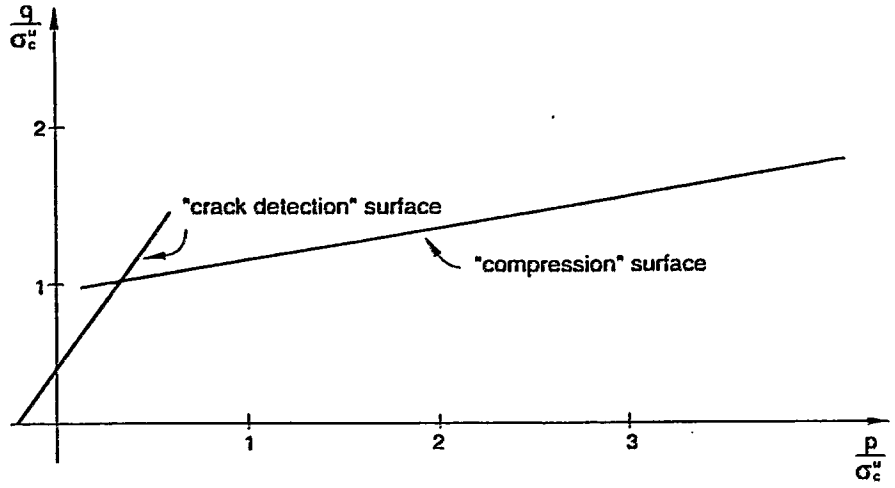

Fig. 5.2 Concrete failure surfaces in the (p-q) plane

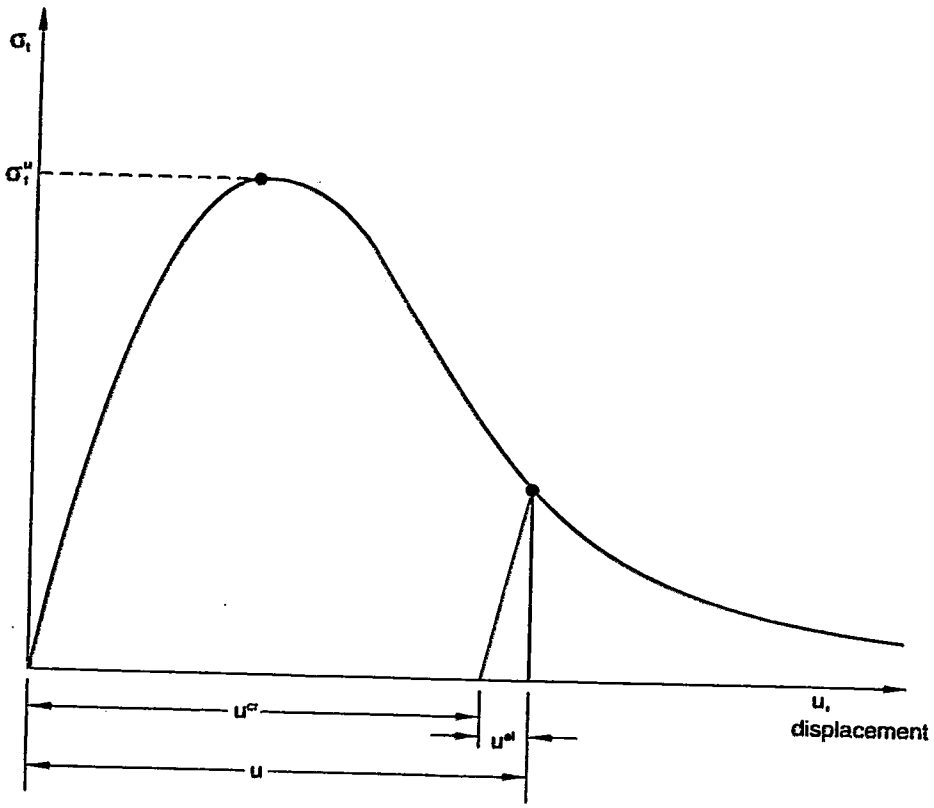

Fig. 5.3 Cracking behaviour based on fracture energy

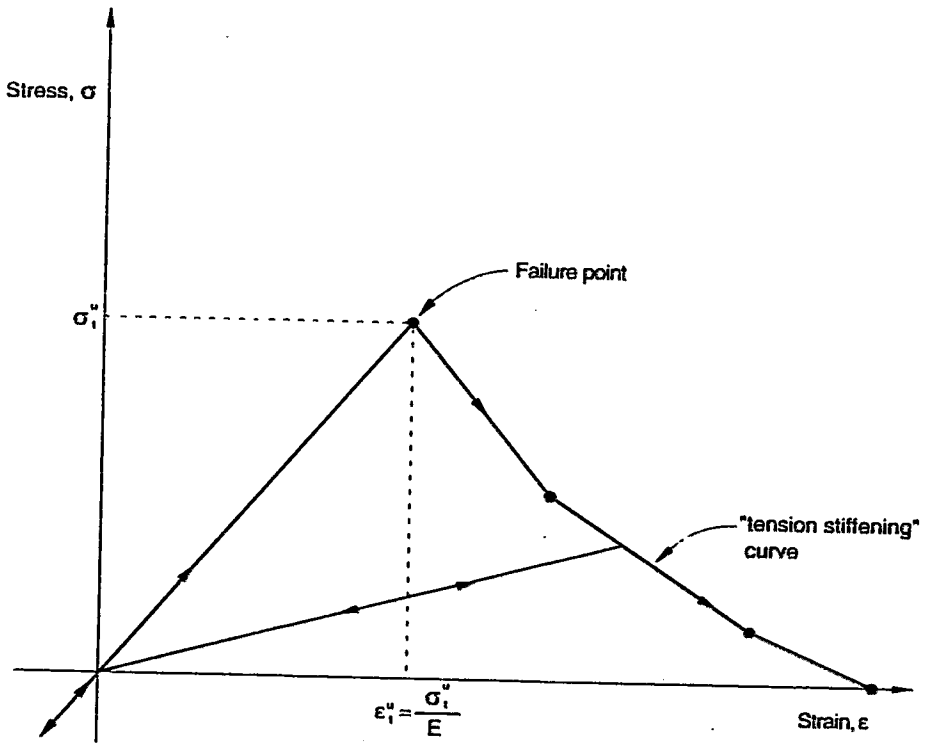

Fig. 5.4 Tension stiffening model

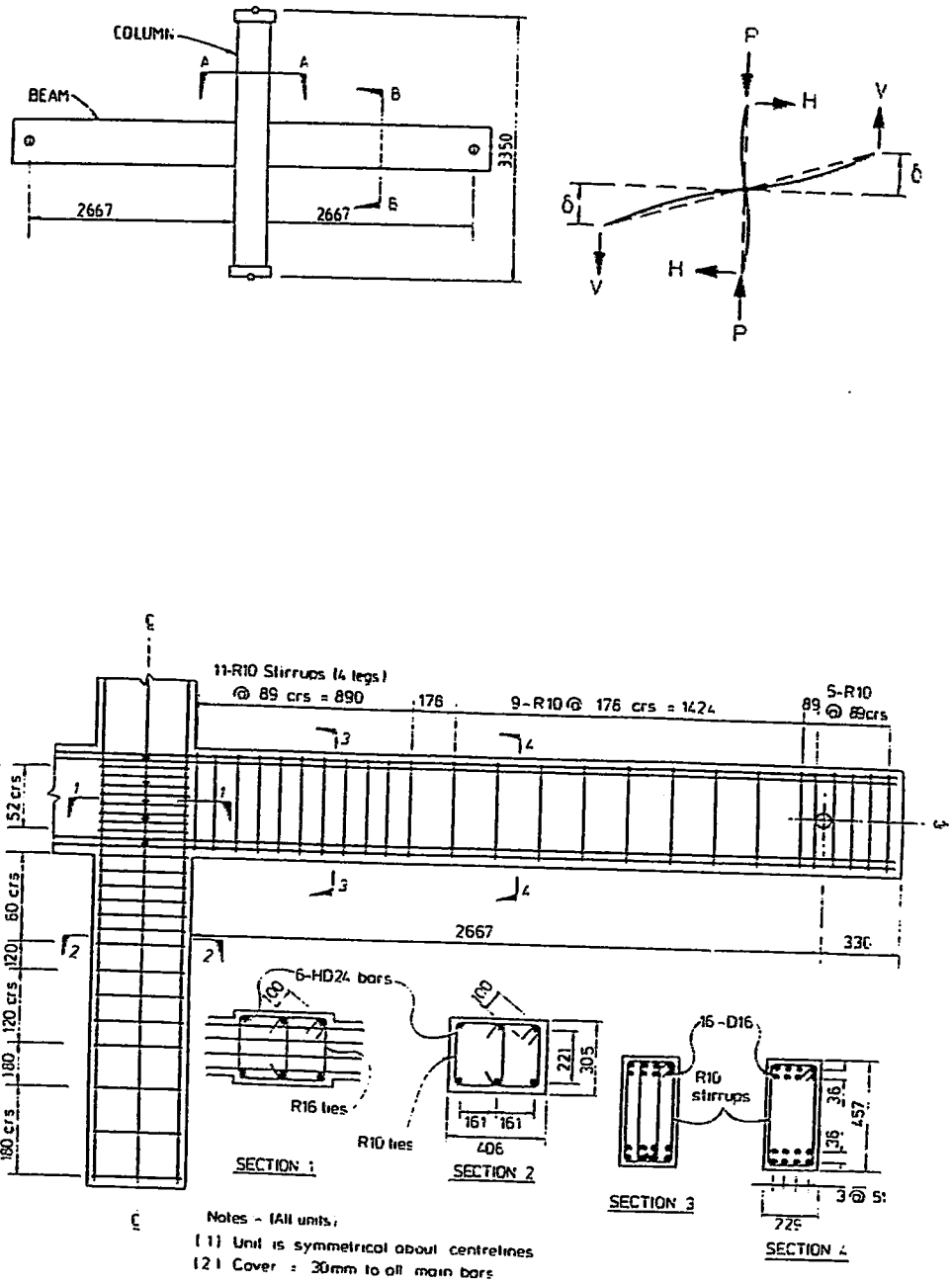

Fig. 5.5 Geometry and reinforcement details along with test set-up

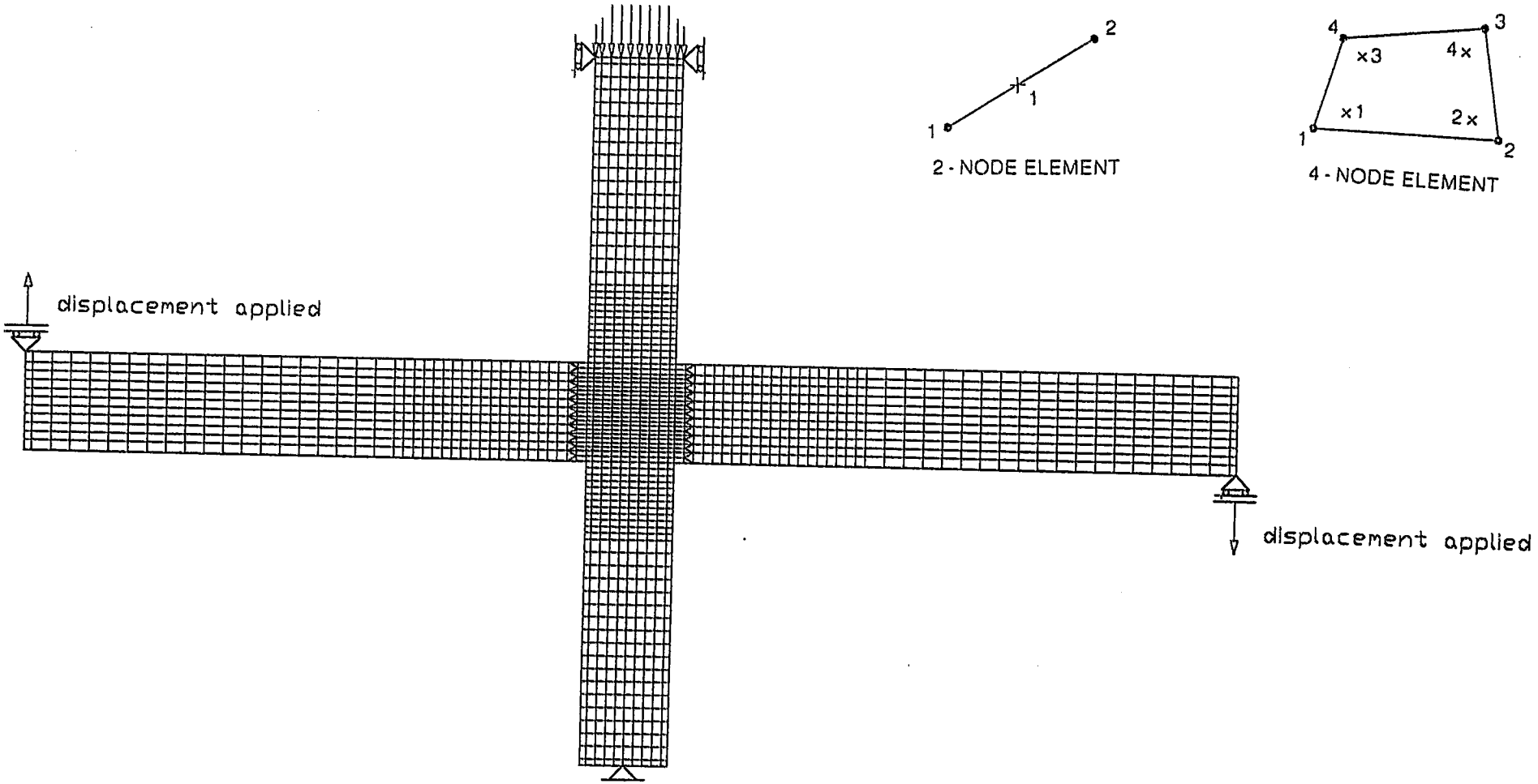

Fig. 5.5 Finite element mesh, with boundary and loading conditions

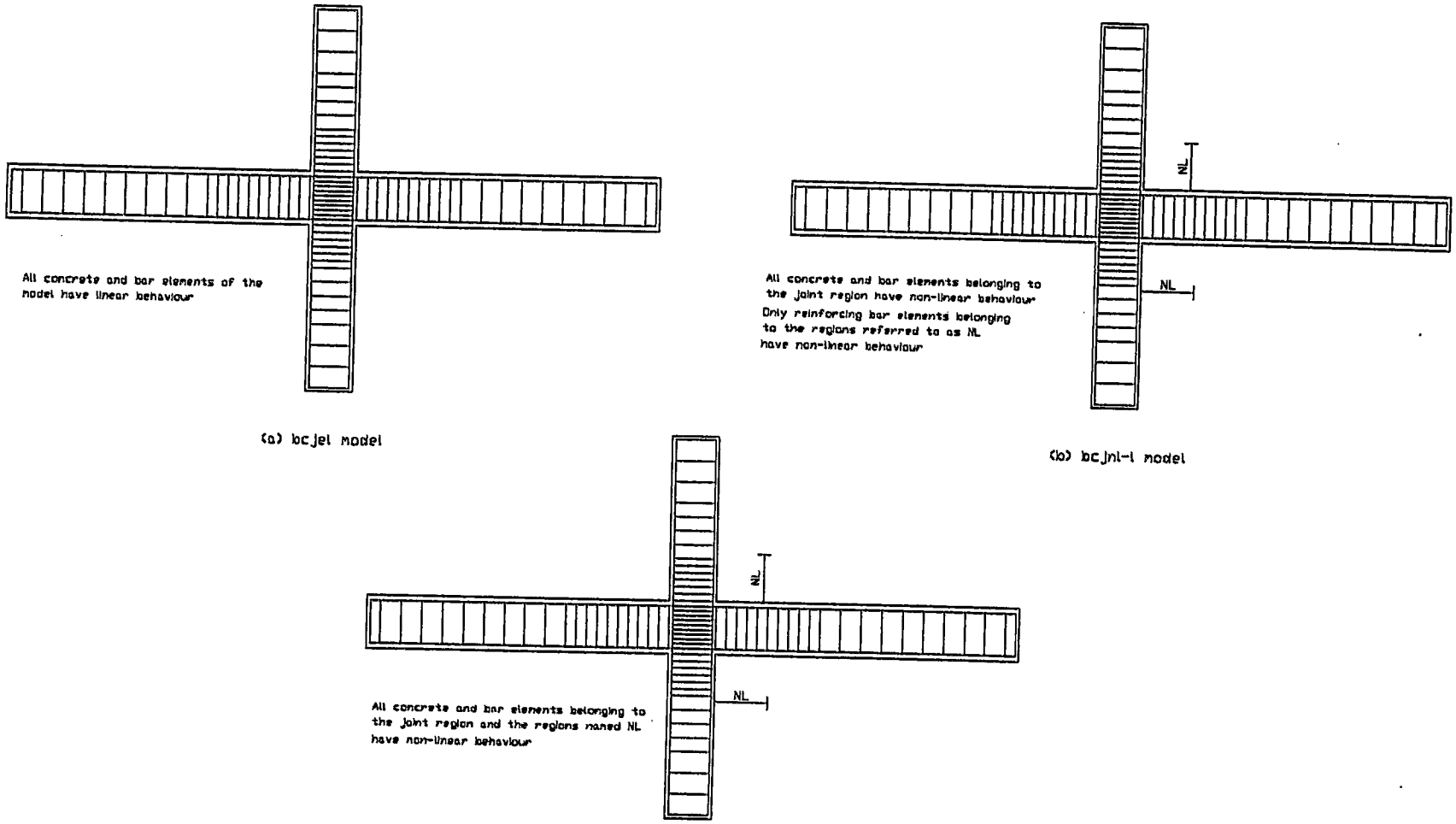

Fig. 5.6 Models analysed in the present study

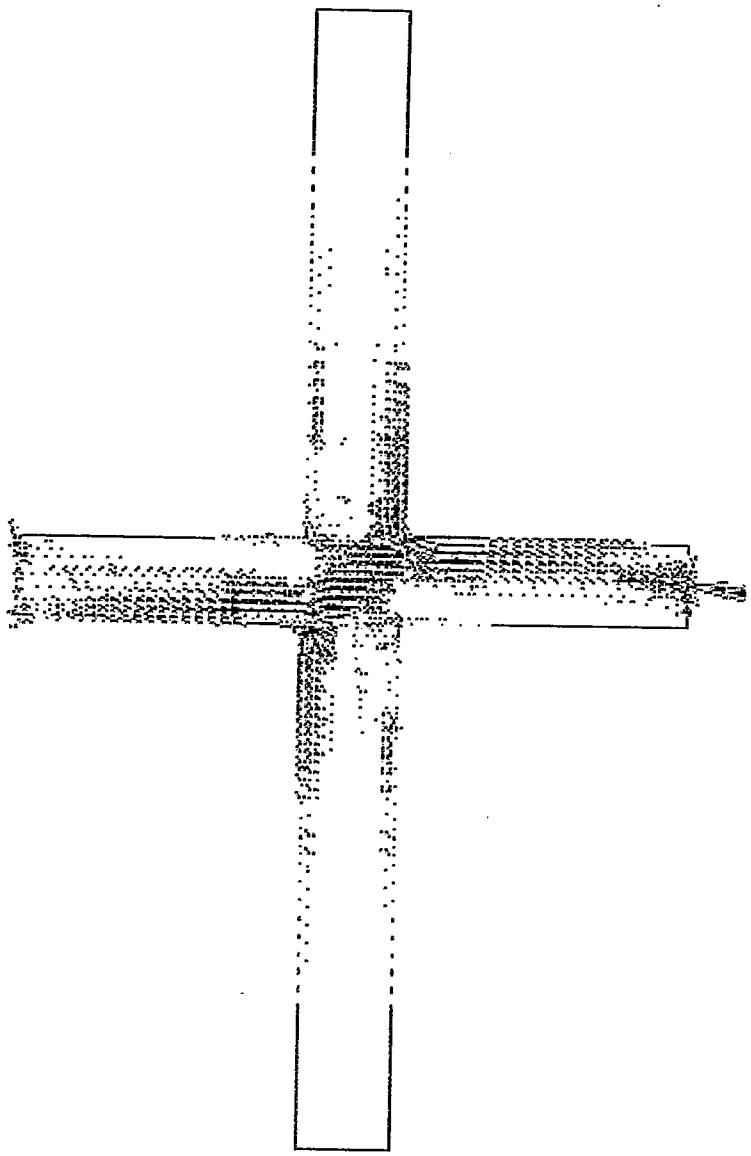

Fig. 5.7 Overview of the principal stresses in the subassemblage, bcjnl model, $\Delta=0.456\Delta_{y,fix}$
red principal tensile stresses
blu principal compressive stresses

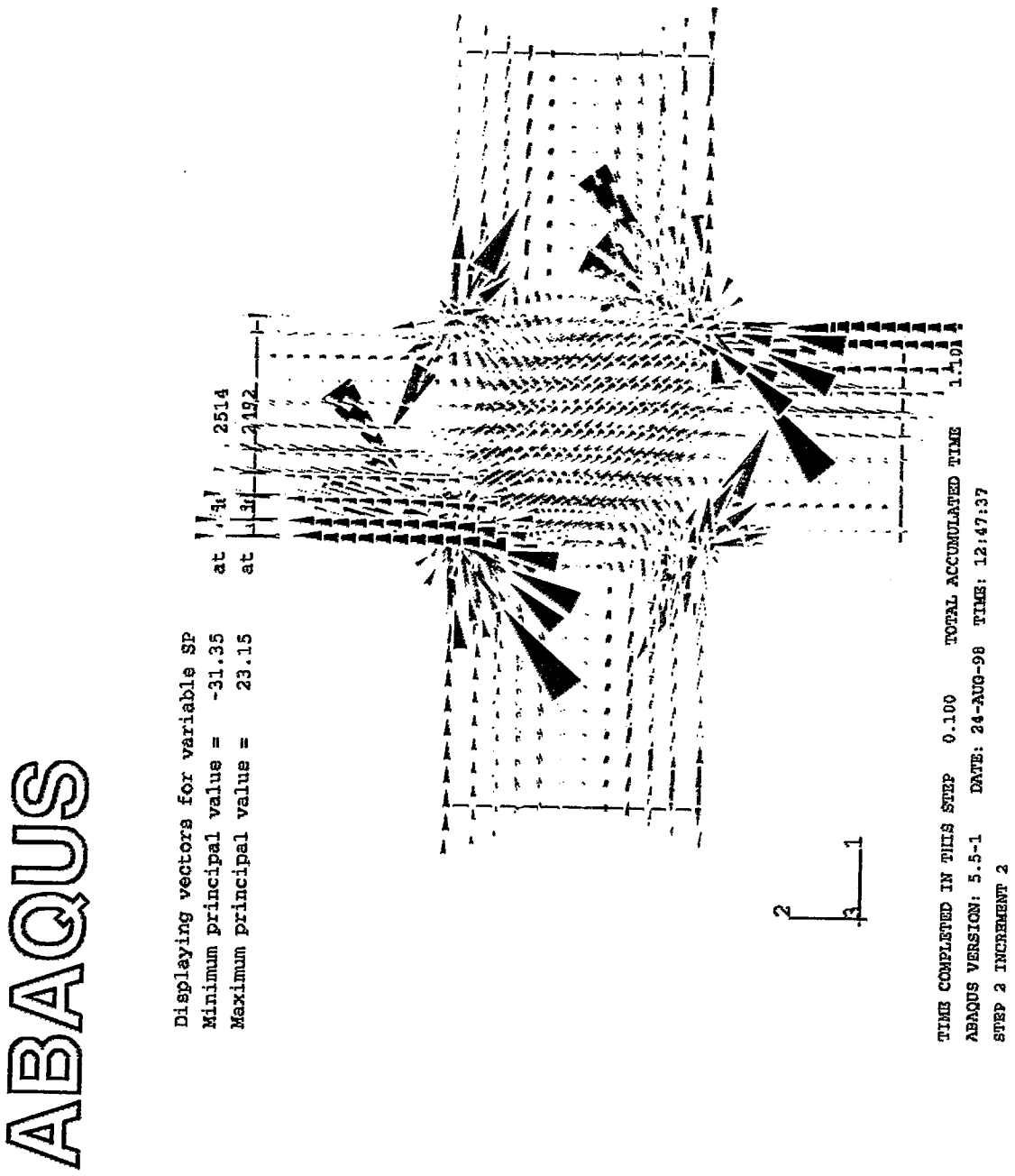

Fig. 5.8a Principal stresses within the joint, **bcjel** model, $\Delta=0.5\Delta_{y,fix}$
red principal tensile stresses
blu principal compressive stresses

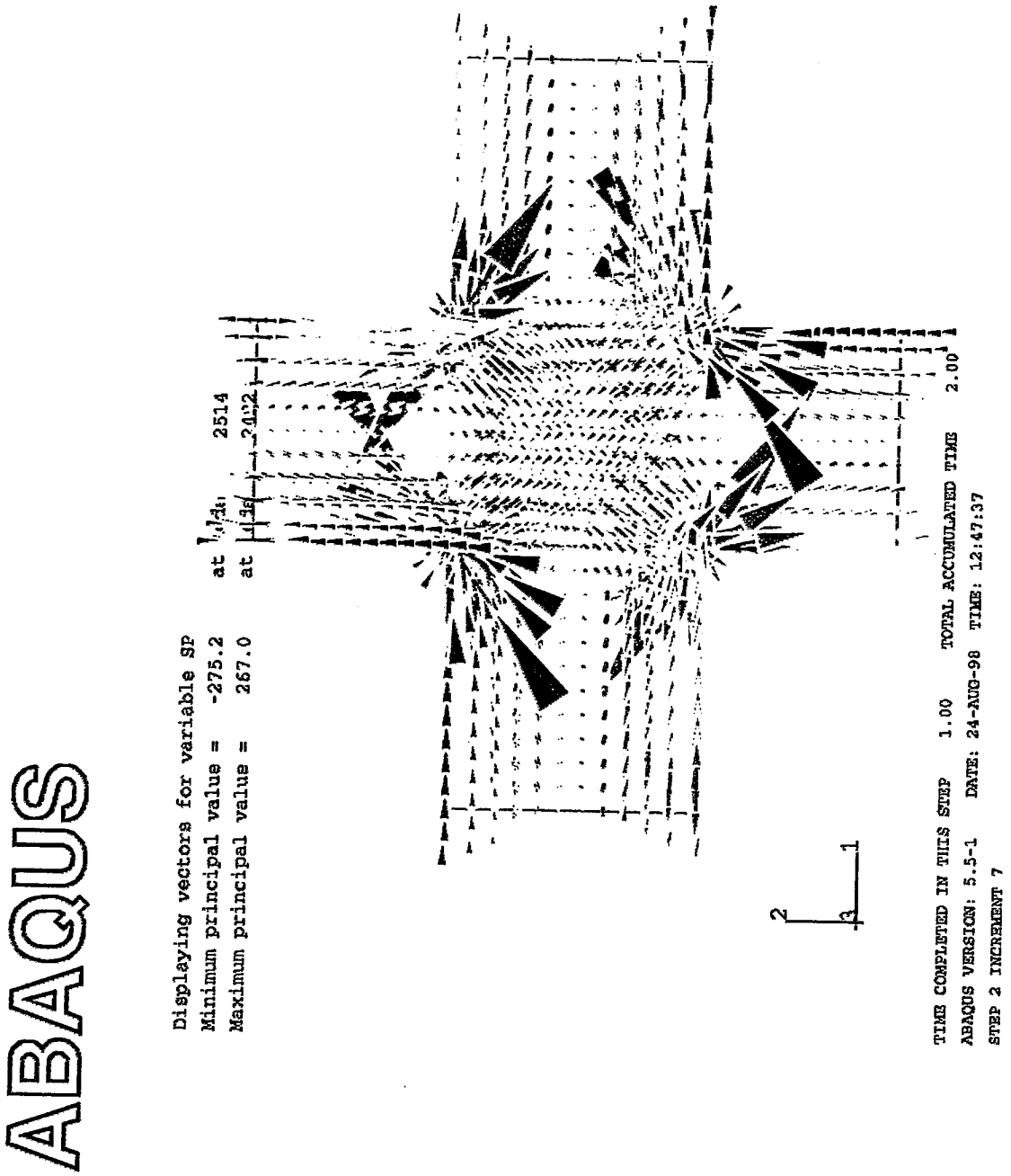

Fig. 5.8b Principal stresses within the joint, **bcjel** model, $\Delta=5\Delta_{y,fix}$
red principal tensile stresses
blu principal compressive stresses

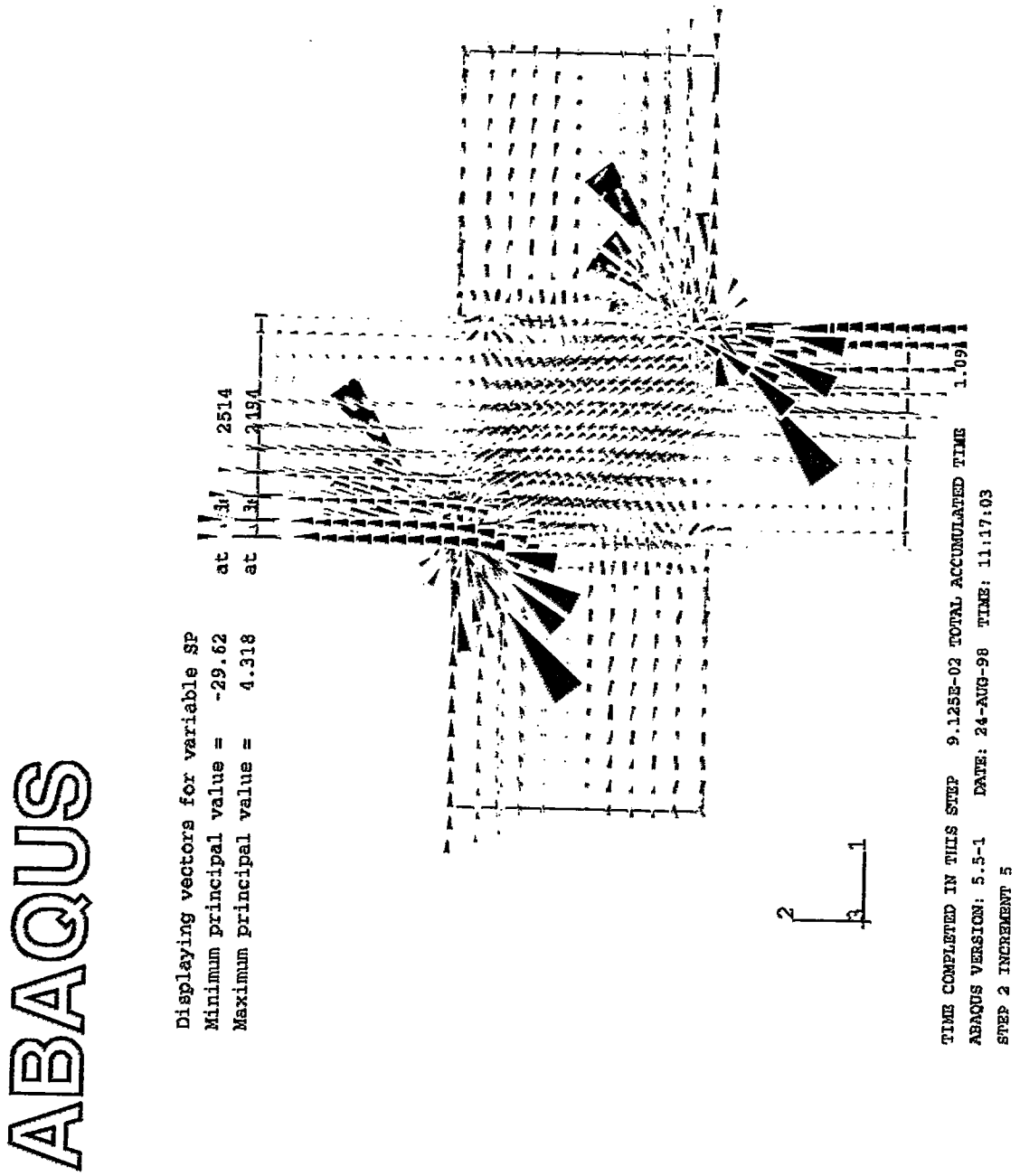

Fig. 5.9a Principal stresses within the joint, **bcjnl** model, $\Delta=0.456\Delta_{y.fix}$
red principal tensile stresses
blu principal compressive stresses

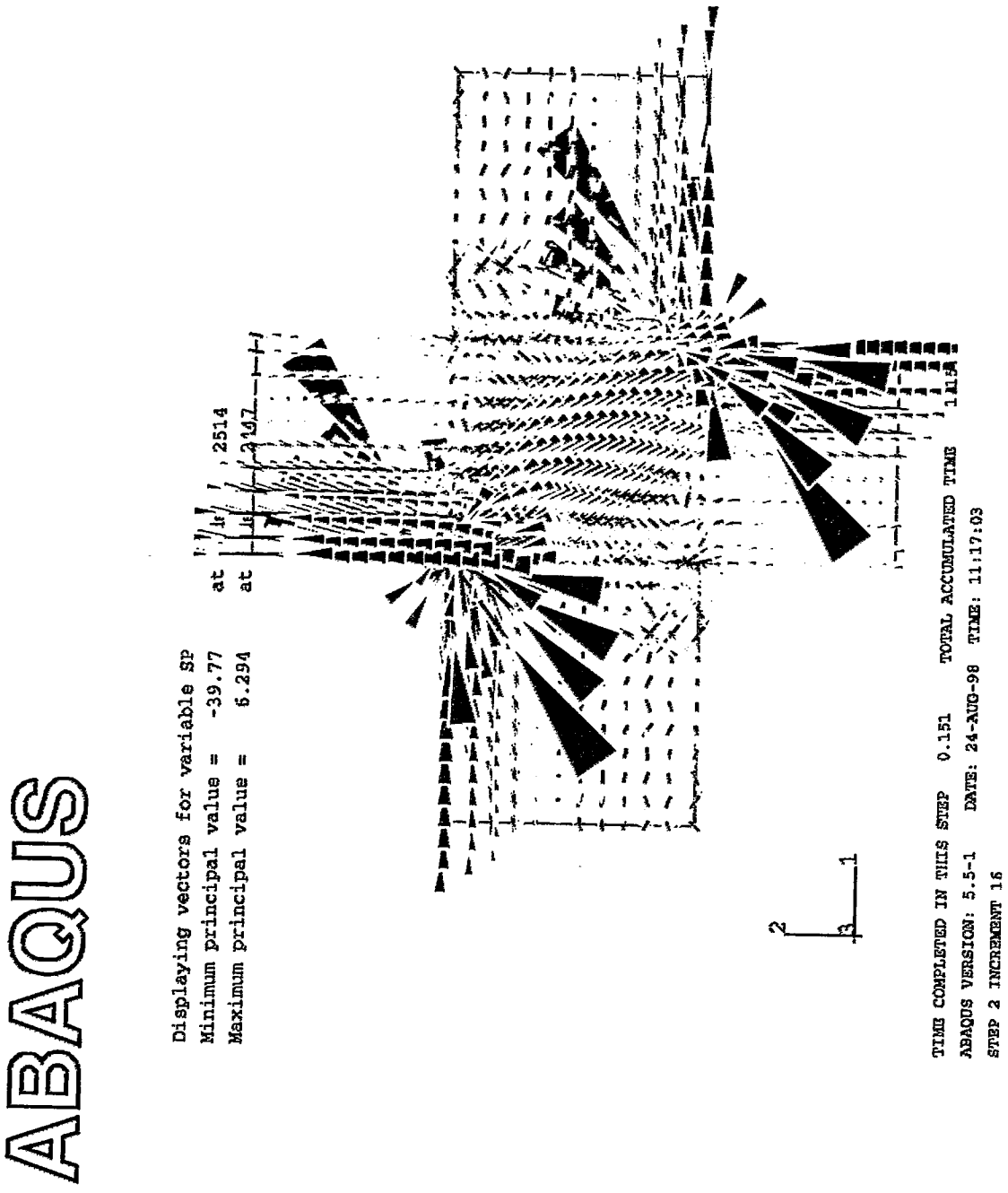

Fig. 5.9b Principal stresses within the joint, **bcjnl** model, $\Delta=0.755\Delta_{y,fix}$
red principal tensile stresses
blu principal compressive stresses

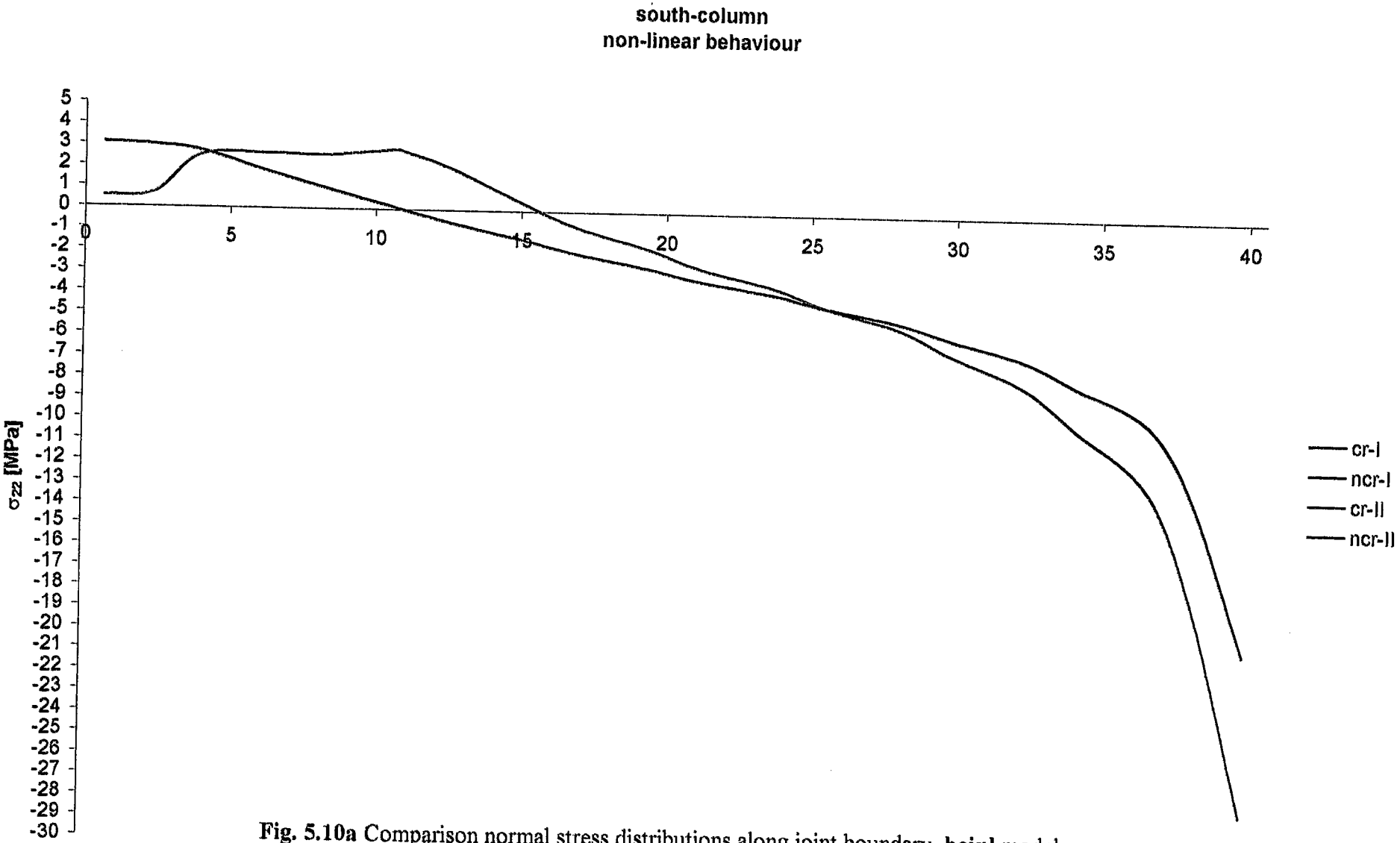

Fig. 5.10a Comparison normal stress distributions along joint boundary, **bcjnl** model

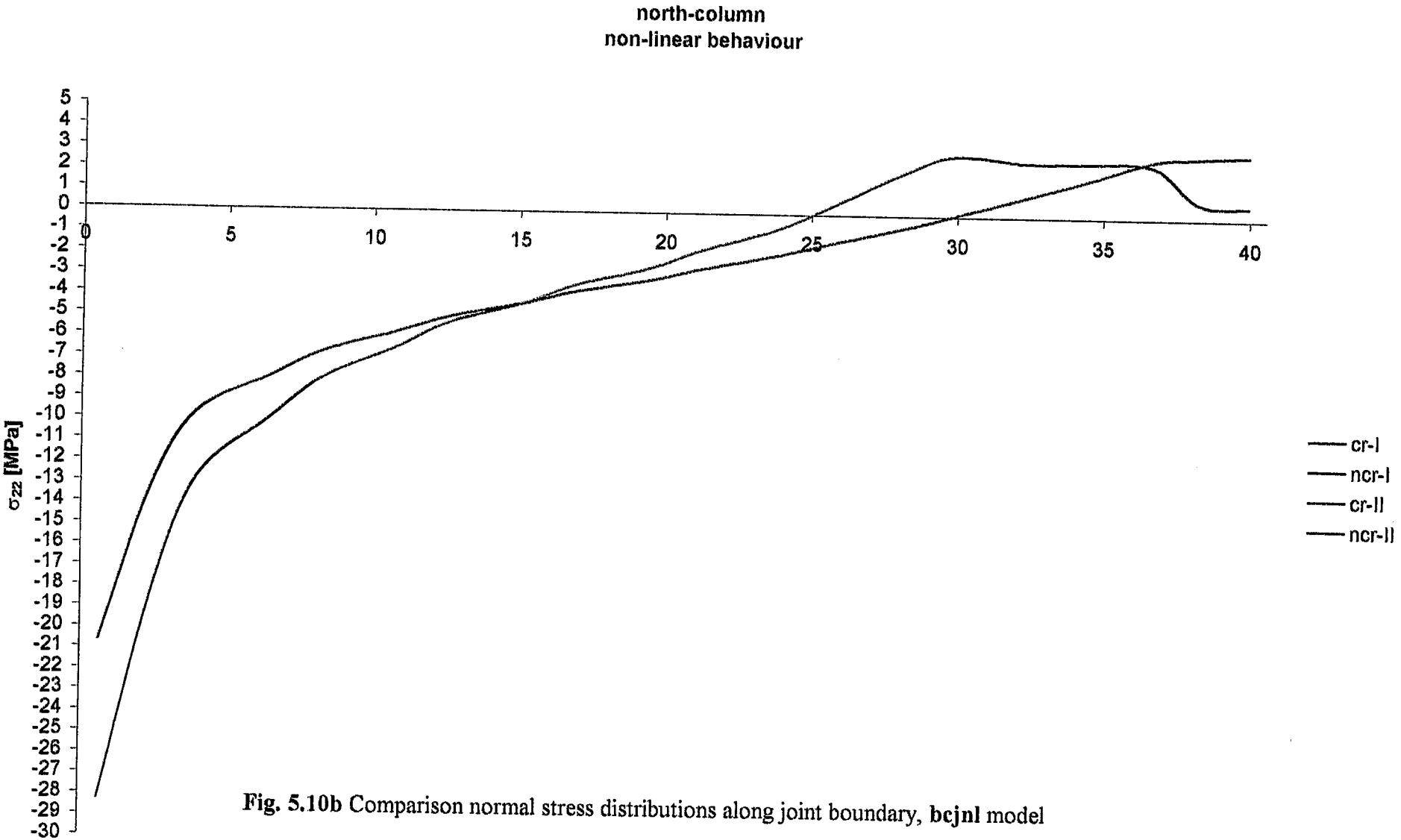

Fig. 5.10b Comparison normal stress distributions along joint boundary, **bcjnl** model

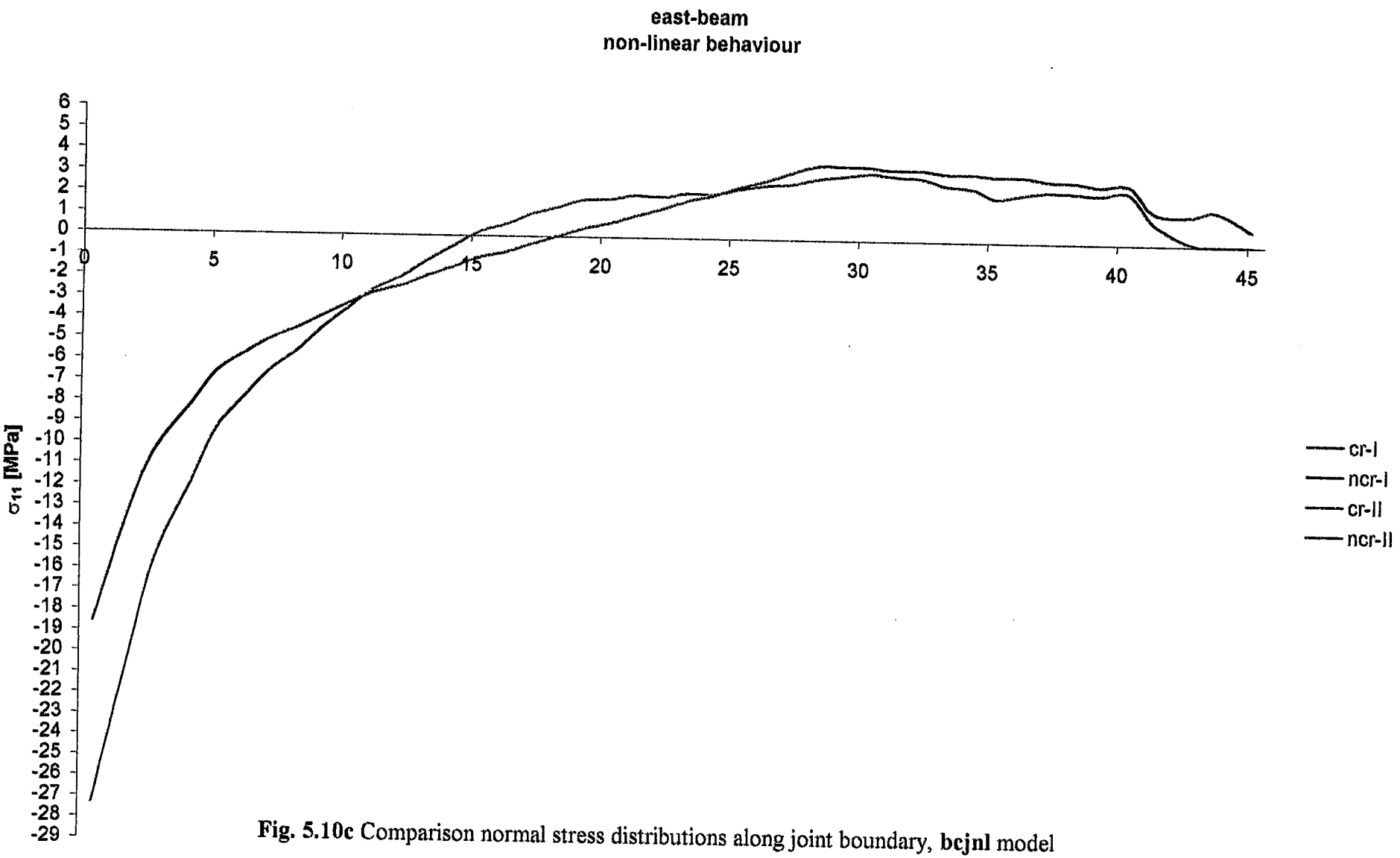

Fig. 5.10c Comparison normal stress distributions along joint boundary, **bcjnl** model

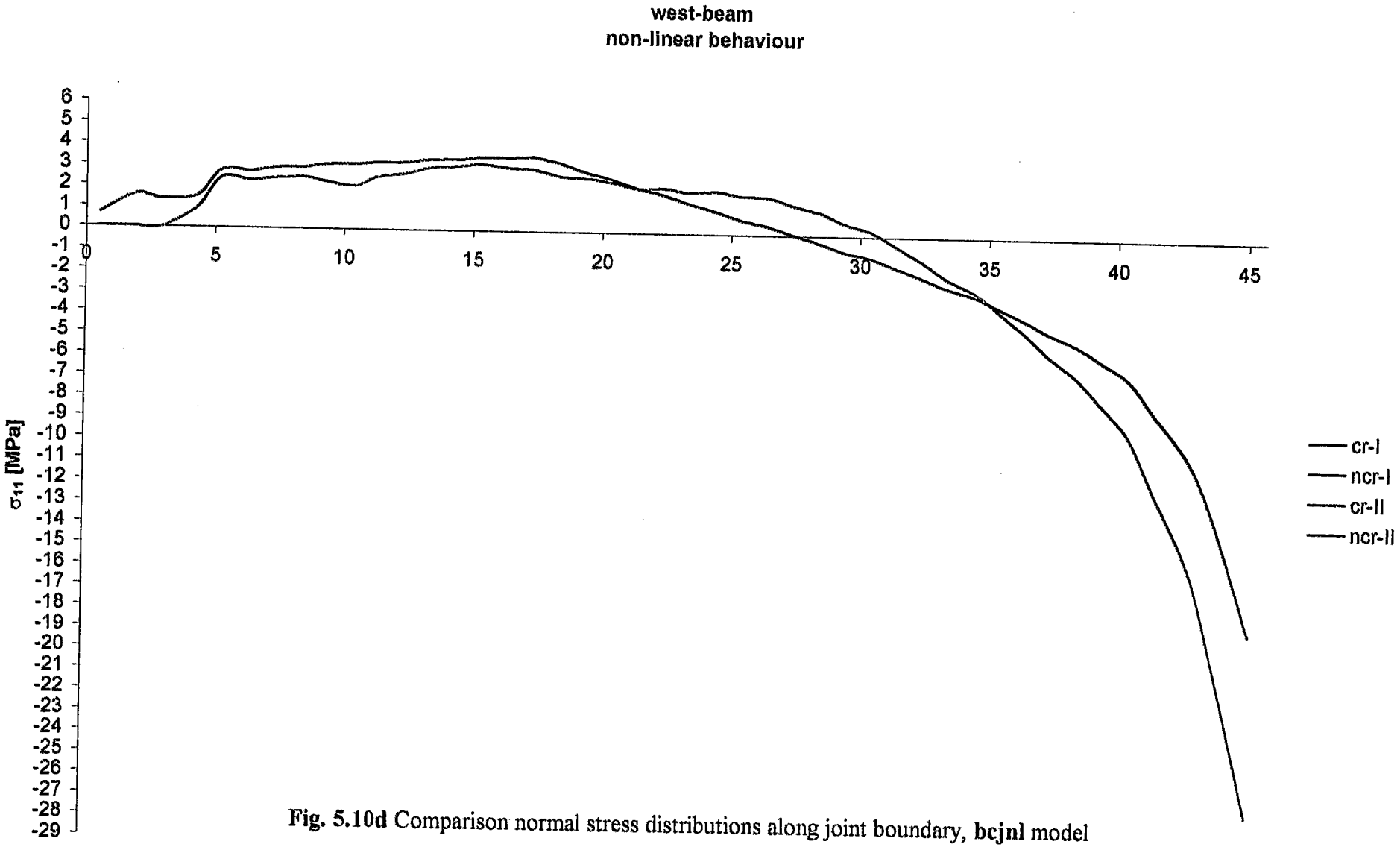

Fig. 5.10d Comparison normal stress distributions along joint boundary, **bcjnl** model

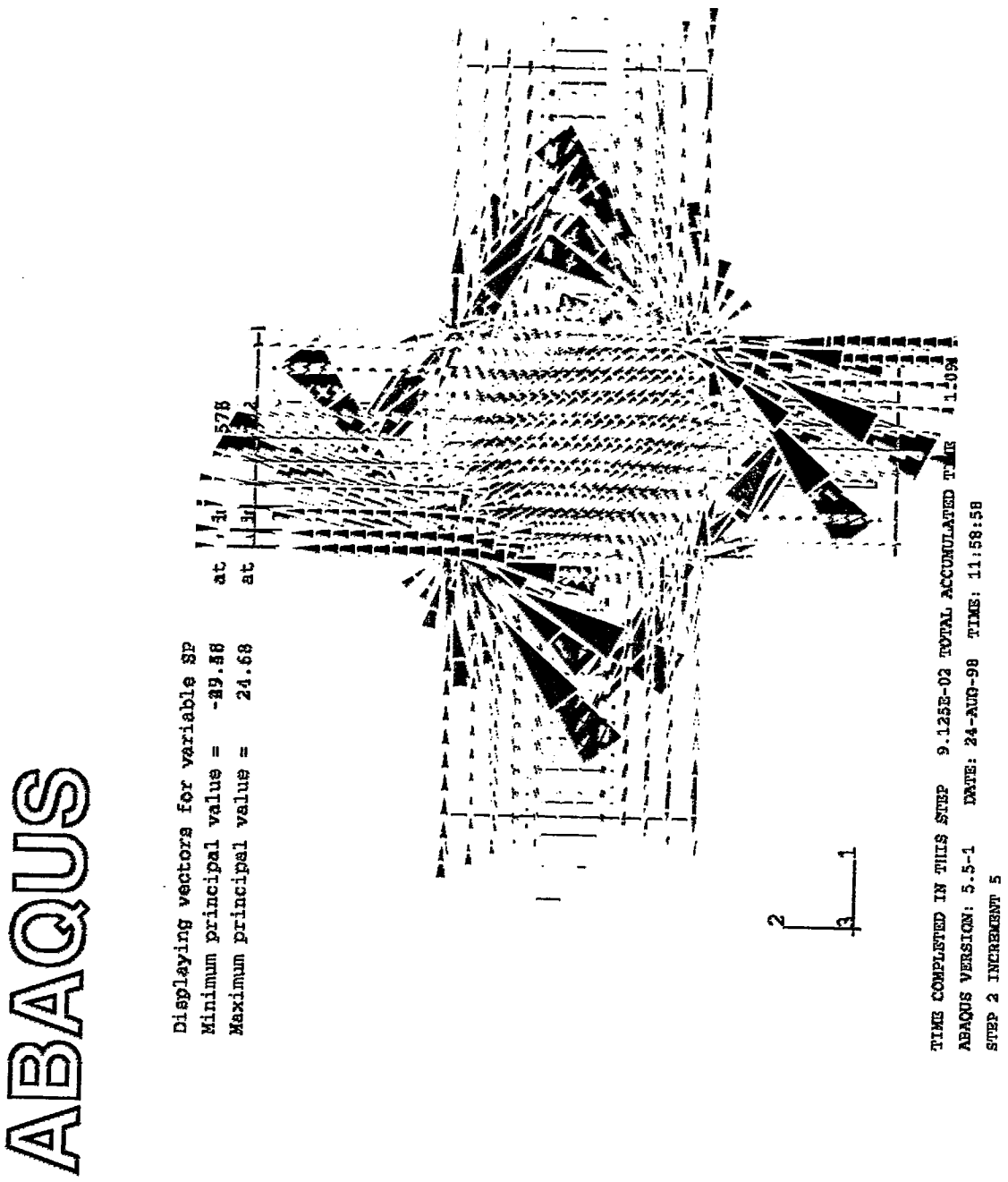

Fig. 5.11a Principal stresses within the joint, **bcjnl-l** model, $\Delta=0.456\Delta_{y,fix}$
red principal tensile stresses
blu principal compressive stresses

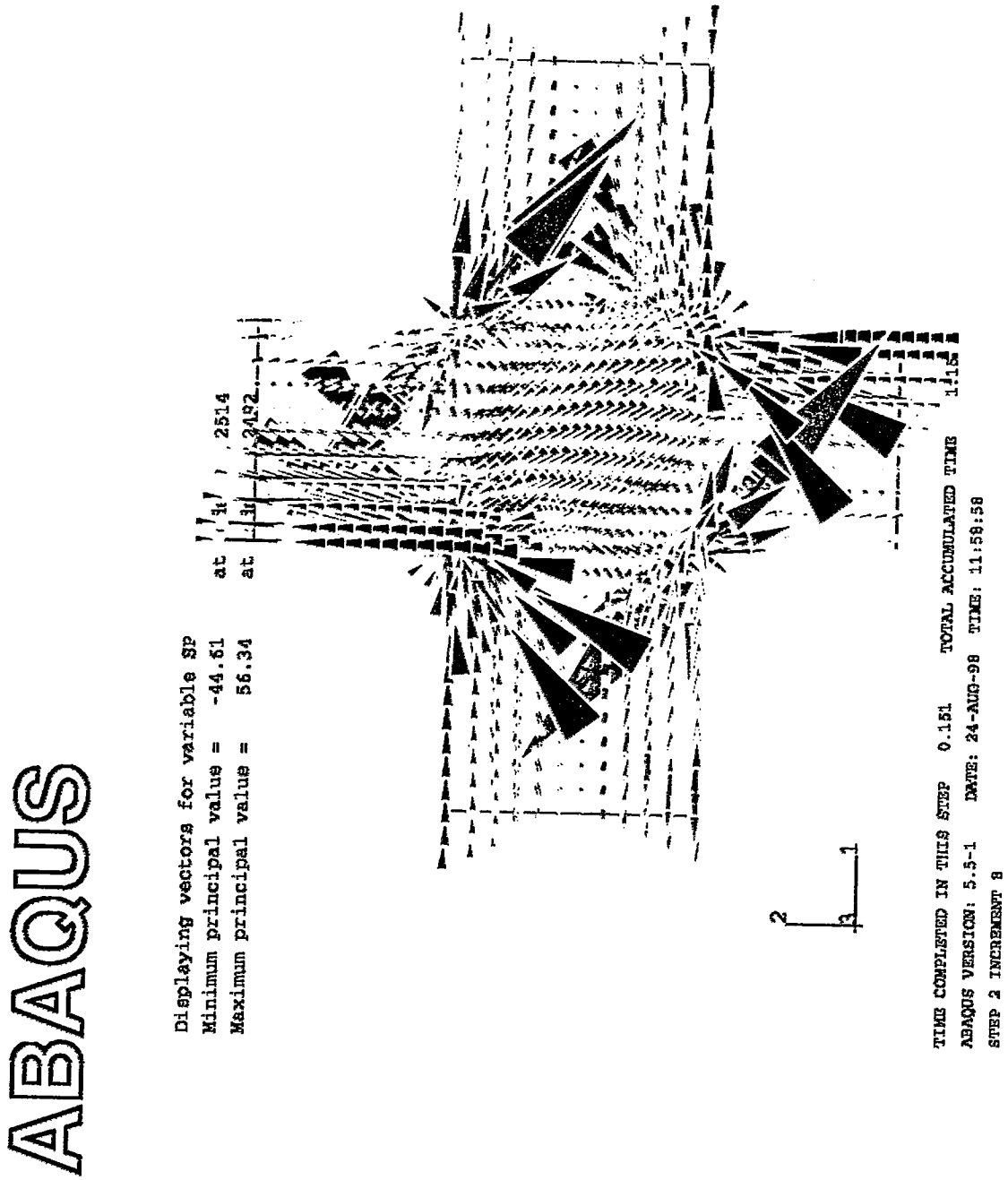

Fig. 5.11b Principal stresses within the joint, **bcjnl-l** model, $\Delta=0.755\Delta_{y,fix}$
red principal tensile stresses
blu principal compressive stresses

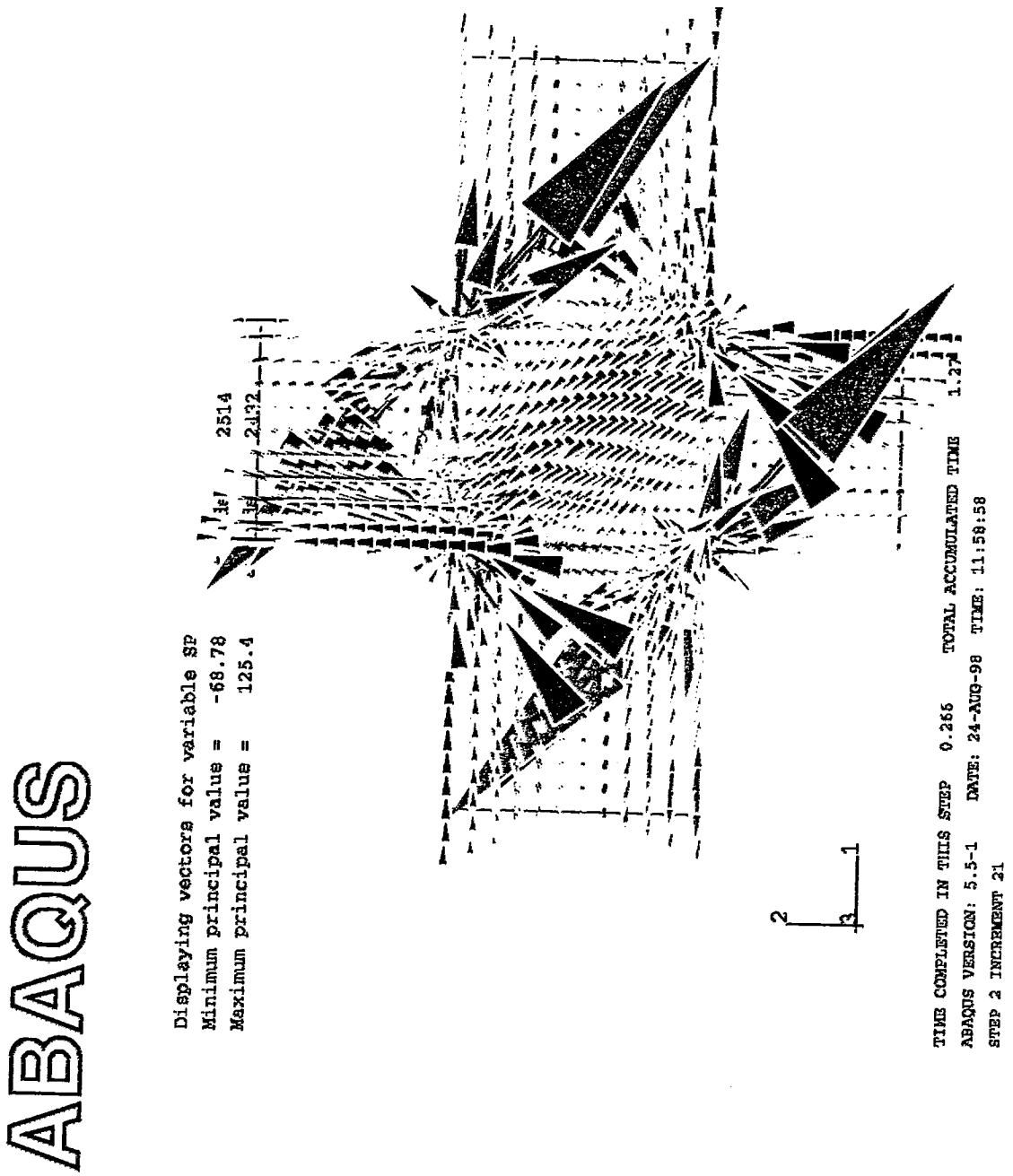

Fig. 5.11c Principal stresses within the joint, **bcjnl-l** model, $\Delta=1.33\Delta_{y.fix}$
red principal tensile stresses
blu principal compressive stresses

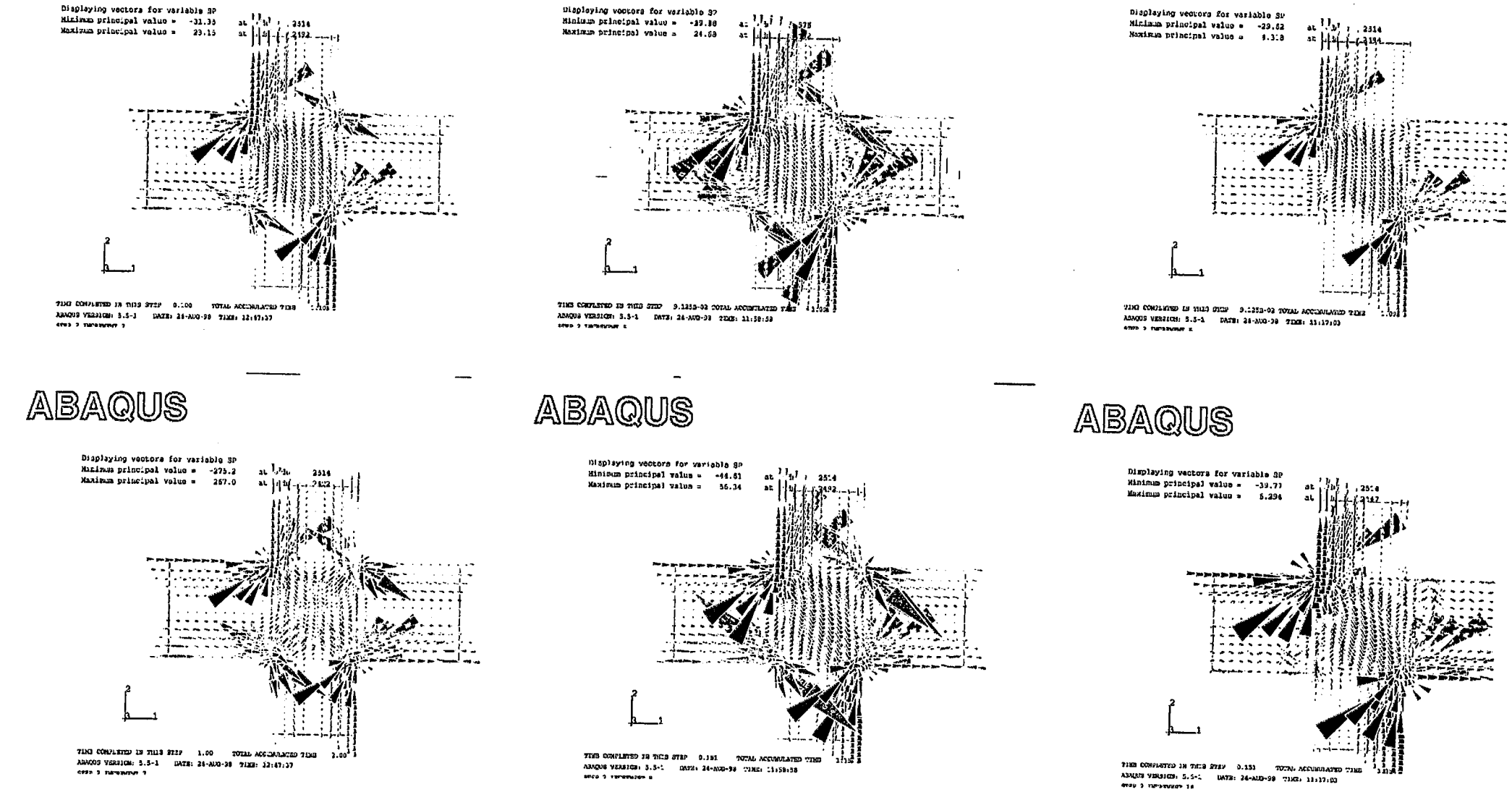

bcjel **bcjnl-l** **bcjnl**

Fig. 5.12 ANALYSIS RESULTS: Principal Stress Paths

red tension
blu compression

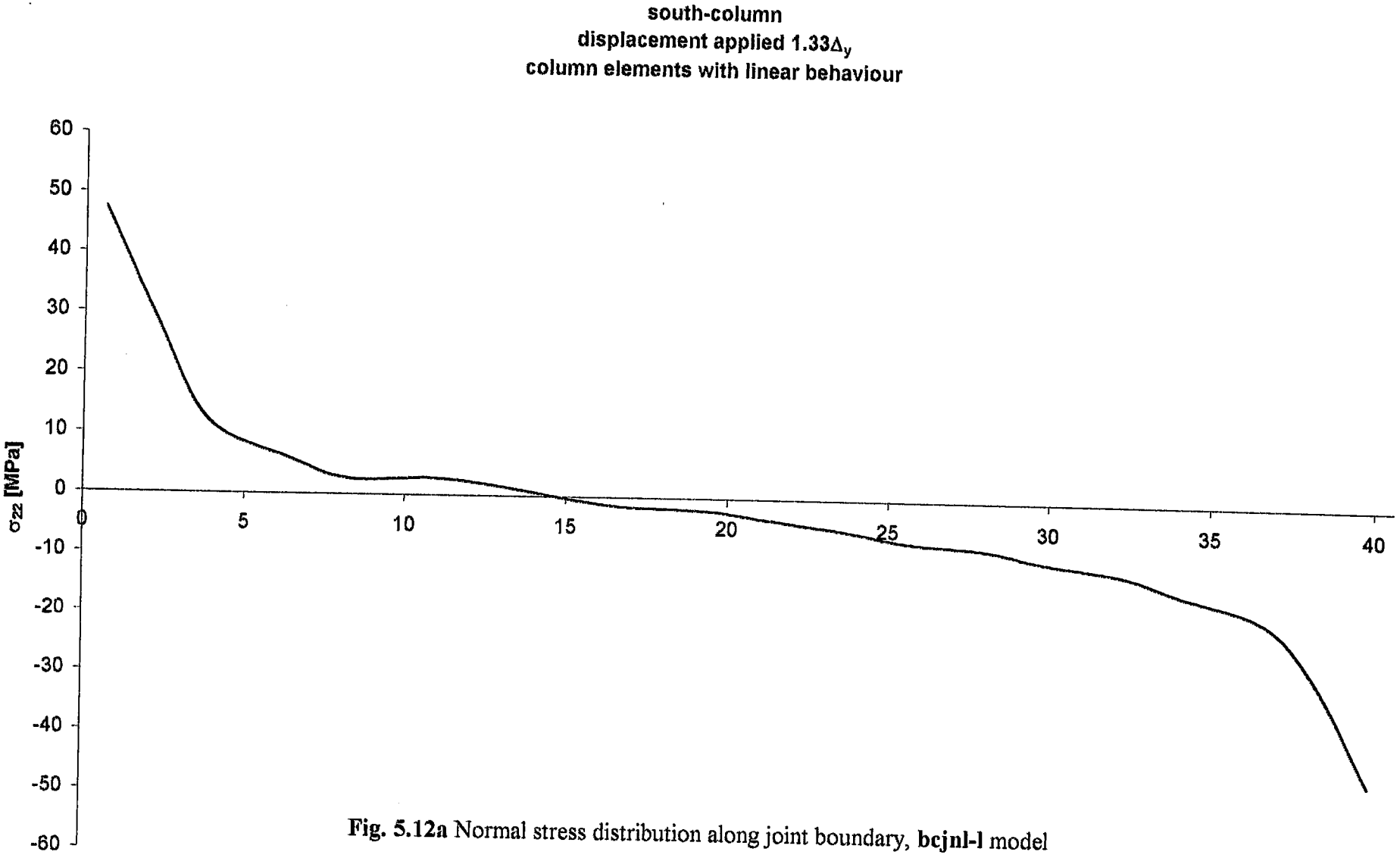

Fig. 5.12a Normal stress distribution along joint boundary, **bcjnl-l** model

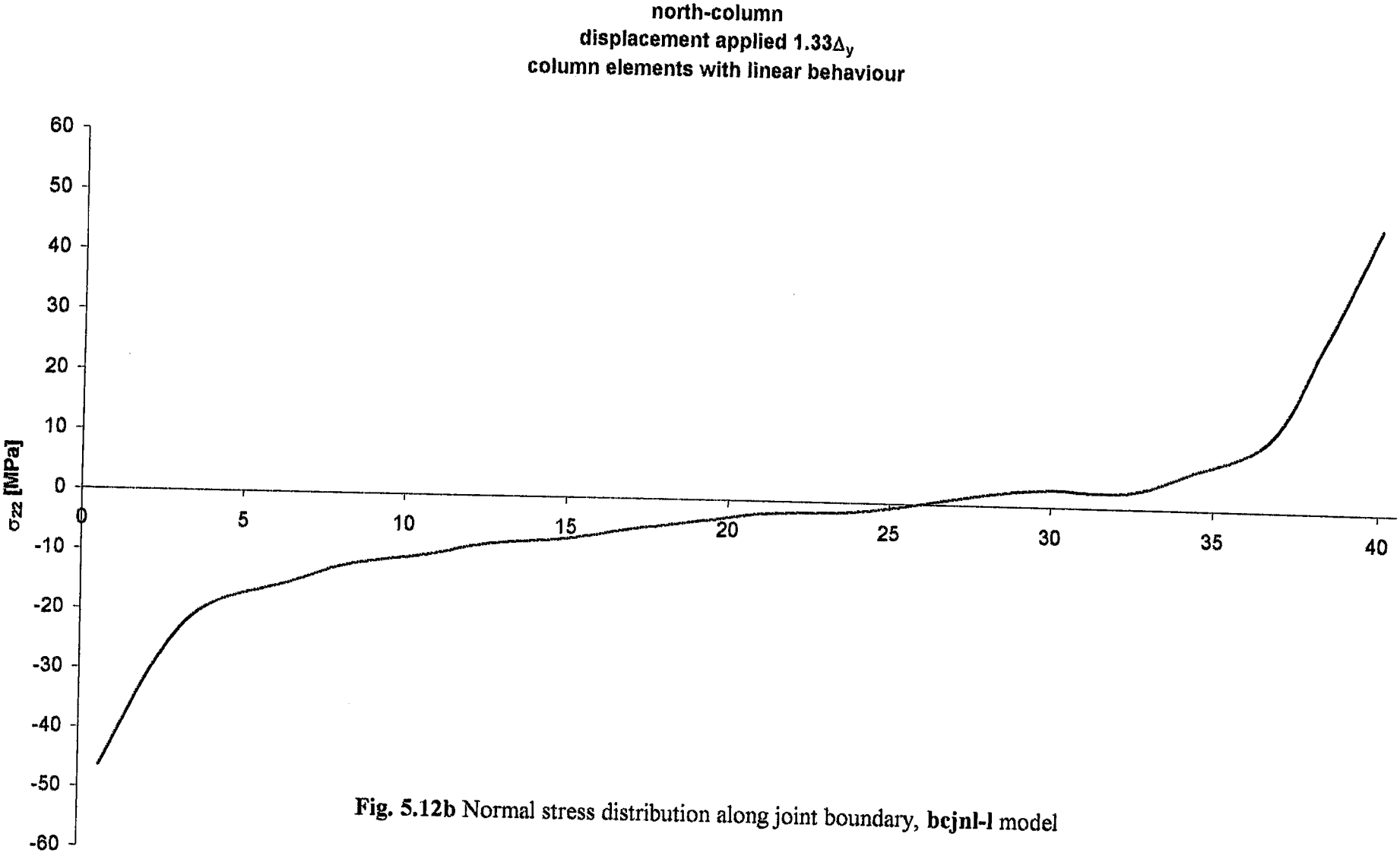

Fig. 5.12b Normal stress distribution along joint boundary, **bcjnl-l** model

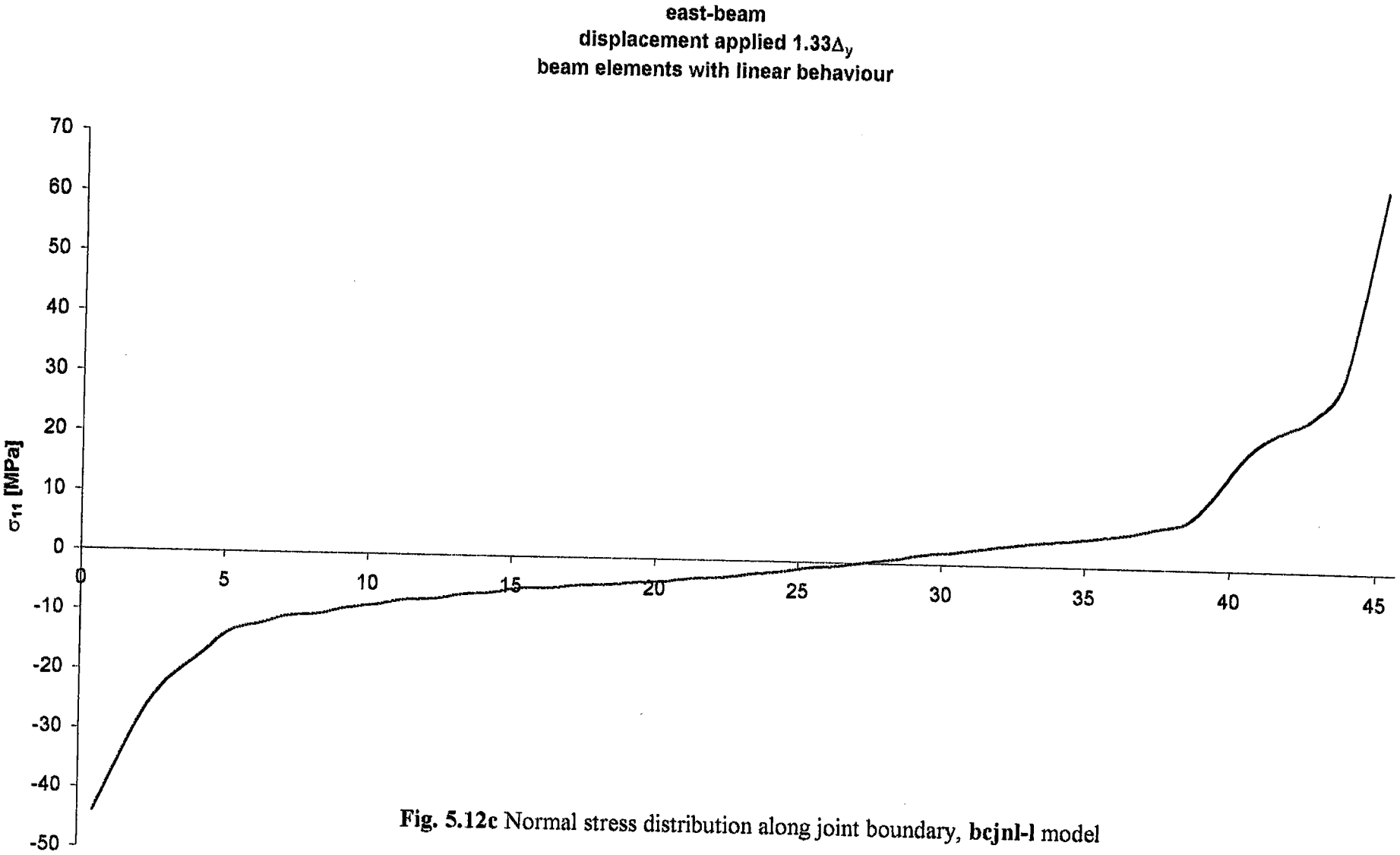

Fig. 5.12c Normal stress distribution along joint boundary, **bcjnl-l** model

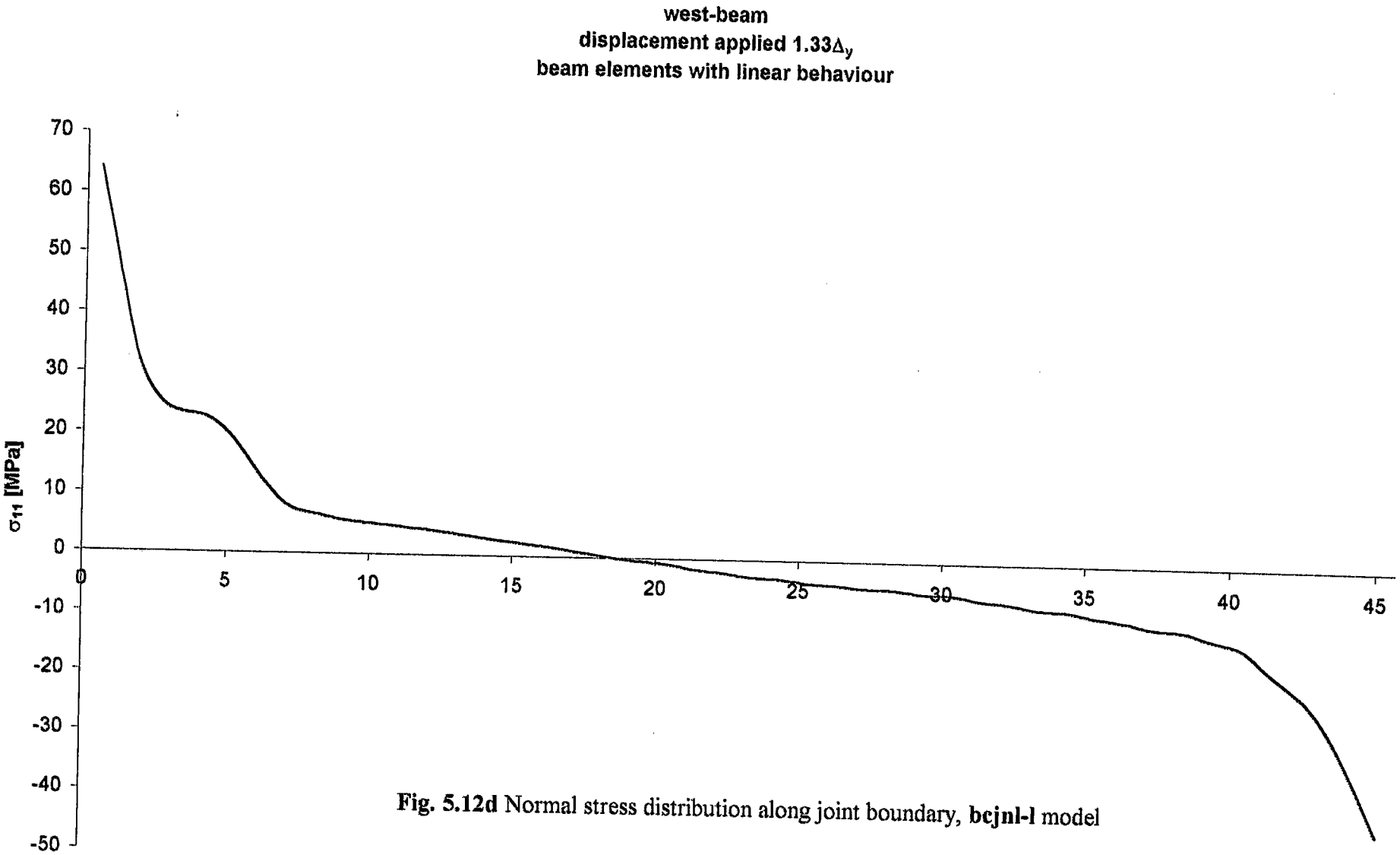

Fig. 5.12d Normal stress distribution along joint boundary, **bcjnl-l** model

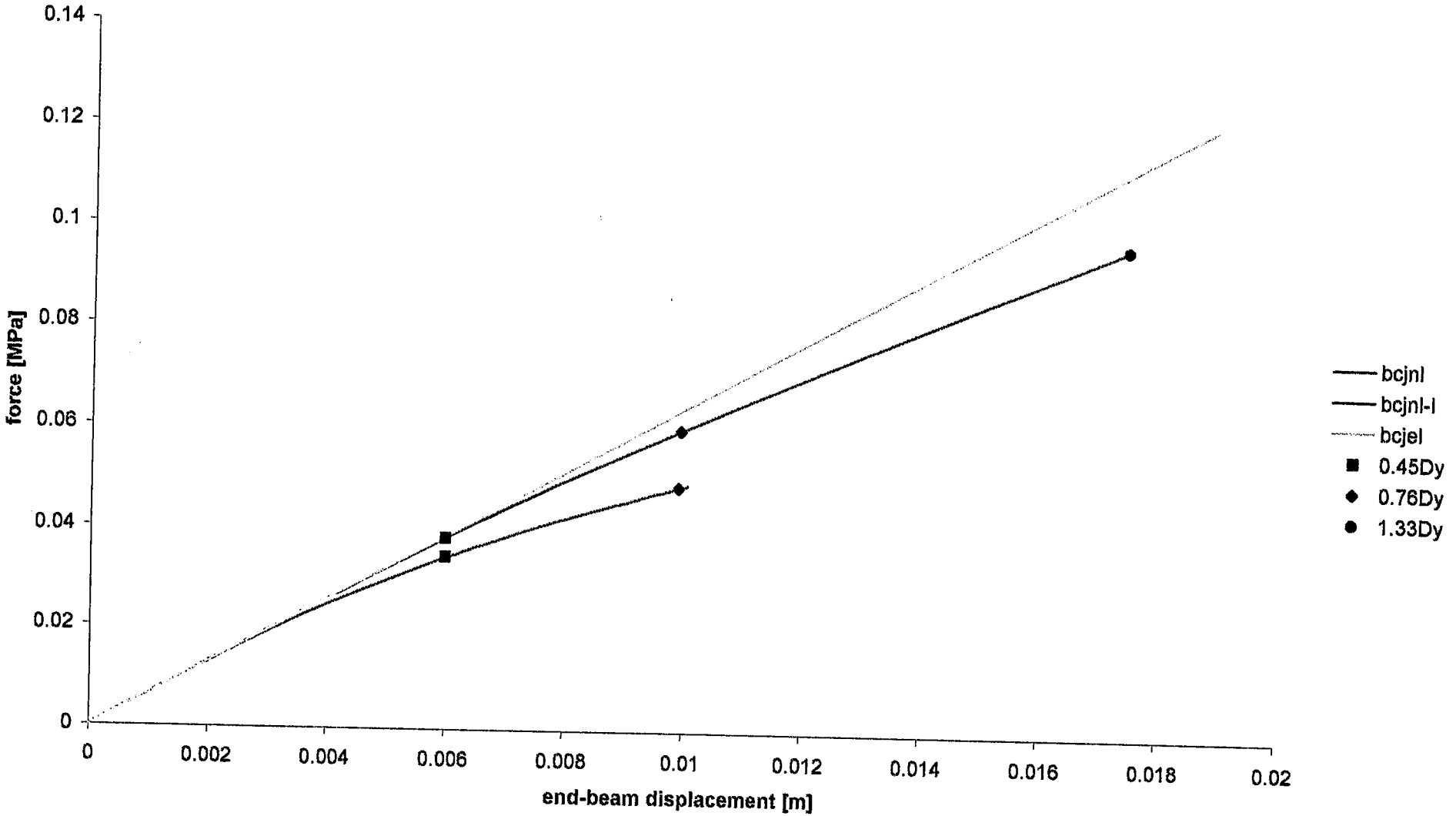

Fig. 5.13a Beam tip load versus beam tip deflection

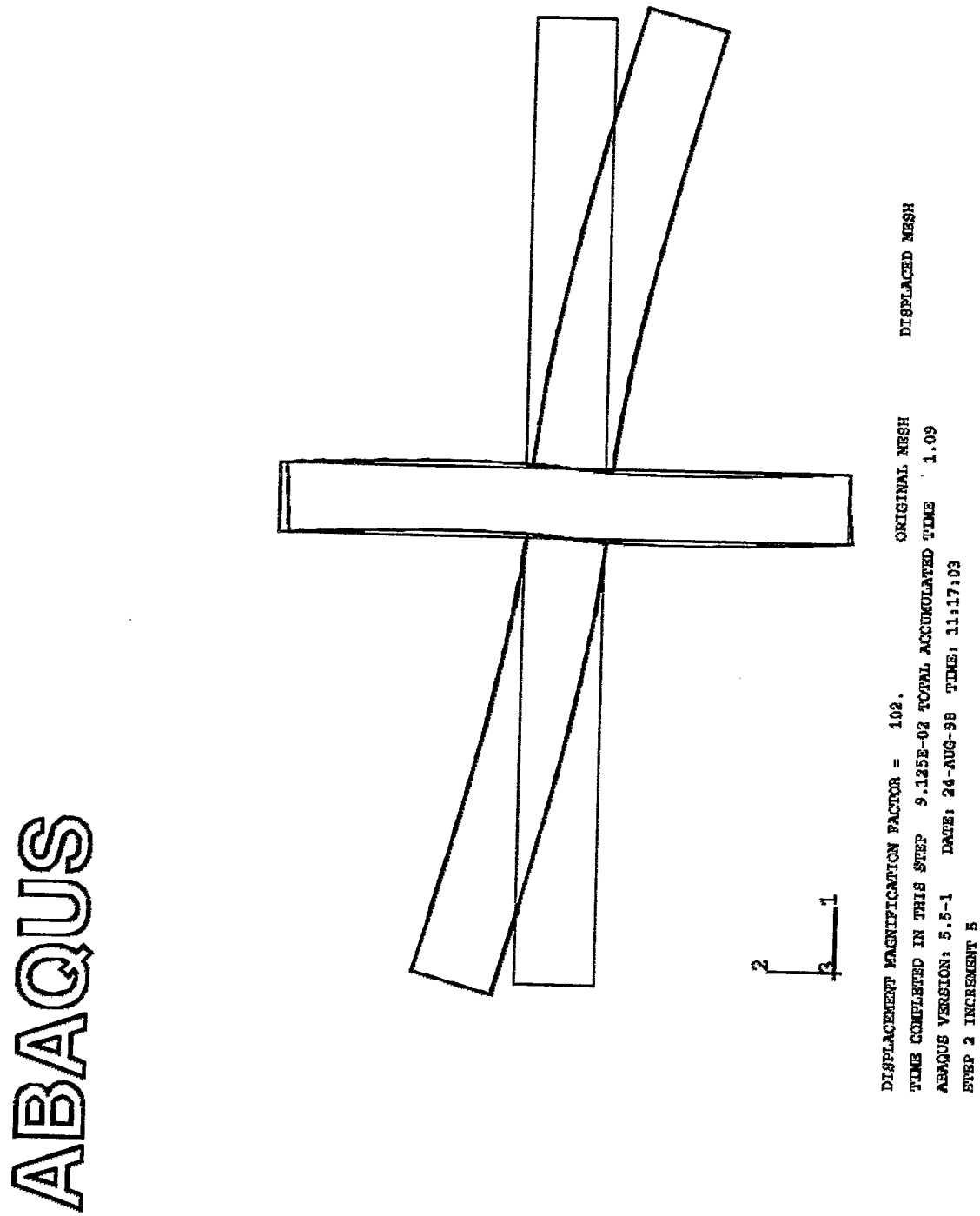

Fig. 5.13b Displacements of the overall subassemblage, **bcjnl** model, $\Delta=0.456\Delta_{y,fix}$

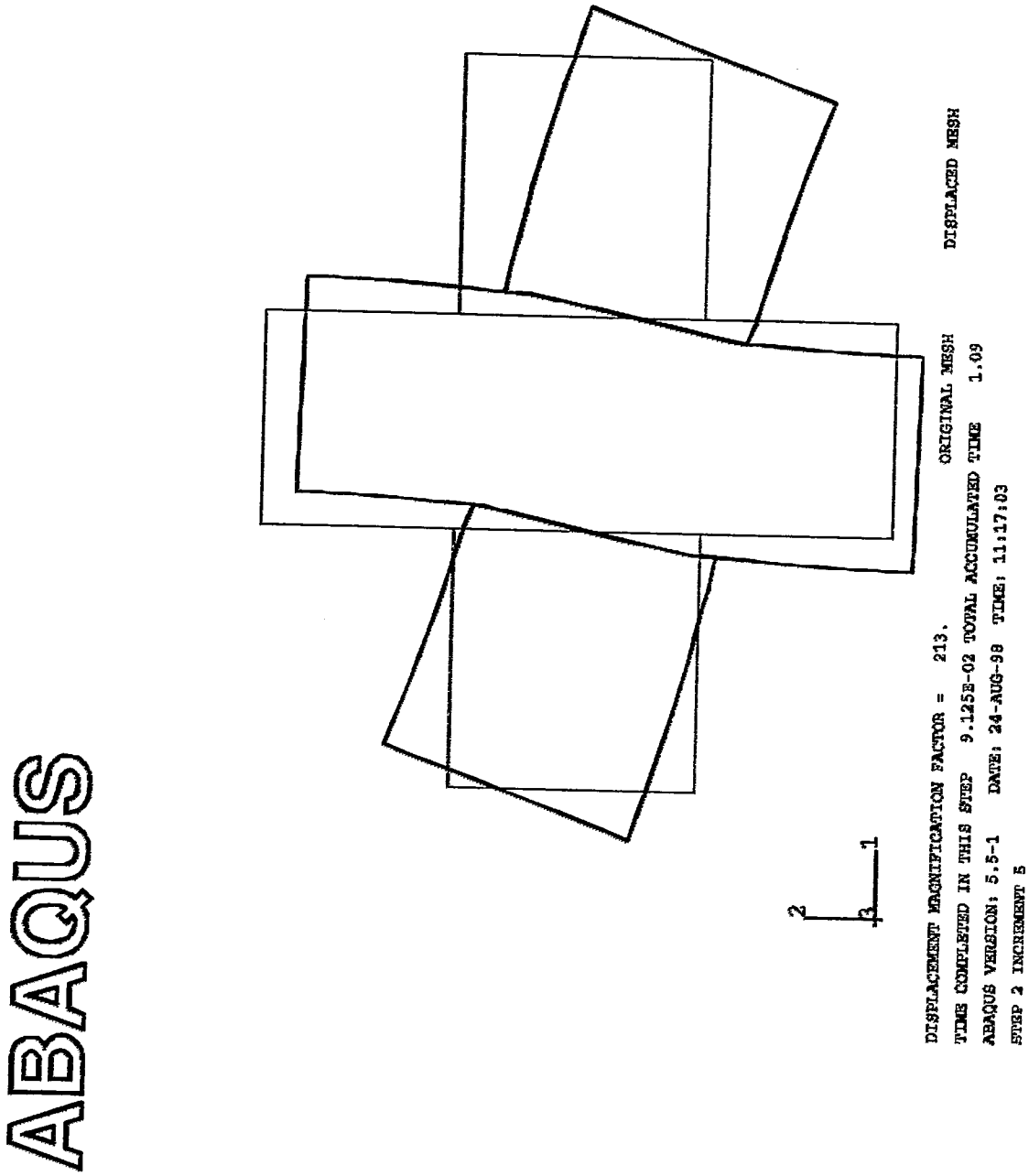

Fig. 5.13c Displacements of the joint, **bcjnl** model, $\Delta=0.456\Delta_{y.fix}$

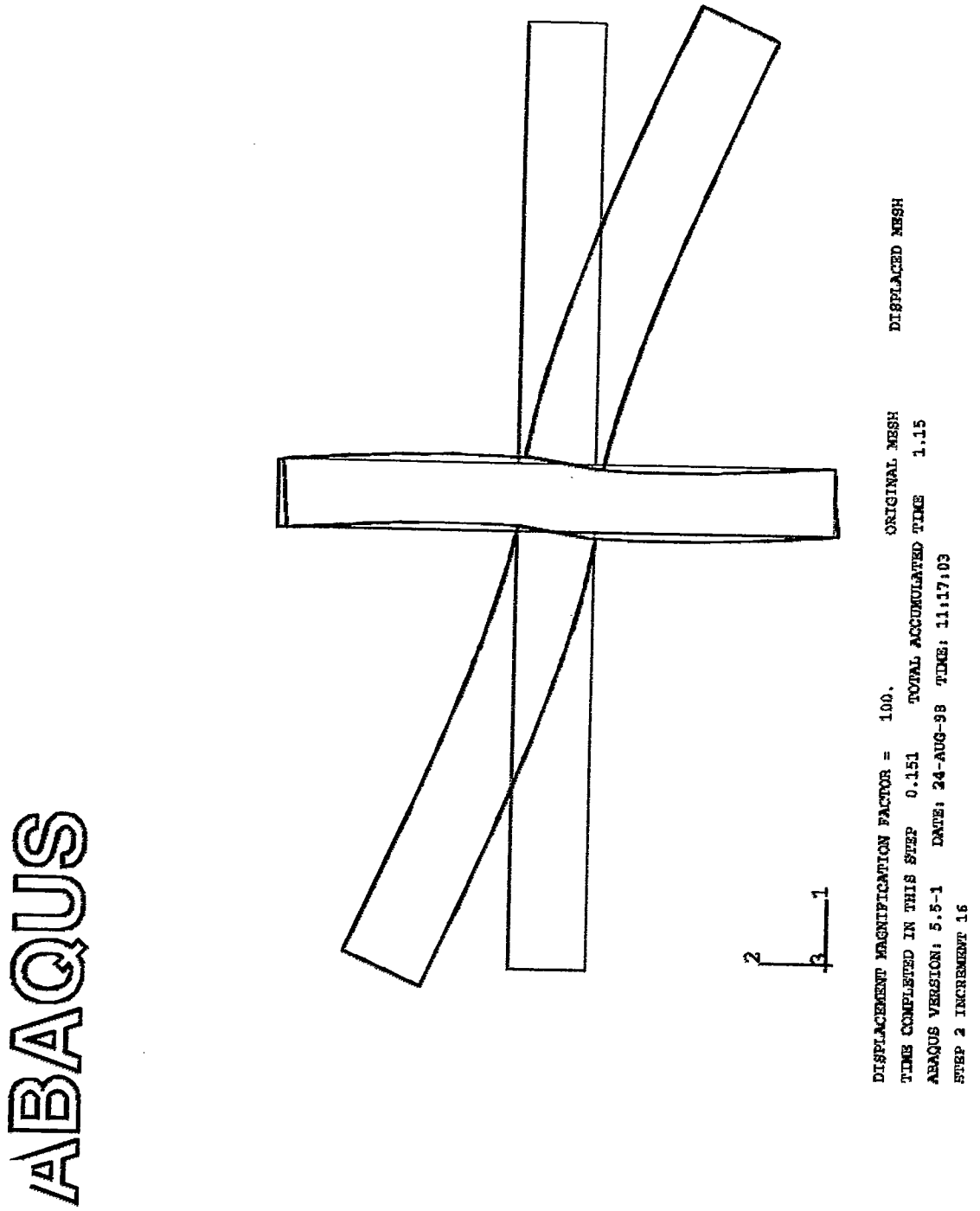

Fig. 5.13d Displacements of the overall subassemblage, **bcjnl** model, $\Delta=0.755\Delta_{y,fix}$

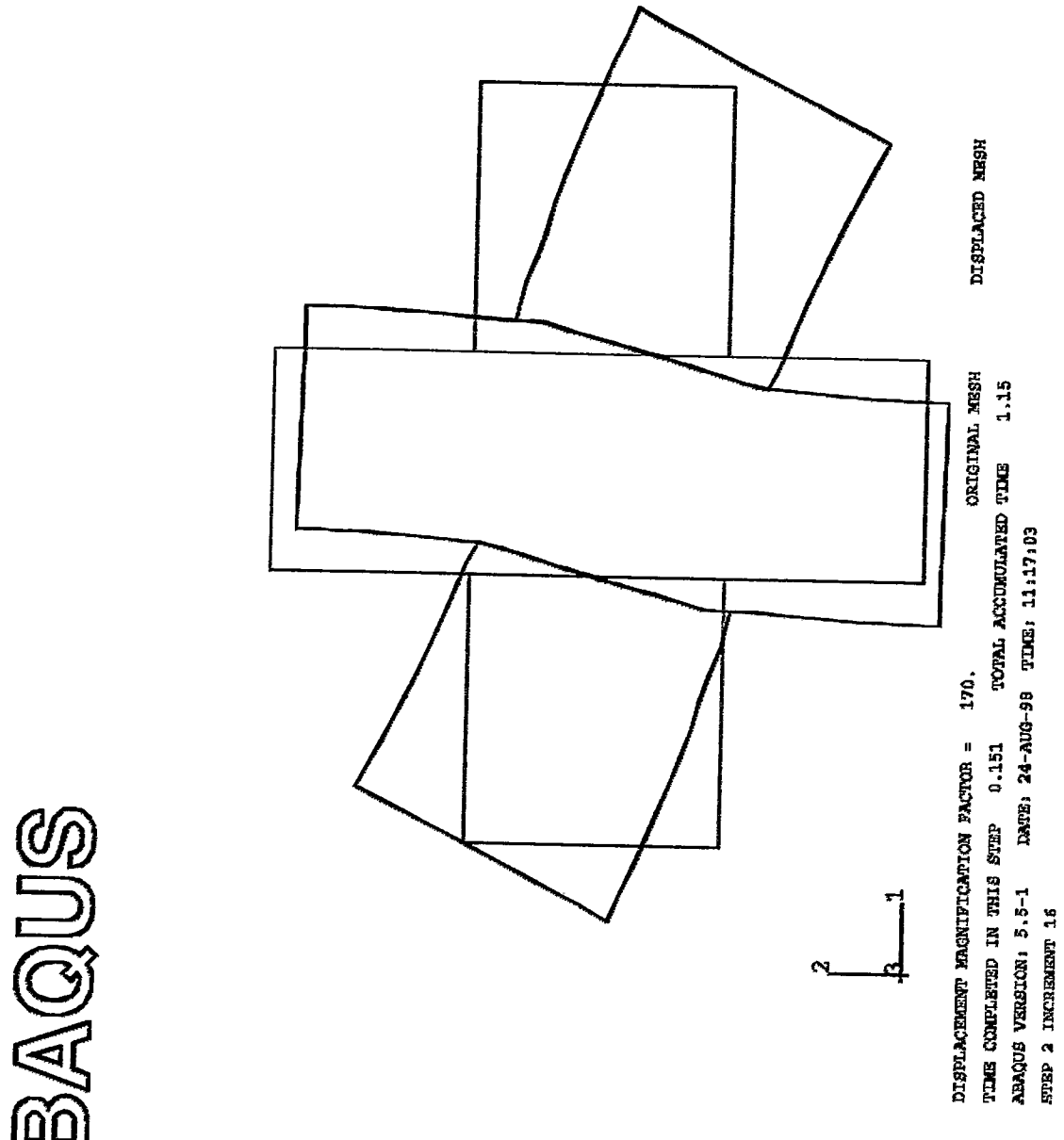

Fig. 5.13e Displacements of the joint, **bcjnl** model, $\Delta=0.755\Delta_{y,fix}$

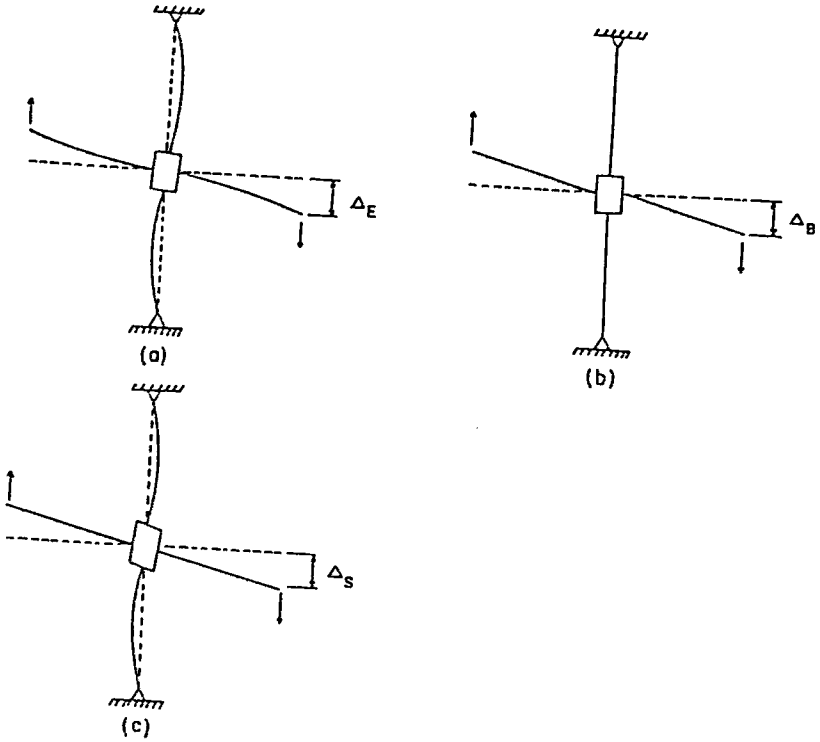

Fig. 5.14 Mechanisms contributing to interstorey displacement

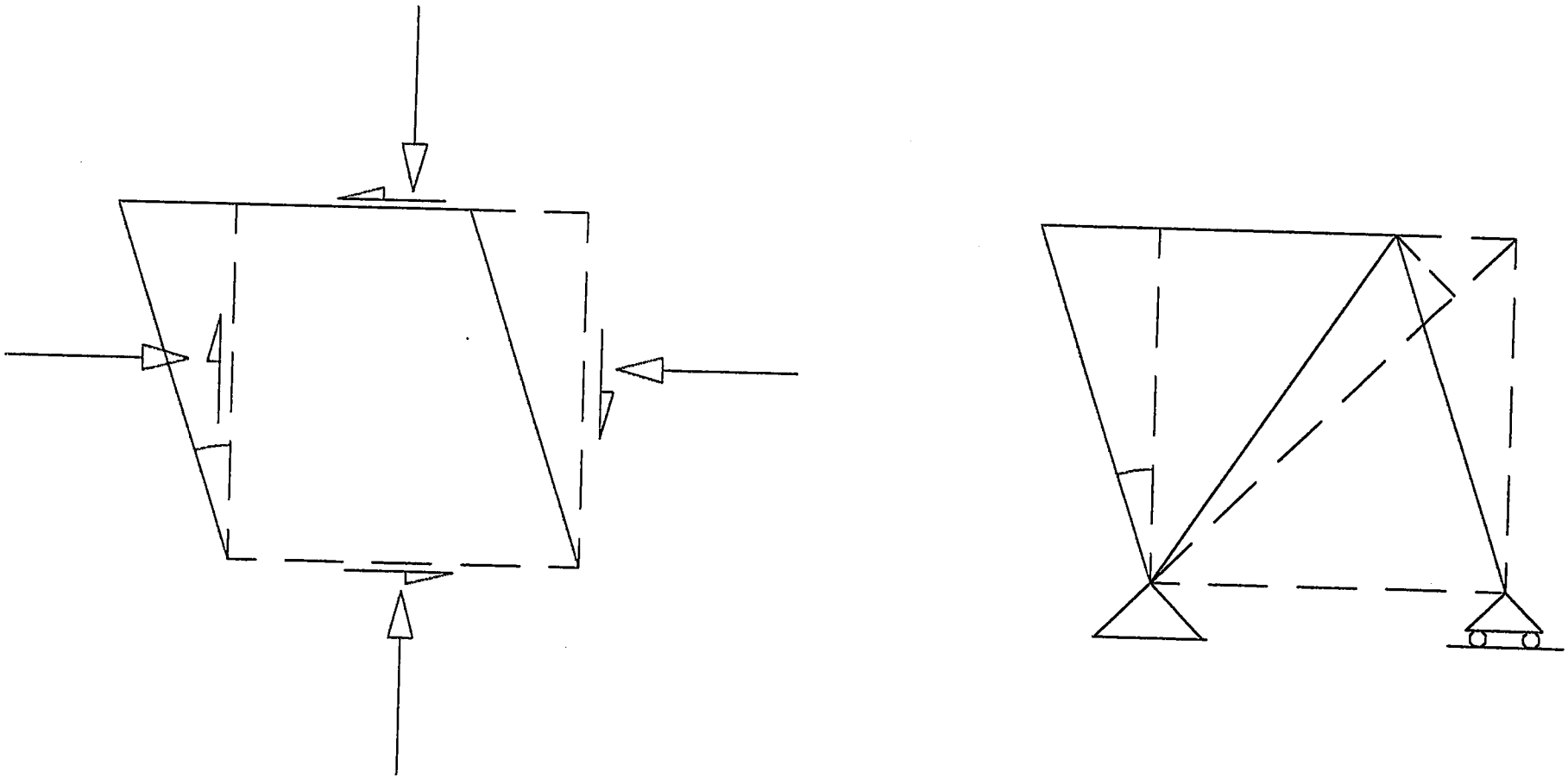

Fig. 5.16 A simple mechanical model

CHAPTER 6

CONCLUSIONS

The study carried out in this research is an effort to expand the understanding of the mechanics of joint response with the objective of identifying the pattern and magnitude of deformation within the joint upon external actions.

At this end a non-linear finite element analysis has been carried out which has given confirmation on some general aspects about the joint behaviour.

The new elements introduced by this research can be identified in the attempt to define underlying principles which a predictive model of the joint behaviour should rely on. Characteristic feature of such model would be its capacity to describe the response of the connection by knowing only geometrical configuration and material properties. The first step in devising the aforementioned model is the identification of the sources of flexibility within the joint and their interaction. It is just the high non-linearity of the interaction between the mechanisms involved in the response of the connection that makes the topic be not an easy task.

The non-linear finite element analysis has shown that when one can rely on very good bond conditions, a first approximation of the joint response can be obtained by considering the panel zone behaviour controlled by only the presence of compressive strut. It has been understood that even under the above assumption, due to the occurrence of cracking at the joint boundary, the size of the compressive strut changes and hence, a system with variable geometry result.

Other parameters, however, need to be considered such as the type of contribution given by the joint shear reinforcement and the influence of the bond conditions on the relative importance among the several response mechanisms as the bond influences the quality of the stress state induced in the joint.

The aforementioned considerations show that there is still need of research in this field. Due attention must be paid not only to the strength characteristic of the joint but also to the stiffness characteristic. This aspect is a main concern in the current earthquake resistant design as result of the use of high strength materials which lead to have columns and beams with reduced sizes and, hence, the joint becomes a region of high distress and a main source of deformability.

REFERENCES

ACI-ASCE Committee 352, Recommendations for design of beam column joints in monolithic reinforced concrete structures, American Concrete Institute Structural Journal, Vol. 73, 1985, pp. 375-393

Agbabian, M.S., Higazy, E.M., Abdel-Ghaffa, A.M., and Elnashai, A.S., Experimental observations on the seismic shear performance of RC beam-to-column connections subjected to varying axial column force, Earthquake Engineering and Structural Dynamics, Vol. 23, 1994, pp. 859-876

Anderson, J.C. and Townsend, W.H., Models for RC frames with degrading stiffness, Journal of Structural Engineering, Vol. 103, 1977, pp. 2361-2376

Aoyama, H., Otani, S., and Kitayama, K., Design criteria for reinforced concrete interior beam-column connections, IX World Conference on Earthquake Engineering, Tokyo-Kyoto, Japan, Vol. IV, 1988, pp.615-6

Banon, H., Biggs, J.M., and Irvine, H.M., Seismic damage in reinforced concrete frames, Journal of Structural Engineering, Vol. 107, 1981, pp. 1713-1729

Bazant, Z.P., and Oh, B.H., Crack band theory for fracture of concrete, Materials and Structures, RILEM, Vol. 16, 1983, pp155-177

Belarbi, A., and Hsu, T.C., Constitutive laws of softened concrete in biaxial tension-compression, American Concrete Institute Structural Journal, Vol. 92, 1995, pp. 562-573

Bicanic, N.,de Borst, R., Gerstle,W., Murray, D.W., Pijaudier-Cabot, G., Saouma, V., William, K.J., and Yamazaki, J., Computational aspects, 1992

Bonacci and Pantazopoulou, Parametric investigation, American Concrete Institute Structural Journal, Vol. 90, 1993, pp. 61-71

CEB Bulletin No 210, RC Elements under cycling loading, 1996, pp. 190

CEB Bulletin No 231, RC frames under earthquake loading, 1996, pp. 303

Ciampi,V., Eligehausen, R., Bertero, V.V., and Popov,E., Analytical model for deformed bar bond under generalized excitations, Transactions IABSE Colloquium on Advanced Mechanics of Reinforced Concrete, Delft, 1981

Collins, M., Towards a rational theory for RC members in shear, Journal of Structural Engineering, Vol. 104, 1978, pp. 649-666

Cosenza, E., and Manfredi, G., Classificazione e comportamento sismico di modelli ciclici degradanti, in Workshop on Cyclic Damage and Pseudodynamic Tests, Ed. Cosenza, E., Naples, Italy, 1994 (in Italian)

Crisfield, M.A., and Wills, J. Solution strategies and softening materials, Computer Methods in Applied Mechanics and Engineering, Vol. 66. 1988, pp.267-289

Crisfield, M.A., and Wills, J., Analysis of R/C panels using different concrete models, Journal of Engineering Mechanics, Vol. 115, 1989, pp.578-597

Crisfield, M.A., and Wills, J., Numerical comparisons involving different 'concrete models', in IABSE, Colloquium on Computational mechanics of concrete structures -Advanced Applications, Delft University Press, Delft, The Netherlands, 1987, pp. 177-188

Crisfield, M.A., Loacl instabilities in the non-linear analysis of reinforced concrete beams and slabs, Proceeding Institution of Civil Enginners, 1982, part 2, pp.135-145

Crisfield, M.A., Non-linear finite element analysis of solids and structures, Vol. I and II, John Wiley & Sons, Inc., 1997

De Borst, R., and Nauta, P., Non-orthogonal cracks in a smeared finite element model, Engineering Computation, Vol. 2, 1985, pp.35-46

Durrani A.J., and Wight, J.K., Behaviour of interior beam-to-column connections under earthquake-type loading, American Concrete Institute Structural Journal, Vol. 82, 1985, pp. 343-349

Durrani, A.J., and Wight, J.K., Experimental study of interior beam to column connections subjected to reversed cyclic loading, VIII World Conference on Earthquake Engineering, San Francisco, California, 1984, pp.429-436

Elnashai, A.S., Introduction to nonlinear material response analysis, Lecture Notes, MSc in Earthquake Engineering and Structural Dynamics, Imperial College, London, 1996

Filippou, F.C. and Issa, A., Nonlinear static and dynamic response of reinforced frames, Proceedings of Fourth U.S. National Conference on Earthquake Engineering, 1990, Palm Springs, California, Vol. 21990

Filippou, F.C. A simple model for reinforcing bar anchorages under cyclic excitations, Journal of Structural Engineering, Vol. 112, 1986, pp. 1639-1659

Filippou, F.C., Popov, E.P., and Bertero, V.V., Modeling of reinforced concrete joints under cyclic excitations, Journal of Structural Engineering, Vol. 109, 1983, pp. 2666-2684

Fujii., S., and Morita, S., Comparison between interior and exterior RC beam-column joint behaviour in Design of beam column joints for seismic resistance, ACI Special Publication SP-123, American Concrete Institute, 1991, pp. 145-165

Giberson, F. The response of nonlinear multistory structures subjected to earthquake excitation, Earthquake Engineering Research Laboratory, California Institute of Technology, Pasadena, CA, EERL Report,1967

Goto, Y., Joh O., and Shibata, T., Influence of transverse reinforcement in beam ends and joints on teh behaviour of R/C beam-column subassemblages, IX World Conference on Earthquake Engineering, Tokyo-Kyoto, Japan, Vol. IV, 1988, pp. 585-590

Hanson, N.W., and Connor, H.W. Seismic resistance of reinforced concrete beam column joints, Journal of Structural Engineering, Vol. 93, 1967, pp. 533-560

Hanson, N.W., Seismic resistance of concrete frames with grade 60 reinforcement, Journal of Structural Engineering, Vol. 97, 1971, pp. 1685-1700

Hibbitt, H.D., Karlsson and Sorensen, ABAQUS Manuals: Vol. 1: User's Manual; Vol. 2: Theory Manual; Vol. 3: Example problems; Version 5.3, 1995, Providence, RI

Higazy, E.M., Seismic Shear Performance of Beam-Column subassemblages in Multistory R/C structures, Ph.D. Dissertation, Civil Engineering Department, University of Southern California, Los Angeles, USA, April 1993

Higazy, E.M., Elnashai. A.S. and Agbabian, M.S., Behaviour of beam-column connections under axial column tension, Journal of Structural Engineering, Vol. 122, 1996, pp. 501-511

Hillerborg, A., Numerical methods to simulate softening and fracture of concrete, in Fracture Mechanics of Concrete, Eds. Sih, G.C., and Di Tommaso, A., Martinus Nijhoff Publishers, 1984

Hsu, T.C., and Zhang, L., Nonlinear analysis of membrane elements by fixed angle softened truss model, American Concrete Institute Structural Journal, Vol. 94, 1997, pp.483-492

Hsu, T.C., Non-linear analysis of concrete membrane elements, American Concrete Institute Structural Journal, Vol. 88, 1991, pp. 552-561

Hsu, T.C., Toward a unified nomenclature for reinforced concrete theory, Journal of Structural Engineering, Vol. 122, 1996, pp. 275-283

Hsu, T.C., Unified Theory of Reinforced Concrete, CRC Press, 1993

Ichinose, T., A rational design procedure for shear reinforcement in R/C interior joint, IX World Conference on Earthquake Engineering, Tokyo-Kyoto, Japan, Vol. IV, 1988, pp.609-614

Ichinose, T., Shear reinforcement of reinforced concrete inelastic interior beam-column joints, Bulletin of the New Zealand National Society for Earthquake Engineering, Vol. 20, 1987, pp.116-126

Izzuddin, B.A., Non-linear solution procedures, Lecture Notes, MSc in Earthquake Engineering and Structural Dynamics, Imperial College, London, 1996

Jirsa, J.O., Meinheit, D.F., and Woolen, J.W. Factors influencing the shear strength of beam-column joints, First US National Conference on Earthquake Engineering, 1975, Ann Arbor, Michigan, EERI, pp.297-305

Joh O., Goto, Y., and Shibata, T., Influence of transverse joint and beam reinforcement and relocation of plastic hinge region on beam-column joint stiffness deterioration, in Design of beam column joints for seismic resistance, ACI Special Publication SP-123, American Concrete Institute, 1991, pp. 187-223

Kitayama, K., Otani, S., and Aoyama, H. Development of design criteria for RC interior beam column joints, in Design of beam column joints for seismic resistance, ACI Special Publication SP-123, American Concrete Institute, 1991, pp. 97-123

Kupfer, H. B., and Gerstle, K. H., Behavior of concrete under biaxial stresses, Journal of Engineering Mechanics, Vol. 99, 1974, pp. 853-866

Kurose, Y., Design of beam-column joints for shear, in Earthquake Resistance of Reinforced Concrete Structures, a Volume honoring Hiroyuki Aoyama, Ed. Okada, T., 1993, pp.276-286

Kwak, H.G., and Filippou, F.C., Finite element analysis of reinforced concrete structures under monotonic and cyclic loads, X World Conference on Earthquake Engineering, Madrid, Spain, 1992, pp.4227-4232

Kwak, H.G., and Filippou, F.C., Nonlinear finite element analysis of R/C structures under monotonic loads, Computer & Structures, Vol. 65, 1997, pp.1-16

Leon, R.T., Anchorage requirements in interior R.C. beam-column joints, IX World Conference on Earthquake Engineering, Tokyo-Kyoto, Japan, Vol. IV, 1988, pp. 585-590

Leon, R.T., Interior joints with variable anchorage lengths, Journal of Structural Engineering, Vol. 115, 1990b, pp. 2261-2275

Leon, R.T., Shear strength and hysteretic behaviour of interior beam column joints, American Concrete Institute Structural Journal, Vol. 87, 1990a, pp. 3-11 1990b

Marti, P., Basic tools of reinforced concrete beam design, American Concrete Institute Structural Journal, Vol. 82, 1985b, pp. 46-56

Marti, P., Truss models in detailing, Concrete International, 1985a, pp. 66-73

Meinheit, D.F., and Jirsa, J.O., Shear strength of RC beam column connections, Journal of Structural Engineering, Vol. 107, 1981, pp. 2227-2244

Morita, S., Fujii, S., Murakami, H., and, Yamada, T., Bond decay of beam bars in joint region under load reversals, X World Conference on Earthquake Engineering, Madrid, Spain, 1992, pp.3157-31620

Noguchi, H. and Naganuma, K., Nonlinear finite element analysis of restoring force characteristics of reinforced concrete beam column joints, VIII World Conference on Earthquake Engineering, San Francisco, California, 1984, pp. 543-550

Noguchi, H., Non linear finite element analysis of reinforced concrete beam-column joints, Transactions IABSE Colloquium on Advanced Mechanics of Reinforced Concrete, Delft, 1981

Otani, S., Inelastic analysis of R/C frame structures, Journal of Structural Engineering, Vol. 100, 1974, pp. 1433-1449

Otani, S., Nonlinear dynamic analysis of reinforced concrete building structures, Canadian Journal of Civil Engineering, 1980, Vol. 7, pp.333-344

Pantazopoulou, S., and Bonacci, J., Considerations of questions about beam-column joints, American Concrete Institute Structural Journal, Vol. 89, 1992, pp. 27-36

Pantazopoulou, S., and Bonacci, J., On earthquake resistant reinforced concrete frame connections, Canadian Journal of Civil Engineering, Vol. 21, 1994, pp. 307-328

Park, R., Gaetry, L., and Stevenson, S.C., Tests on an interior reinforced concrete beam-column joint, Bulletin of the New Zealand National Society for Earthquake Engineering, Vol. 13, 1980, pp. 81-92

Park, R., and Dai Ruitong, A comparison of the behaviour of reinforced concrete beam column joints designed for ductility and limited ductility, Bulletin of the New Zealand National Society for Earthquake Engineering, Vol. 21, 1988, pp. 255-278

Park, R., and Keong, Y.S., Tests on structural concrete beam-column joints with intermediate column bars, Bulletin of the New Zealand National Society for Earthquake Engineering, Vol. 12, 1979, pp. 189-203

Park, R., and Milburn, J.R., Comparison of recent New Zealand and United States seismic design provisions for reinforced concrete beam-column joints and test results from four units designed according to the New Zealand Code, Bulletin of the New Zealand National Society for Earthquake Engineering, Vol. 16, 1983, pp.3-23

Park, R., and Paulay, P., Reinforced Concrete Structures, John Wiley & Sons, Inc., 1975, 769pp.1975

Paulay, P., Park, R., and Priestley, M.J.N., Reinforced concrete beam column joints under seismic actions, American Concrete Institute Structural Journal, Vol. 75, 1978, pp. 585-593

Paulay, T. and Priestley, M.J.N., Seismic design of concrete and masonry buildings, John Wiley & Sons, Inc., 1992

Paulay, T., Developments in the seismic design of reinforced concrete frames in New Zealand, Canadian Journal of Civil Engineering, Vol. 8, 1981, pp. 91-113

Penelis and Kappos, Earthquake-resistant concrete structures, E&FN Spon Chapman & Hall, 1997, 576 pp.

Rots., J.G., and Blaauwendraad, J., Crack models for concrete: discrete or smeared? Fixed, multi-directional or rotating?, Heron Journal, Vol. 34, 1989, 59pp

Russo, G., Zoingone, G., and Romano, F., Analytical solution for bond-slip of reinforcing bars in R.C. joints, Journal of Structural Engineering, Vol. 116, 1990, pp. 336-355

Schnobrich, W.C., The role of finite element analysis of reinforced concrete structures, in Finite Element Analysis of Reinforced Concrete Structures, Eds. Meyer, C. and Okamura, H., ASCE, 1986

Solemani, D., Popov, E.P., and Betero, V.V., Hysteretic behaviour of reinforced concrete beam-column subassemblages, American Concrete Institute, 1979, Vol. 76, pp.1179-1195

Sozen, M.A., Hysteresis in structural elements, Applied Mechanic in Earthquake Engineering, ASME, Vol.8, 1974, pp.63-73

Stevens, N.J., Uzumeri, S.M., and Collins, M.P., Reinforced concrete elements subjected to reversed shear, IX World Conference on Earthquake Engineering, Tokyo-Kyoto, Japan, Vol. VIII, 1988, pp.635-640

Stevens, N.J., Uzumeri, S.M., and Collins, M.P., Reinforced concrete subjected to reversed cyclic shear- experiments and constitutive model, American Concrete Institute Structural Journal, Vol. 88, 1991, pp. 135-147

Stevens, N.J., Uzumeri, S.M., Collins, M.P., and Will, Constitutive model for reinforced concrete finite element analysis, American Concrete Institute Structural Journal, Vol. 88, 1991, pp. 49-59

Tassios, T.P., Properties of bond between concrete and steel under load cycles idealizing seismic actions, Bulletin CEB No 131-132, Rome 1979, pp. 67-122

Tassios, T.P., Specific rules for concrete structure-justification note no. 8: A rational simplified model for beam-column joint behaviour, in Background Document for Eurocode 8-Part 1, Vol 2-Design Rules, Brussells, pp. 55-64

Townsend, W.H., and Hanson, R.D., Hysteresis loops for reinforced concrete beam-column connections, V World Conference on Earthquake Engineering, Rome, 1972, pp. 1131-1134

Uzumeri, S.M., and Seckin, M., Behaviour of joints and ductility of reinforced concrete frames, V European Conference on Earthquake Engineering, Instabul, 1975, paper 94, chapter 4

Uzumeri, S.M., Strength and ductility of cast in place beam column joints, in Reinforced concrete structures in seismic zones, ACI Special Publication SP-53, American Concrete Institute, 1977, pp. 293-350

Vecchio, F.J., and Collins, M.P., The modified compression field theory for reinforced concrete elements subjected to shear, American Concrete Institute Structural Journal, Vol. 183, 1986, pp. 219-231

Vecchio, F.J., and Collins, M.P., Stress-strain characteristics of reinforced concrete in pure shear, Transactions IABSE Colloquium on Advanced Mechanics of Reinforced Concrete, Delft, 1981

Watanabe, K. and Noguchi, H., Analysis of shear resistance mechanisms of RC beam-column connections subject to seismic forces, IX World Conference on Earthquake Engineering, Tokyo-Kyoto, Japan, 1988, Vol. IV, pp.603-608

Wong, P.K.C., Priesltey, M.J.N., and Park, R., Seismic resistance of frames with vertically distributed longitudinal reinforcement in beams, American Concrete Institute Structural Journal, Vol. 87, 1990, pp. 488-498

Yunfei,H., Chingchang, H., and Yufeng, C., Further studies on the behaviour of reinforced concrete beam column joint under reversed cyclic loading, VIII World Conference on Earthquake Engineering, San Francisco, California, 1984, pp. 485-492

Zhang, L. and Jirsa, J.O., A study of shear behaviour of reinforced concrete beam column joints, PMFSEL Report No 82-1, The University of Texas, 1982

Appendix A

Listing of a Fortran program to solve the two-dimensional panel model

```
      Program Main
c
c Program to describe the shear stress - shear strain relationship in biaxial
c tension-compression state. As the softening effect is related to tensile strain,
c the use of the softening coefficient holds if epsr>0. The output data correspond
c to positive value for epsr.
c Note that in uniaxial compressive law a tensile strain is present.
c Values greater than this implies the presence of a tensile stress.
c
      real sigmal,sigmat,rol,rot,Es,fy,scuniax,epso,epsdmax,toll
      real epsd,epsr,soft,c,a,sigmad,sigmar,epsy,epsl,epst
      real b1,b2,epsr1,alpha,b,tlt,glt,d,sdmax
      real scl,sct,fl,ft,scleq,scteq,epsleq,epsteq
      character*20 fileinp,fileout,resul
c
      write(*,'(A)')' Please Input File Data Name?'
      read(*,'(A)')fileinp
c
      write(*,'(A)')' Please Output File Name?'
      read(*,'(A)')fileout
c
      write(*,'(A)')' Please Output Results File for plotting ?'
      read(*,'(A)')resul
c
      open(5,File=fileinp,status='old')
      open(6,File=fileout,status='unknown')
      open(7,File=resul,status='unknown')
c
      read(5,*)sigmal,sigmat,rol,rot
      read(5,*)Es,fy
      read(5,*)scuniax,epso,epsdmax
      read(5,*)toll
c
c IMPLEMENTATION of the compressive constitutive law proposed by Collins and Vecchio, 1986
c
      epsy=fy/Es
      write(6,*)epsy
c
      epsd=-0.00010
20    epsr=0.
10    if (epsr.LT.(-0.2*epso/0.34)) then
            soft=1.0
      else
            soft=1./(0.8-0.34*(epsr/epso))
      end if
c
      c=epsd/epso
      sigmad=soft*scuniax*(2*c-c**2)
c
```

```
        sigmar=0.
c
        a=(epsr-epsd)/(sigmar-sigmad)
c
        a1=(sigmar-sigmad)*epsr+(epsr-epsd)*(sigmal-sigmar)
        a2=sigmar-sigmad+rol*Es*(epsr-epsd)
        epsl=a1/a2
        if (epsl.GE.0.)then
                if (epsl.GE.epsy)then
                        epsl=epsr+a*(sigmal-sigmar-rol*fy)
                end if
        end if
        if (epsl.LE.0.)then
                if (epsl.LE.-epsy)then
                        epsl=epsr+a*(sigmal-sigmar+rol*fy)
                end if
        end if
c
        b1=(sigmar-sigmad)*epsr+(epsr-epsd)*(sigmat-sigmar)
        b2=sigmar-sigmad+rot*Es*(epsr-epsd)
        epst=b1/b2
        if (epst.GE.0.)then
                if (epst.GE.epsy)then
                        epst=epsr+a*(sigmat-sigmar-rot*fy)
                end if
        end if
        if (epst.LE.0.)then
                if (epst.LE.-epsy)then
                        epst=epsr+a*(sigmat-sigmar+rot*fy)
                end if
        end if
c
        epsr1=epsl+epst-epsd
        d=abs(epsr1-epsr)
        if (abs(epsr1-epsr).GT.toll) then
                epsr=epsr1
                goto 10
        end if
c
        epsr=epsr1
        if (epsr.GE.0) then
                b=(epsl-epsd)/(epst-epsd)
                alpha=atan(SQRT(b))
                tlt=(sigmar-sigmad)*sin(alpha)*cos(alpha)
                glt=(2*(epsr-epsd)*sin(alpha)*cos(alpha))
                scl=sigmad*(cos(alpha))**2+sigmar*(sin(alpha))**2
                sct=sigmad*(sin(alpha))**2+sigmar*(cos(alpha))**2
                epsleq=epsd*(cos(alpha))**2+epsr*(sin(alpha))**2
                epsteq=epsd*(sin(alpha))**2+epsr*(cos(alpha))**2
                alpha=alpha*180./3.14159265359
                sdmax=soft*scuniax
c
                if (abs(epsl).LE.epsy) then
                        fl=Es*epsl
                else
                        if (epsl.LT.0) then
                                fl=-fy
                        else
                                fl=fy
                        end if
                end if
c
```

```
                if (abs(epst).LE.epsy) then
                        ft=Es*epst
                else
                        if (epst.LT.0) then
                                ft=-fy
                        else
                                ft=fy
                        end if
                end if
c
                scleq=sigmal-rol*fl
                scteq=sigmat-rot*ft
                write(6,100)alpha
        write(6,100)glt,tlt,epsr,epsd
                write(6,100)epst,epsteq,epsl,epsleq
                write(6,100)scl,scleq,sct,scteq
                write(6,100)sigmal,fl,sigmat,ft
                write(6,*)
                write(7,110)glt,tlt,epst,epsl,sigmad,sdmax
        end if
c
        epsd=epsd-0.00002
        if (epsd.GT.epsdmax) then
                goto 10
c
c  Note that in this way we keep the last value of epsr for the following value for epsd
c because I have observed that epsr increases as epsd increases.
c
        end if
c
        stop
100     Format(T1,F12.8,T16,F12.8,T32,F12.8,T48,F12.8)
110     Format(T1,F12.8,T16,F12.8,T31,F12.8,T46,F12.8,T61,F7.3,T71,F7.3)
        close(5)
        close(6)
        close(7)
        end
```

Input Files

File: specimenA

```
-3.45,0.1725,0.04,0.01    :sigmal, sigmat, rol, rot
200000,300                :Es, fy
-34.5,-0.002,-0.0035      :scuniax, epso, epsdmax
0.0000001                 :toll
```

File: specimenB

```
-3.45,0.1725,0.025,0.01   :sigmal, sigmat, rol, rot
200000,300                :Es, fy
-51.75,-0.002,-0.0035     :scuniax, epso, epsdmax
0.0000001                 :toll
```

File: specimenC

```
-3.45,0.1725,0.06,0.06    :sigmal, sigmat, rol, rot
200000,300                :Es, fy
-34.5,-0.002,-0.0035      :scuniax, epso, epsdmax
0.0000001                 :toll
```

Appendix B

End Deflection of the Subassemblage's Beam

The beam of the subassemblage is assumed fix at the joint boundary and is subjected to a point load at the free end.

The maximum end beam displacement with the beam still in linear elastic range is given by:

$$\Delta_{ct} = \frac{\sigma_{ct} L_b^3}{3E_c(h - x)} \tag{B.1}$$

where

E_s is the concrete Young modulus
σ_{ct} is the concrete tensile strength
x is the neutral axis depth
h is the cross-section height
L is the beam span

$\Delta_{y.fix}$ denotes the free end displacement when the moment that produces the first yielding is reached at the critical section. It is evaluated considering a linear distribution of the curvature along the beam with the maximum ordinate obtained without accounting for concrete in tension. Hence,

$$\Delta_{y.fix} = \frac{\Phi_y L_b^2}{3} \tag{B.2}$$

with

$$\Phi_y = \frac{f_y}{E_s d(1 - \zeta)} \tag{B.3}$$

where

E_s is the steel Young modulus
f_y is the steel yield strength
d is the effective height
ζ is the ratio of the neutral axis depth to the effective height

The data of the problem are:

L=2.611m h=0.457m b=0.229m

A_1(top) =16.08cm^2 (8D16) d_1=4.8cm
A_2(bottom) =16.08cm^2 (8D16) d_2=4.8cm

E_c=30000MPaf_c=**40MPa** σ_{ct}=0.09f_c=**3.6MPa**

E_s=200000Mpa f_y=**320MPa**

$d=h-d_2=(0.457-0.048)m=0.409m$
$x=0.5h=0.5*0.457m=0.2285m$ (neutral axis depth with contribution of tensile concrete. The cross section is symmetrically reinforced)
$x_{cr}=\zeta d=0.326*0.409m=0.133m$ (neutral axis depth without contribution of tensile concrete)

Hence,

$$\Delta_{ct} = \mathbf{0.0011934m} \quad (B.4)$$
$$\Delta_{y,fix} = \mathbf{0.01319m} \quad (B.5)$$

The values of the point loads associated with the above displacements by considering only flexural deformations are given by:

$$F_{ct} = \frac{3E_c I_{eq} \Delta_{ct}}{L_b^3} \quad (B.6)$$

$$F_{y,fix} = \frac{3E_c I_{cr} \Delta_y}{L_b^3} \quad (B.7)$$

The actual average second order area moment is a value between I_{cr} and I_{eq} due to tension stiffening, that is the capacity of the concrete to bear tensile stresses among cracks where the concrete is intact and not cracked. Hence, a value for F_y between $3E_cI_{cr}\Delta_y/L^3$ and $3E_cI_{eq}\Delta_y/L^3$ should be anticipated.

As for the displacement of the beam-end in the subassemblage, assuming a linear behaviour and only the contribution of flexural deformation, it needs to account for the column deformability, as well.

For a simply supported beam with a moment *M* applied at the mid span, the ensuing section rotation is equal to

$$\varphi = \frac{ML}{12EI} \quad (B.8)$$

Hence, let

$$\Delta=\Delta_{fix}+\Delta_M \quad (B.9)$$

then

$$\Delta_{fix} = \frac{FL_b^3}{3EI_b} \quad (B.10)$$

$$\Delta_M=\varphi^* L_b \quad (B.11)$$

where

φ is the rotation of the mid-section of the whole column under the action of a moment *M* equal to $F*2L_b$.

The whole column has a length equal to $2L_c$, hence

$$\varphi = \frac{F(2L_b)(2L_c)}{12EI_c} = \frac{FL_bL_c}{3EI_c} \tag{B.12}$$

Thus,

$$\Delta_M = \frac{FL_bL_c}{3EI_c}L_b \tag{B.13}$$

So

$$\Delta = \Delta_{fix} + \Delta_M = \frac{FL_b^3}{3EI_b} + \frac{FL_b^2L_c}{3EI_c} = \frac{FL_b^3}{3EI_b}[1 + \frac{I_bL_c}{I_cL_b}] \tag{B.14}$$

Appendix C

Input File for ABAQUS (*bcjnl* model)

```
*HEADING
bcjnl.inp
**
** Beam Column Joint
**
** Non linear material is assumed for elements belonging
** to the joint and regions of column and beams adjacent to the joint.
**
** The Actions are given by column axial load in the first step
** and Imposed Displacement at ends beams in the second step.
**
** Units:
** Force  MNewton (MN)
** Length meters  (m)
**
*PREPRINT,ECHO=NO,MODEL=NO
**
** MODEL DEFINITION
**
** COLUMN NODES
**
*NODE
1,0.,0.
2,0.03,0.
10,0.376,0.
11,0.406,0.
**
12,0.,0.03
13,0.03,0.03
21,0.376,0.03
22,0.406,0.03
**
199,0.,1.05
200,0.03,1.05
208,0.376,1.05
209,0.406,1.05
**
331,0.,1.41
332,0.03,1.41
340,0.376,1.41
341,0.406,1.41
**
353,0.,1.458
354,0.03,1.458
362,0.376,1.458
363,0.406,1.458
**
551,0.,1.819
552,0.03,1.819
560,0.376,1.819
561,0.406,1.819
**
573,0.,1.867
574,0.03,1.867
```

```
582,0.376,1.867
583,0.406,1.867
**
705,0.,2.227
706,0.03,2.227
714,0.376,2.227
715,0.406,2.227
**
892,0.,3.247
893,0.03,3.247
901,0.376,3.247
902,0.406,3.247
**
903,0.,3.277
904,0.03,3.277
912,0.376,3.277
913,0.406,3.277
**
**
**
*NGEN,NSET=CS-END
2,10,1
*NGEN,NSET=CS01
13,21,1
*NGEN,NSET=CS02
200,208,1
*NGEN,NSET=CS03
332,340,1
*NGEN,NSET=CS04
354,362,1
*NGEN,NSET=CN01
552,560,1
*NGEN,NSET=CN02
574,582,1
*NGEN,NSET=CN03
706,714,1
*NGEN,NSET=CN04
893,901,1
*NGEN,NSET=CN-END
904,912,1
*NGEN,NSET=CSE01
12,199,11
*NGEN,NSET=CSE02
199,331,11
*NGEN,NSET=CSE03
331,353,11
*NGEN,NSET=CSE-NE
353,551,11
*NGEN,NSET=CNE01
551,573,11
*NGEN,NSET=CNE02
573,705,11
*NGEN,NSET=CNE03
705,892,11
*NGEN,NSET=CSW01
22,209,11
*NGEN,NSET=CSW02
209,341,11
*NGEN,NSET=CSW03
341,363,11
*NGEN,NSET=CSW-NW
363,561,11
*NGEN,NSET=CNW01
561,583,11
*NGEN,NSET=CNW02
583,715,11
*NGEN,NSET=CNW03
715,902,11
*NFILL,NSET=CS-01
CS01,CS02,17,11
```

```
*NFILL,NSET=CS-02
CS02,CS03,12,11
*NFILL,NSET=CS-03
CS03,CS04,2,11
*NFILL,NSET=CS-N
CS04,CN01,18,11
*NFILL,NSET=CN-01
CN01,CN02,2,11
*NFILL,NSET=CN-02
CN02,CN03,12,11
*NFILL,NSET=CN-03
CN03,CN04,17,11
**
** The following Node Sets are generated
** JEB        Joint East Beam Boundary Nodes:
**           The joint boundary nodes common to the east beam
** JWB        Joint West Beam Boundary Nodes:
**           The joint boundary nodes common to the west beam
** JOINT      The nodes belonging to the joint region of column
** SOU-COL    The nodes belonging to the south column but the joint
** NOR-COL    The nodes belonging to the north column but the joint
** CS-ENDAL   All the nodes belonging to the end south column for the B.C.
** CN-ENDAL   All the nodes belonging to the end north column for the B.C.
**
*NSET,NSET=JWB,GENERATE
331,573,11
*NSET,NSET=JEB,GENERATE
341,583,11
*NSET,NSET=JOINT,GENERATE
331,583,1
*NSET,NSET=SOU-COL,GENERATE
1,330,1
*NSET,NSET=NOR-COL,GENERATE
584,913,1
*NSET,NSET=CS-ENDAL,GENERATE
1,11,1
*NSET,NSET=CN-ENDAL,GENERATE
903,913,1
*NSET,NSET=JTSH,GENERATE
331,341,1
*NSET,NSET=JBSH,GENERATE
341,583,11
**
**
** EAST-BEAM NODES
**
*NODE
1001,3.017,1.410
1002,3.017,1.458
1011,3.017,1.819
1012,3.017,1.867
**
1013,2.987,1.410
1014,2.987,1.458
1023,2.987,1.819
1024,2.987,1.867
**
1241,1.296,1.410
1242,1.296,1.458
1251,1.296,1.819
1252,1.296,1.867
**
1457,0.495,1.410
1458,0.495,1.458
1467,0.495,1.819
1468,0.495,1.867
**
1469,0.4505,1.410
1470,0.4505,1.434
1471,0.4505,1.458
```

```
1489,0.4505,1.819
1490,0.4505,1.843
1491,0.4505,1.867
**
1492,0.406,1.410
1493,0.406,1.434
1494,0.406,1.458
1512,0.406,1.819
1513,0.406,1.843
1514,0.406,1.867
**
*NGEN,NSET=EB-EEND
1002,1011,1
*NGEN,NSET=BE01
1014,1023,1
*NGEN,NSET=BE02
1242,1251,1
*NGEN,NSET=BE03
1458,1467,1
*NGEN,NSET=BE04
1471,1489,1
*NGEN,NSET=BE05
1494,1512,1
*NGEN,NSET=BES01
1013,1241,12
*NGEN,NSET=BES02
1241,1457,12
*NGEN,NSET=BEN01
1024,1252,12
*NGEN,NSET=BEN02
1252,1468,12
*NFILL,NSET=BE-01
BE01,BE02,19,12
*NFILL,NSET=BE-02
BE02,BE03,18,12
*NFILL,NSET=BE-02
BE02,BE03,18,12
**
** The following set nodes are generated:
** EBALNOD  East Beam All Nodes
** EBJ      East Beam Boundary Nodes common to the Joint
**          where to force constraints with the corresponding
**          column joint nodes
** EB-JT    East Beam Nodes adjacent to the Joint
** EB-ENDAL All the nodes belonging to the end east beam for the B.C.
**
*NSET,NSET=EBALNOD,GENERATE
1001,1514,1
*NSET,NSET=EBJ,GENERATE
1492,1514,1
*NSET,NSET=EB-JT,GENERATE
1373,1514,1
*NSET,NSET=EB-ENDAL,GENERATE
1001,1012,1
**
** WEST-BEAM NODES
**
*NCOPY,CHANGE NUMBER=1000,OLDSET=EBALNOD,REFLECT=LINE
0.203,0.,0.,0.203,3.277,0.
**
**
** The following set nodes are generated:
** WBALNOD  West Beam All Nodes
** WBJ      West Beam Boundary Nodes common to the Joint
**          where to force constraints with the corresponding
**          column joint nodes
** WB-JT    West Beam Nodes adjacent to the Joint
** WB-ENDAL All the nodes belonging to the end west beam for the B.C.
**
*NSET,NSET=WBALNOD,GENERATE
```

```
2001,2514,1
*NSET,NSET=WBJ,GENERATE
2492,2514,1
*NSET,NSET=WB-JT,GENERATE
2373,2514,1
*NSET,NSET=WB-ENDAL,GENERATE
2001,2012,1
**
**Constraint between column and adjacent beams
**
*EQUATION
2
JWB,1,1.0,WBJ,1,-1.0
2
JWB,2,1.0,WBJ,2,-1.0
2
JEB,1,1.0,EBJ,1,-1.0
2
JEB,2,1.0,EBJ,2,-1.0
**
**
**
**
** GENERATION COLUMN ELEMENTS
**
*ELEMENT,TYPE=CPS4
1,1,2,13,12
*ELGEN,ELSET=COLALL
1,10,1,1,82,11,10
**
** The following Elemnt Sets are generated:
** S-COLEL Elements belonging to south column but the joint
** SCADJ  South Column Adjacent Joint Elements
** JOINTEL Elements belonging to the joint
** N-COLEL Elements belonging to north column but the joint
** NCADJ  North Column Adjacent Joint Elements
** ELCNLB  Elements Column with Non Linear Behaviour
** ELCLB  Elements Column with Linear Behaviour
** SCIADJ  South Column elements Immediately Adjacent Joint
** NCIADJ  North Column elements Immediately Adjacent Joint
**
*ELSET,ELSET=S-COLEL,GENERATE
1,300,1
*ELSET,ELSET=SCADJ,GENERATE
181,300,1
*ELSET,ELSET=JOINTEL,GENERATE
301,520,1
*ELSET,ELSET=N-COLEL,GENERATE
521,820,1
*ELSET,ELSET=NCADJ,GENERATE
521,640,1
*ELSET,ELSET=ELCNLB,GENERATE
181,640,1
*ELSET,ELSET=ELCLB,GENERATE
1,180,1
641,820,1
*ELSET,ELSET=SCIADJ,GENERATE
291,300,1
*ELSET,ELSET=NCIADJ,GENERATE
521,530,1
**
**
** GENERATION EAST BEAM ELEMENTS
**
*ELEMENT,TYPE=CPS4
1001,1001,1002,1014,1013
1452,1492,1469,1470,1493
**
** Generation Rectangular Elements
**
```

```
*ELGEN,ELSET=EBEAM
1001,11,1,1,38,12,11
1452,22,1,1,1
**
**Triangular Elements
**
*ELEMENT,TYPE=CPS3
1419,1457,1458,1470
1420,1458,1459,1472
1421,1459,1460,1474
1422,1460,1461,1476
1423,1461,1462,1478
1424,1462,1463,1480
1425,1463,1464,1482
1426,1464,1465,1484
1427,1465,1466,1486
1428,1466,1467,1488
1429,1467,1468,1490
**
1430,1469,1457,1470
1432,1471,1458,1472
1434,1473,1459,1474
1436,1475,1460,1476
1438,1477,1461,1478
1440,1479,1462,1480
1442,1481,1463,1482
1444,1483,1464,1484
1446,1485,1465,1486
1448,1487,1466,1488
1450,1489,1467,1490
**
1431,1470,1458,1471
1433,1472,1459,1473
1435,1474,1460,1475
1437,1476,1461,1477
1439,1478,1462,1479
1441,1480,1463,1481
1443,1482,1464,1483
1445,1484,1465,1485
1447,1486,1466,1487
1449,1488,1467,1489
1451,1490,1468,1491
**
**
** The following element sets are generated:
** EBALEL East Beam All Elements
** ELEBNLB Elements East Beam with Non Linear Behaviour
** ELEBLB  Elements East Beam with Linear Behaviour
** EBIAJ   East Beam elements Immediately Adjacent Joint
**
*ELSET,ELSET=EBALEL,GENERATE
1001,1473,1
*ELSET,ELSET=ELEBNLB,GENERATE
1320,1473,1
*ELSET,ELSET=ELEBLB,GENERATE
1001,1319,1
*ELSET,ELSET=EBIAJ,GENERATE
1452,1473,1
**
**
** GENERATION WEST BEAM ELEMENTS
**
*ELCOPY,ELEMENT SHIFT=1000,SHIFT NODES=1000,OLDSET=EBALEL,REFLECT
**
** The following element sets are generated:
** WBALEL West Beam All Elements
** ELWBNLB Elements West Beam with Non Linear Behaviour
** ELWBLB  Elements West Beam with Linear Behaviour
** WBIAJ   West Beam elements Immediately Adjacent Joint
**
```

```
*ELSET,ELSET=WBALEL,GENERATE
2001,2473,1
*ELSET,ELSET=ELWBNLB,GENERATE
2320,2473,1
*ELSET,ELSET=ELWBLB,GENERATE
2001,2319,1
*ELSET,ELSET=WBIAJ,GENERATE
2452,2473,1
**
**
** COLUMN BARS
**
** Hoops
**
*ELEMENT, TYPE=T2D2
3001,13,14
3041,134,135
3141,376,377
3221,574,575
3321,794,795
*ELGEN
3001,8,1,1,4,33,10
3041,8,1,1,10,22,10
3141,8,1,1,8,22,10
3221,8,1,1,10,22,10
3321,8,1,1,4,33,10
**
** The following Elemnt Sets are generated:
**     SCHO   Hoop Elements belonging to South Column but the joint
**     JCHO   Hoop Elements belonging to the joint
**     NCHO   Hoop Elements belonging to North Column but the joint
**     HESCNLB Hoop Elements South Column Non Linear Behaviour
**     HENCNLB Hoop Elements North Column Non Linear Behaviour
**
*ELSET,ELSET=SCHO,GENERATE
3001,3131,10
3002,3132,10
3003,3133,10
3004,3134,10
3005,3135,10
3006,3136,10
3007,3137,10
3008,3138,10
*ELSET,ELSET=JCHO,GENERATE
3141,3211,10
3142,3212,10
3143,3213,10
3144,3214,10
3145,3215,10
3146,3216,10
3147,3217,10
3148,3218,10
*ELSET,ELSET=NCHO,GENERATE
3221,3351,10
3222,3352,10
3223,3353,10
3224,3354,10
3225,3355,10
3226,3356,10
3227,3357,10
3228,3358,10
*ELSET,ELSET=HESCNLB,GENERATE
3071,3131,10
3072,3132,10
3073,3133,10
3074,3134,10
3075,3135,10
3076,3136,10
3077,3137,10
3078,3138,10
```

```
*ELSET,ELSET=HENCNLB,GENERATE
3221,3281,10
3222,3282,10
3223,3283,10
3224,3284,10
3225,3285,10
3226,3286,10
3227,3287,10
3228,3288,10
*ELSET,ELSET=HESCLB,GENERATE
3001,3061,10
3002,3062,10
3003,3063,10
3004,3064,10
3005,3065,10
3006,3066,10
3007,3067,10
3008,3068,10
*ELSET,ELSET=HENCLB,GENERATE
3291,3351,10
3292,3352,10
3293,3353,10
3294,3354,10
3295,3355,10
3296,3356,10
3297,3357,10
3298,3358,10
**
** Longitudinal Bars
**
*ELEMENT, TYPE=T2D2
4001,13,24
*ELGEN
4001,80,11,1,3,4,100
**
** The following Element Sets are generated:
**     SWCLB   South West side Column Longitudinal Bars
**     SMCLB   South Middle side Column Longitudinal Bars
**     SECLB   South East side Column Longitudinal Bars
**     NWCLB   North West side Column Longitudinal Bars
**     NMCLB   North Middle side Column Longitudinal Bars
**     NECLB   North East side Column Longitudinal Bars
**     SWCADJLB  South West side Column Adjacent Joint Longitudinal Bars
**     SMCADJLB  South Middle side Column Adjacent Joint Longitudinal Bars
**     SECADJLB  South East side Column Adjacent Joint Longitudinal Bars
**     NWCADJLB  North West side Column Adjacent Joint Longitudinal Bars
**     NMCADJLB  North Middle side Column Adjacent Joint Longitudinal Bars
**     NECADJLB  North East side Column Adjacent Joint Longitudinal Bars
**     WCJLB     West side Column Joint Longitudinal Bars
**     MCJLB     Middle side Column Joint Longitudinal Bars
**     ECJLB     East side Column Joint Longitudinal Bars
**     LBECNLB   Longitudinal Bars East side Column Non Linear Behaviour
**     LBMCNLB   Longitudinal Bars Middle side Column Non Linear Behaviour
**     LBWCNLB   Longitudinal Bars West side Column Non Linear Behaviour
**     LBECLB    Longitudinal Bars East side Column Linear Behaviour
**     LBMCLB    Longitudinal Bars Middle side Column Linear Behaviour
**     LBWCLB    Longitudinal Bars West side Column Linear Behaviour
**
*ELSET,ELSET=SWCLB,GENERATE
4001,4029,1
*ELSET,ELSET=SMCLB,GENERATE
4101,4129,1
*ELSET,ELSET=SECLB,GENERATE
4201,4229,1
*ELSET,ELSET=NWCLB,GENERATE
4052,4080,1
*ELSET,ELSET=NMCLB,GENERATE
4152,4180,1
*ELSET,ELSET=NECLB,GENERATE
4252,4280,1
```

```
*ELSET,ELSET=SWCADJLB,GENERATE
4018,4029,1
*ELSET,ELSET=SMCADJLB,GENERATE
4118,4129,1
*ELSET,ELSET=SECADJLB,GENERATE
4218,4229,1
*ELSET,ELSET=NWCADJLB,GENERATE
4052,4063,1
*ELSET,ELSET=NMCADJLB,GENERATE
4152,4163,1
*ELSET,ELSET=NECADJLB,GENERATE
4252,4263,1
*ELSET,ELSET=WCJLB,GENERATE
4030,4051,1
*ELSET,ELSET=MCJLB,GENERATE
4130,4151,1
*ELSET,ELSET=ECJLB,GENERATE
4230,4251,1
*ELSET,ELSET=LBWCNLB,GENERATE
4018,4063,1
*ELSET,ELSET=LBMCNLB,GENERATE
4118,4163,1
*ELSET,ELSET=LBECNLB,GENERATE
4218,4263,1
*ELSET,ELSET=LBWCLB,GENERATE
4001,4017,1
4064,4080,1
*ELSET,ELSET=LBMCLB,GENERATE
4101,4117,1
4164,4180,1
*ELSET,ELSET=LBECLB,GENERATE
4201,4217,1
4264,4280,1
**
**
**
** EAST-BEAM BARS
**
** Hoops
**
*ELEMENT,TYPE=T2D2
5001,1014,1015
5011,1026,1027
5201,1494,1495
*ELGEN
5001,9,1,1,1
5011,9,1,1,19,24,10
5201,18,1,1,1
**
** The following Element Sets are generated:
**     EBALST   East Beam All Stirrups
**     STEBNLB  Stirrups East Beam Non Linear Behaviour
**     STEBLB   Stirrups East Beam Linear Behaviour
**
**
*ELSET,ELSET=EBALST,GENERATE
5001,5191,10
5002,5192,10
5003,5193,10
5004,5194,10
5005,5195,10
5006,5196,10
5007,5197,10
5008,5198,10
5009,5199,10
5201,5218,1
*ELSET,ELSET=STEBNLB,GENERATE
5151,5191,10
5152,5192,10
5153,5193,10
```

```
5154,5194,10
5155,5195,10
5156,5196,10
5157,5197,10
5158,5198,10
5159,5199,10
5201,5218,1
*ELSET,ELSET=STEBLB,GENERATE
5001,5141,10
5002,5142,10
5003,5143,10
5004,5144,10
5005,5145,10
5006,5146,10
5007,5147,10
5008,5148,10
5009,5149,10
**
**
** Longitudinal Bars
**
*ELEMENT,TYPE=T2D2
5501,1014,1026
**
5538,1458,1471
5539,1471,1494
5638,1467,1489
5639,1489,1512
*ELGEN
5501,37,12,1,2,9,100
**
**
** The following Element Sets are generated:
**     EBTLB    East Beam Top Longitudinal Bars
**     EBBLB    East Beam Bottom Longitudinal Bars
**     EBTLBNLB East Beam Top Longitudinal Bars Non Linear Behaviour
**     EBTLBLB  East Beam Top Longitudinal Bars Linear Behaviour
**     EBBLBNLB East Beam Bottom Longitudinal Bars Non Linear Behaviour
**     EBBLBLB  East Beam Bottom Longitudinal Bars Linear Behaviour
**     EBALLB   East Beam All Longitudinal Bars
**
*ELSET,ELSET=EBTLB,GENERATE
5601,5639,1
*ELSET,ELSET=EBBLB,GENERATE
5501,5539,1
*ELSET,ELSET=EBTLBNLB,GENERATE
5629,5639,1
*ELSET,ELSET=EBTLBLB,GENERATE
5601,5628,1
*ELSET,ELSET=EBBLBNLB,GENERATE
5529,5539,1
*ELSET,ELSET=EBBLBLB,GENERATE
5501,5528,1
*ELSET,ELSET=EBALLB,GENERATE
5501,5539,1
5601,5639,1
**
**
** GENERATION WEST BEAM REINFORCEMENT
**
** Generation Stirrups West Beam
**
*ELCOPY,ELEMENT SHIFT=1000,SHIFT NODES=1000,OLDSET=EBALST
**
**
** Generation Longitudinal Bars West Beam
**
*ELCOPY,ELEMENT SHIFT=1000,SHIFT NODES=1000,OLDSET=EBALLB
**
** The following Element Sets are generated:
```

```
**     WBALST  West Beam All Stirrups
**     STWBNLB  Stirrups West Beam Non Linear Behaviour
**     STWBLB  Stirrups West Beam Linear Behaviour
**
**
*ELSET,ELSET=WBALST,GENERATE
6001,6191,10
6002,6192,10
6003,6193,10
6004,6194,10
6005,6195,10
6006,6196,10
6007,6197,10
6008,6198,10
6009,6199,10
6201,6218,1
*ELSET,ELSET=STWBNLB,GENERATE
6151,6191,10
6152,6192,10
6153,6193,10
6154,6194,10
6155,6195,10
6156,6196,10
6157,6197,10
6158,6198,10
6159,6199,10
6201,6218,1
*ELSET,ELSET=STWBLB,GENERATE
6001,6141,10
6002,6142,10
6003,6143,10
6004,6144,10
6005,6145,10
6006,6146,10
6007,6147,10
6008,6148,10
6009,6149,10
**
**
** The following Element Sets are generated:
**     WBTLB   West Beam Top Longitudinal Bars
**     WBBLB   West Beam Bottom Longitudinal Bars
**     WBTLBNLB West Beam Top Longitudinal Bars Non Linear Behaviour
**     WBTLBLB  West Beam Top Longitudinal Bars Linear Behaviour
**     WBBLBNLB West Beam Bottom Longitudinal Bars Non Linear Behaviour
**     WBBLBLB  West Beam Bottom Longitudinal Bars Linear Behaviour
**     WBALLB   West Beam All Longitudinal Bars
**
*ELSET,ELSET=WBTLB,GENERATE
6601,6639,1
*ELSET,ELSET=WBBLB,GENERATE
6501,6539,1
*ELSET,ELSET=WBTLBNLB,GENERATE
6629,6639,1
*ELSET,ELSET=WBTLBLB,GENERATE
6601,6628,1
*ELSET,ELSET=WBBLBNLB,GENERATE
6529,6539,1
*ELSET,ELSET=WBBLBLB,GENERATE
6501,6528,1
*ELSET,ELSET=WBALLB,GENERATE
6501,6539,1
6601,6639,1
**
**
** BEAM BARS THROUGH THE JOINT
**
*ELEMENT,TYPE=T2D2
7001,353,354
*ELGEN
```

```
7001,10,1,1,2,198,100
**
** The following Element Sets are generated:
**     JBTLB   Joint Beam Top Longitudinal Bars
**     JBBLB   Joint Beam Bottom Longitudinal Bars
**
*ELSET,ELSET=JBTLB,GENERATE
7001,7010,1
*ELSET,ELSET=JBBLB,GENERATE
7101,7110,1
**
**
** The following Elements Sets are generated:
**     TLB Top Longitudinal Bars
**     BLB Bottom Longitudinal Bars
**     CLB Column Longitudinal Bars
**
*ELSET,ELSET=TLB,GENERATE
5638,5639,1
7101,7110,1
6638,6639,1
**
*ELSET,ELSET=BLB,GENERATE
5538,5539,1
7001,7010,1
6538,6539,1
**
*ELSET,ELSET=CLB,GENERATE
4028,4053,1
4128,4153,1
4228,4253,1
**
** D E F I N I T I O N   G E O M E T R I C A L   P R O P E R T I E S
**   C O N C R E T E   C O N T I N U U M   E L E M E N T S
**
** They are defined by giving the depth of the cross section
**
*SOLID SECTION, ELSET=ELCNLB,MATERIAL=NLBCON
0.305
*SOLID SECTION, ELSET=ELCLB,MATERIAL=LBCON
0.305
*SOLID SECTION, ELSET=ELEBNLB,MATERIAL=NLBCON
0.229
*SOLID SECTION, ELSET=ELEBLB,MATERIAL=LBCON
0.229
*SOLID SECTION, ELSET=ELWBNLB,MATERIAL=NLBCON
0.229
*SOLID SECTION, ELSET=ELWBLB,MATERIAL=LBCON
0.229
**
** D E F I N I T I O N   G E O M E T R I C A L   P R O P E R T I E S
**         B A R   E L E M E N T S
** They are defined by giving the cross section area of the bar
**
** L O N G I T U D I N A L   B A R S
**
** NLBSTLB Non Linear Behaviour Steel for Longitudinal Bars
** LBSTLB  Linear Behaviour Steel for Longitudinal Bars
** NLBSTST Non Linear Behaviour Steel for Stirrups
** LBSTST  Linear Behaviour Steel for Stirrupss
**
** East Beam
**
** Top Area 8D16
*SOLID SECTION, ELSET=EBTLBNLB,MATERIAL=NLBSTLB
0.001608
*SOLID SECTION, ELSET=EBTLBLB,MATERIAL=LBSTLB
0.001608
**
** Bottom Area 8D16
```

```
*SOLID SECTION, ELSET=EBBLBNLB,MATERIAL=NLBSTLB
0.001608
*SOLID SECTION, ELSET=EBBLBLB,MATERIAL=LBSTLB
0.001608
**
** West Beam
**
** Top Area 8D16
*SOLID SECTION, ELSET=WBTLBNLB,MATERIAL=NLBSTLB
0.001608
*SOLID SECTION, ELSET=WBTLBLB,MATERIAL=LBSTLB
0.001608
**
** Bottom Area 8D16
*SOLID SECTION, ELSET=WBBLBNLB,MATERIAL=NLBSTLB
0.001608
*SOLID SECTION, ELSET=WBBLBLB,MATERIAL=LBSTLB
0.001608
**
** Joint Longitudinal Beam Bars
**
** Top Area 8D16
*SOLID SECTION, ELSET=JBTLB,MATERIAL=NLBSTLB
0.00229
** Bottom Area 8D16
*SOLID SECTION, ELSET=JBBLB,MATERIAL=NLBSTLB
0.00229
**
** Column
**
** Bars on the East side: 2HD24
*SOLID SECTION, ELSET=LBECNLB,MATERIAL=NLBSTLB
0.000904
*SOLID SECTION, ELSET=LBECLB,MATERIAL=LBSTLB
0.000904
** Bars on the Middle side: 2HD24
*SOLID SECTION, ELSET=LBMCNLB,MATERIAL=NLBSTLB
0.000904
*SOLID SECTION, ELSET=LBMCLB,MATERIAL=LBSTLB
0.000904
** Bars on the West side: 2HD24
*SOLID SECTION, ELSET=LBWCNLB,MATERIAL=NLBSTLB
0.000904
*SOLID SECTION, ELSET=LBWCLB,MATERIAL=LBSTLB
0.000904
**
**
** S T I R R U P S  and  H O O P S
**
** East Beam
**
** R10 with 4 legs
*SOLID SECTION,ELSET=STEBNLB,MATERIAL=NLBSTST
0.000316
** R10 with 2 legs
*SOLID SECTION,ELSET=STEBLB,MATERIAL=LBSTST
0.000158
**
**
** West Beam
**
** R10 with 4 legs
*SOLID SECTION,ELSET=STWBNLB,MATERIAL=NLBSTST
0.000316
** R10 with 2 legs
*SOLID SECTION,ELSET=STWBLB,MATERIAL=LBSTST
0.000158
**
** Joint
**
```

```
** R16 with 2 legs
*SOLID SECTION, ELSET=JCHO,MATERIAL=NLBSTST
0.000402
**
** South Column
**
** R10 with 2 legs
*SOLID SECTION, ELSET=HESCNLB,MATERIAL=NLBSTST
0.000158
** R10 with 2 legs
*SOLID SECTION, ELSET=HESCLB,MATERIAL=LBSTST
0.000158
**
** North Column
**
** R10 with 2 legs
*SOLID SECTION, ELSET=HENCNLB,MATERIAL=NLBSTST
0.000158
** R10 with 2 legs
*SOLID SECTION, ELSET=HENCLB,MATERIAL=LBSTST
0.000158
**
**
** DEFINITION MATERIAL PROPERTIES
**
** The properties of the following materials are to be defined:
** NLBCON  Non Linear Behaviour Concrete
** LBCON   Linear Behaviour Concrete
** NLBSTLB Non Linear Behaviour Steel for Longitudinal Bars
** LBSTLB  Linear Behaviour Steel for Longitudinal Bars
** NLBSTST Non Linear Behaviour Steel for Stirrups and Hoops
** LBSTST  Linear Behaviour Steel for Stirrups and Hoops
**
**
*MATERIAL, NAME=LBCON
*ELASTIC
** Young Modulus, Poisson Coefficient
3.0E4,0.18
**
*MATERIAL, NAME=NLBCON
*ELASTIC
** Young Modulus, Poisson Coefficient
3.0E4,0.18
*CONCRETE
28.,0.
40.,.000666
32.,.001931
*TENSION STIFFENING
1.,0.
0.,2.E-3
**
*MATERIAL, NAME=NLBSTLB
*ELASTIC
** Young Modulus, Poisson Coefficient
2.0E5,0.20
*PLASTIC
320.,0.
430.,0.0131
**
*MATERIAL, NAME=LBSTLB
*ELASTIC
** Young Modulus, Poisson Coefficient
2.0E5,0.20
**
*MATERIAL, NAME=NLBSTST
*ELASTIC
** Young Modulus, Poisson Coefficient
2.0E5,0.20
*PLASTIC
320.,0.
```

```
430.,0.0131
**
*MATERIAL, NAME=LBSTST
*ELASTIC
** Young Modulus, Poisson Coefficient
2.0E5,0.20
**
**
**
** B O U N D A R Y  C O N D I T I O N
**
*BOUNDARY
6,1,2
**
903,1
913,1
**
**
*RESTART,WRITE
**
**
** HISTORY DEFINITION
**
**
** F I R S T  S T E P
**
** Axial Load
**
*STEP, INC=100
*STATIC
0.1,1.
**
** The load is assigned as concentrated in the nodes
** The Units are MN (see Elements Library)
**
*CLOAD
903,2,-0.0183
904,2,-0.0447
905,2,-0.0528
906,2,-0.0528
907,2,-0.0528
908,2,-0.0528
909,2,-0.0528
910,2,-0.0528
911,2,-0.0528
912,2,-0.0447
913,2,-0.0183
*NODE PRINT,NSET=EB-ENDAL
U,
RF
*ELPRINT,ELSET=ELCNLB
S,
E,
CRACK,CONF
*ELPRINT,ELSET=ELEBNLB
S,
E,
CRACK,CONF
*ELPRINT,ELSET=ELWBNLB
S,
E,
CRACK,CONF
*MONITOR,NODE=1007,DOF=2
*END STEP
**
** S E C O N D  S T E P
**
** Displacement Control
**
*STEP, INC=100
```

```
*STATIC
0.01,1,1.0E-6
**
** The following command is suggested by the User Manual page 8.3.2-5
**
** The first parameter Io denotes the number of equilibrium iterations
** after which the check is made that the residuals are not increasing
** in both of two consecutive iterations. This parameter is particularly
** useful if the initial convergence (check on the residuals at ecah
** iteration) is nonmonotonic. [4]
** The second parameter Ir is the number of equilibrium iterations after
** which the logarithmic rate of convergence check begins. [8]
**
*CONTROLS,PARAMETERS=TIME INCREMENTATION
8,10
*BOUNDARY
**
** The imposed displacement corresponds to 5*Dy.
** Dy is the end displacement of the beam evaluated considering a
** linear variation of the curvature along the whole length of the beam.
** fy, which is the curvature of the fix section corresponding to
** reinforcement yielding, has been evaluated neglecting the
** contribution of the tensile concrete between the cracks.
** Dy=fy*L^2/3
**
EB-ENDAL,2,,-0.06595
WB-ENDAL,2,,+0.06595
*MONITOR,NODE=1007,DOF=2
*END STEP
```